AD A132 215   ON THE UNSTEADY RESPONSE OF AN OCEANIC FRONT TO LOCAL   1/2
                ATMOSPHERIC FORCING(U) NAVAL POSTGRADUATE SCHOOL
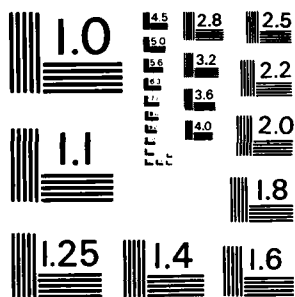   MONTEREY CA   C J HALL JUN 83
UNCLASSIFIED   F/G 8/3   N(

MICROCOPY RESOLUTION TEST CHART

NATIONAL BUREAU OF STANDARDS-1963-A

NAVAL POSTGRADUATE SCHOOL
Monterey, California

THESIS

ON THE UNSTEADY RESPONSE OF AN
OCEANIC FRONT TO LOCAL ATMOSPHERIC FORCING

by

Christopher James Hall

June 1983

Thesis Advisor: Roland W. Garwood, Jr.

Approved for public release; distribution unlimited

REPORT DOCUMENTATION PAGE	READ INSTRUCTIONS BEFORE COMPLETING FORM

1. REPORT NUMBER	2. GOVT ACCESSION NO. A132215	3. RECIPIENT'S CATALOG NUMBER

| 4. TITLE (and Subtitle)

On the Unsteady Response of an Oceanic Front to Local Atmospheric Forcing | 5. TYPE OF REPORT & PERIOD COVERED

Master's Thesis
June 1983 |
|---|---|
| | 6. PERFORMING ORG. REPORT NUMBER |

| 7. AUTHOR(s)

Christopher James Hall	8. CONTRACT OR GRANT NUMBER(s)

| 9. PERFORMING ORGANIZATION NAME AND ADDRESS

Naval Postgraduate School
Monterey, California 93940	10. PROGRAM ELEMENT, PROJECT, TASK AREA & WORK UNIT NUMBERS

| 11. CONTROLLING OFFICE NAME AND ADDRESS

Naval Postgraduate School
Monterey, California 93940 | 12. REPORT DATE

June 1983 |
|---|---|
| | 13. NUMBER OF PAGES

120 |

14. MONITORING AGENCY NAME & ADDRESS(if different from Controlling Office)	15. SECURITY CLASS. (of this report)
	15a. DECLASSIFICATION/DOWNGRADING SCHEDULE

16. DISTRIBUTION STATEMENT (of this Report)

Approved for public release; distribution unlimited

17. DISTRIBUTION STATEMENT (of the abstract entered in Block 20, if different from Report)

18. SUPPLEMENTARY NOTES

19. KEY WORDS (Continue on reverse side if necessary and identify by block number)

oceanic front
density front

20. ABSTRACT (Continue on reverse side if necessary and identify by block number)

The unsteady response of two oceanic density fronts to local atmospheric forcing, using combinations of wind stress and surface heat flux, is investigated with an embedded mixed layer-general circulation model. The adjustment of the frontal structure is dependent upon the wind stress direction and whether there is surface heating or cooling. In cases of an applied wind stress alone where denser water is transported

toward less dense water, the frontal structure diffuses, the mixed layer depth deepens, and cross-frontal mixing occurs. In cases where less dense water is transported toward denser water, the frontal strucure is preserved, mixed layer depth is preserved and cross-frontal mixing is minimized. The addition of surface heating shallows the mixed layer and inhibits vertical mixing. Inertial oscillations are observed in the across-front velocity field.

Accession For	
NTIS GRA&I	☒
DTIC TAB	☐
Unannounced	☐
Justification	

By
Distribution/
Availability Codes

Dist	Avail and/or Special
A	

DTIC
COPY
INSPECTED
2

2

On the Unsteady Response
of an Oceanic Front to Local Atmospheric Forcing

by

Christopher J. Hall
Lieutenant, United States Navy
B.S., United States Naval Academy, 1975

Submitted in partial fulfillment of the
requirements for the degree of

MASTER OF SCIENCE IN METEORLOGY AND OCEANOGRAPHY

from the

NAVAL POSTGRADUATE SCHOOL
June 1983

Author: _____

Approved by: _____
Thesis Advisor

_____
Second Reader

_____
Chairman, Department of Oceanography

_____
Dean of Science and Engineering

3

ABSTRACT

The unsteady response of two oceanic density fronts to local atmospheric forcing, using combinations of wind stress and surface heat flux, is investigated with an embedded mixed layer-general circulation model. The adjustment of the frontal structure is dependent upon the wind stress direction and whether there is surface heating or cooling. In cases of an applied wind stress alone where denser water is transported toward less dense water, the frontal structure diffuses, the mixed layer depth deepens, and cross-frontal mixing occurs. In cases where less dense water is transported toward denser water, the frontal structure is preserved, mixed layer depth is preserved and cross-frontal mixing is minimized. The addition of surface heating shallows the mixed layer and inhibits vertical mixing. Inertial oscillations are observed in the across-front velocity field.

TABLE OF CONTENTS

LIST OF TABLES

7

LIST OF FIGURES

8

ACKNOWLEDGEMENT

I. INTRODUCTION

A. BACKGROUND AND PURPOSE

During recent years, there have been a number of scientific studies that describe the nature and existence of oceanic fronts. Cromwell and Reid (1956) identified a front by an abrupt horizontal density change at the sea surface. Roden (1976) stated that a front should be considered to exist wherever any oceanic state variable (density, temperature or salinity) reaches a relative maximum value in its horizontal gradient.

The motivation for studying fronts and ocean prediction has been stressed by Roden (1976), Elsberry and Garwood (1979), and Niiler (1982). Elsberry and Garwood (1979) specifically point out antisubmarine warfare applications, fisheries management and a resource for climate research data, as viable and pertinent reasons for further study. Many important physical processes which are accompanied by attendant air-sea interactions occur in frontal regions. Latent and sensible heat transfer, evaporative and precipitative processes, baroclinic currents, salt fluxes, mass and momentum transport, inertial-internal wave activity and mixing all can occur. Oceanic frontal areas are areas of sound

11

speed changes and often are areas of increased biological activity.

This thesis examines the time-dependent response of a numerically- simulated oceanic front to local atmospheric forcing. The model used in this work incorporates the forcings of wind stress and surface heating with a 20-level primitive equation ocean circulation model with embedded mixed layer dynamics.

B. OBSERVATIONAL STUDIES

Cromwell and Reid (1956) described a simple case of an upper layer of warm, less dense water overlying a layer of cool, denser water in the ocean. The front in this case is a density front formed by the horizontal temperature gradient. Observations showed surface convergence along the front, sinking motion in the immediate vicinity of the front and divergence at lower depths. They observed that the wind affected the front by mixing the upper layer, reducing the horizontal surface temperature gradient, and enhancing the temperature jump at the base of the mixed layer.

Voorhis and Hersey (1964) observed a wintertime thermal front in the Sargasso Sea. They found an average temperature gradient of ; deg C/10 km, and a maximum in one

instance of 1.5 deg C/5 km. This was accompanied by a 60 cm/s jet flowing to the east along the edge of the front. The depth of the front corresponded to the mixed layer depth. The water on either side of the front was found to be well-mixed.

Katz (1969) continued the work of Voorhis and Hersey and derived temperature-salinity correlations for a front observed in the Sargasso Sea in May. He found the front to be a separation of two distinct water masses, with a transition zone of only a few meters in the vertical. He deduced that water transport along the front maintained the sharp transition. Although not observed, Katz presumed mixing must occur at the interface, but the along-front current prevented any build-up of well-mixed waters in that area. He also hypothesized that a vertical component to the current must exist at the interface. Thus, the interface would be preserved by both horizontal and vertical motions, and the vertical velocity would account for the observed accumulation of well-mixed waters below the front.

Bang (1973) studied a front at the southern end of the Benguela Current. This was an intense front with a horizontal temperature gradient of 1.6 deg C/km and a temperature

change of 8-10 deg C across it. There was also local upwelling occurring due to an offshore transport. As might be expected from Ekman theory, Bang found the front to intensify under southerly winds (Ekman transport being to the left of the wind in the Southern Hemisphere). Under a northwest gale, the front rapidly weakened. It reintensified as the wind steadied from the south.

Roden has made significant and extensive contributions to the literature on oceanic fronts, especially on the large-scale fronts in the Pacific Ocean. In a series of papers, he has observed and examined the Pacific subarctic front (Roden 1975, 1977), the subtropical front (Roden 1974, 1975, 1980), the doldrum front (Roden 1974, 1975), and the subarctic-subtropical transition zone (Roden 1971, 1972). In the 1971 paper, Roden concentrated on the subarctic-subtropical transition zone and found that the wind stress played an important role in determining the location of heat and salt flux divergence zones. Roden (1972) focused on the temperature and salinity fronts located at the boundaries of the transition zone; the subarctic front to the north and the subtropical front (which is also a density front) to the south. The origins of both fronts were found to be related

to the wind stress, geostrophic flow fields and heat and salt flux divergence. The doldrum front was included in a study of the subtropical front (Roden 1974). Further work on all three fronts was conducted by Roden (1975) with reference to the wind and to the energy flux fields. He observed that the depth of the mixed layer changed dramatically across the subarctic front in winter and spring; from 100 m on the north side to 300 m on the south side. The subtropical front is highly dependent on the wind and energy flux fields at the sea surface, as the front occurs in an area of Ekman transport convergence. The doldrum front is a front due to a salinity gradient only, with a baroclinic eastward-flowing current at the surface and a faster westward-flowing undercurrent.

For the subarctic front, Roden (1977) found atmospheric forcing (that is, wind stress, radiative heat flux, precipitation and turbulent energy fluxes) to be the primary cause of frontal movement, intensification and decay. Roden has shown repeatedly that the roles of wind stress, Ekman transport and heating are inextricable from the dynamics of frontogenesis. Roden (1980) again examined the subtropical frontal zone (within which are located a number of

individual fronts) and showed that Ekman transport led to a concentration of the temperature and salinity gradients in the upper ocean. Thus, frontogenesis was due to horizontal convergence and confluence of the flow field.

While Roden's work has dealt primarily with frontogenesis and in explaining the dynamics of several identified North Pacific fronts, his findings are pertinent to this thesis, i.e., local atmospheric forcing plays a major role in the dynamics of oceanic fronts.

C. MODEL STUDIES

Garvine has concentrated on a modelling approach to fronts. In one of his earlier papers (1974), he investigated the dynamics of small-scale fronts, though without regard to atmospheric forcing. Such fronts propagate into the ambient water via the unbalanced horizontal pressure gradient. Because of minimal cross-frontal mixing, he found strong convergence and sinking at the front. He later expanded this model to include the effects of wind stress (Garvine 1979a, 1979b). However, because of the need to maintain steady state in the model, he prescribed wind stress to be of secondary importance relative to the horizontal pressure gradient. Buoyancy and energy budgets were added later to the model (Garvine 1980).

Kao (1980) investigated the Gulf Stream as a large-scale density front in the upper ocean. The heart of his work was performing a scale analysis, which revealed three length scales: an inertial or deformation length scale, a buoyancy length scale, and a diffusive length scale. Kao's conclusion was that the front was maintained by the cross-Gulf Stream circulation, but his model included no wind stress or heating.

Cushman-Roisin's (1981) model was based on Roden's work on large-scale frontogenesis, and it does have some similarities to the model used in this thesis because it includes mixed layer dynamics. An important difference is in the scales. Cushman-Roisin investigates large-scale and long-term spin-up of a front in response to a wind stress curl. The model in this thesis is used to investigate local response of a pre-existing front to local winds and heating. Surface wind stress is a primary means of forcing in both models, but Cushman-Roisin applies a strong wind stress curl in the form of a wind field that changes direction at the latitude of the zonally-oriented front. We, on the other hand, spin up a horizontally uniform wind stress over six hours, after which it maintains a constant value. The

results obtained by Cushman-Roisin depend much upon the curl of the wind stress. Cushman-Roisin finds the mixed layer depth is at a minimum in the middle of the front, while Ekman downwelling is at a maximum. This is probably due to a lack of any wind stress at the front itself, although the curl is large.

Camerlengc (1982) studied the large-scale response of upper ocean fronts, specifically the Pacific subarctic front. His model has a variable-spaced horizontal grid with highest resolution in the frontal area. Vertical mixing was not included in the model. Assuming a pre-existing front, Camerlengc applied different wind stresses, and found that except in the case of the passage of a strong cyclone, the effects of wind forcing were limited to the upper 150 m. One case of a uniform wind stress did show Ekman transport and a horizontal displacement of the front.

II. DESCRIPTION OF THE PROBLEM

A. GENERAL

The response of a pre-existing oceanic front to local atmospheric forcing (wind stress and surface heating) over a time period of two days is examined. An embedded mixed layer-ocean circulation model is used, and two different frontal structures are treated. The first numerically-inserted front, hereafter referred to as Front 1, is somewhat of an artifact in that the isotherms become horizontal at a relatively shallow depth (see Figs. 1, 2, and 3 for the initial conditions), so that Front 1 is manifested only within the upper 60 m. The temperature field is vertically stratified below approximately 70 m. The front is about 10 km wide. The maximum horizontal temperature gradient at the surface is 1.5 deg C/1.6 km. The mixed layer depth is a numerically-inserted approximation to what the actual mixed layer depth would be. A geostrophic along-front velocity is calculated from the initial temperature field. It has a maximum speed of 32 cm/s with its axis located at the surface on the warm side of the front. The across-front geostrophic

velocity is zero. Front 1 is a viable representation of a smaller mesoscale upper layer front, and the model results will be important in this context. The second type of front, hereafter referred to as Front 2, is a simulation of a more typical front, similar to those reported by Roden (1980). The horizontal temperature gradient at the surface is 1.5 deg C/3.2 km. The front is not only evident at the surface, but also its effect on the temperature field extends throughout the thermocline of the model (see Figs. 4, 5, and 6 for the initial conditions). The mixed layer depth again is a numerically-inserted approximation based on the shape of the temperature field. It is felt that adjustments which occur shortly after the start of integration of the model will compensate for any errors in the initial field. A geostrophic along-front velocity is calculated from the initial temperature field. Its maximum value is 100 cm/s and the axis lies at the surface on the warm side of the front. The across-front geostrophic velocity is zero. With both fronts oriented in a right-hand coordinate system, z increases upwards, y increases to the right, and x increases out of the page.

B. HYPOTHESES

It is expected that the direction of the wind relative to the orientation of the front plays an important role in the near-frontal circulation and density structure. Ekman transport across the front should cause upwelling and down-welling features near the surface manifestation of the front. Jchannessen, et al (1977) observed that the thermocline through the Maltese front shallowed in certain areas, which indicated upwelling, and also that the thermocline spatially deepened after isotherms surfaced. In Johannessen's case, this was attributed to the presence of an eddy. If the water masses had been of similar types, it would have been indicative of downwelling.

With regard to one-dimensional mixing, Niiler's (1975) mixed layer model used an impulsive wind stress and no heating, and showed that initially the mixed layer deepened rapidly. Strong inertial motions can be generated which can lead to a large increase in available turbulent energy and thus to a rapid(within the first half pendulum-day) deepening of the mixed layer. Mellor and Durbin (1975) also used an impulsive wind stress of 2 cm^2 /s^2 (approximately 2 dynes/cm^2) and no heating. They showed that the mixed layer

T at hour 0
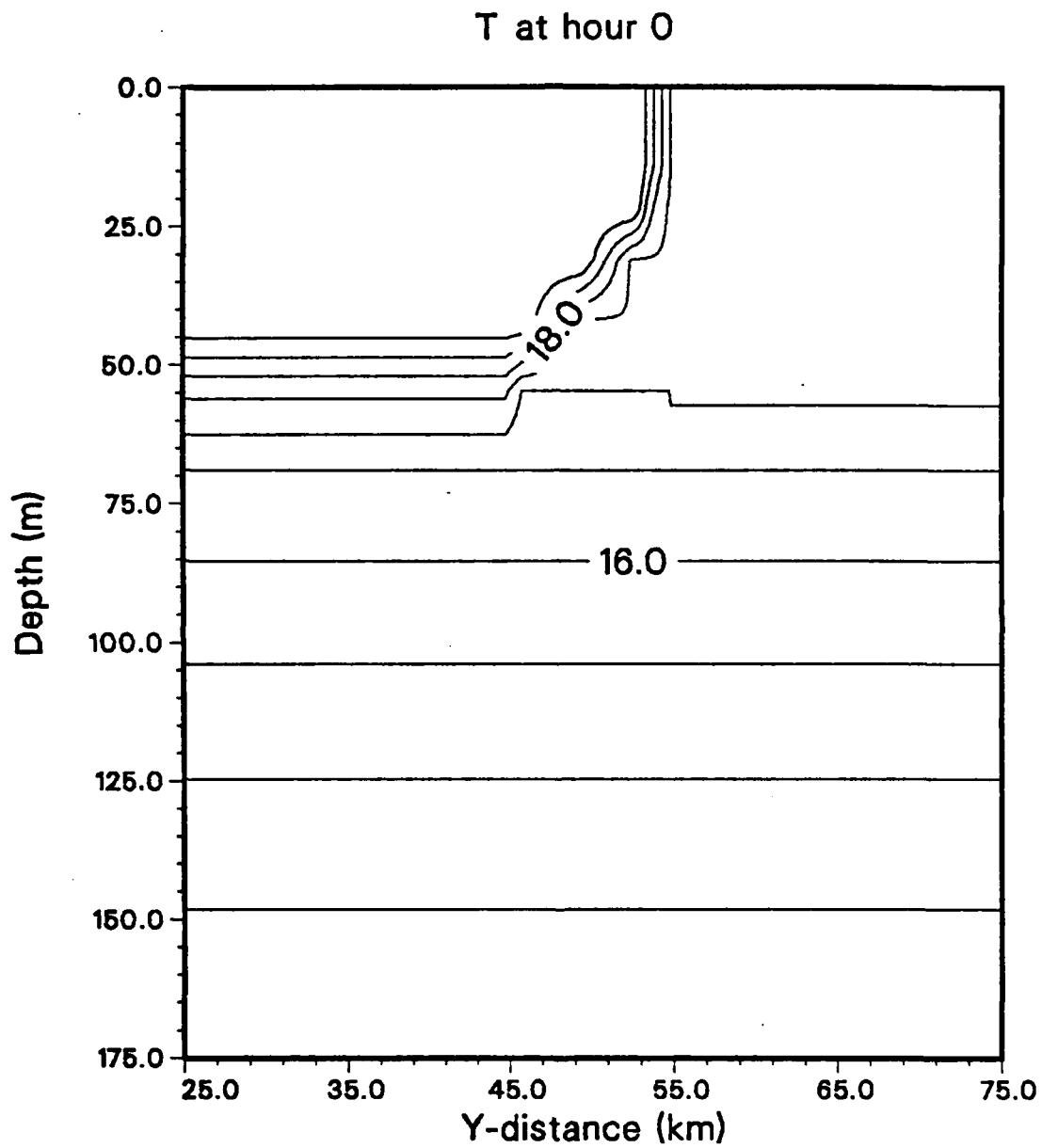
Figure 1. Front 1 Initial Temperature. Only the middle section of the grid and the upper 175 m are shown. Contour interval is 0.5 deg C.

H at hour 0
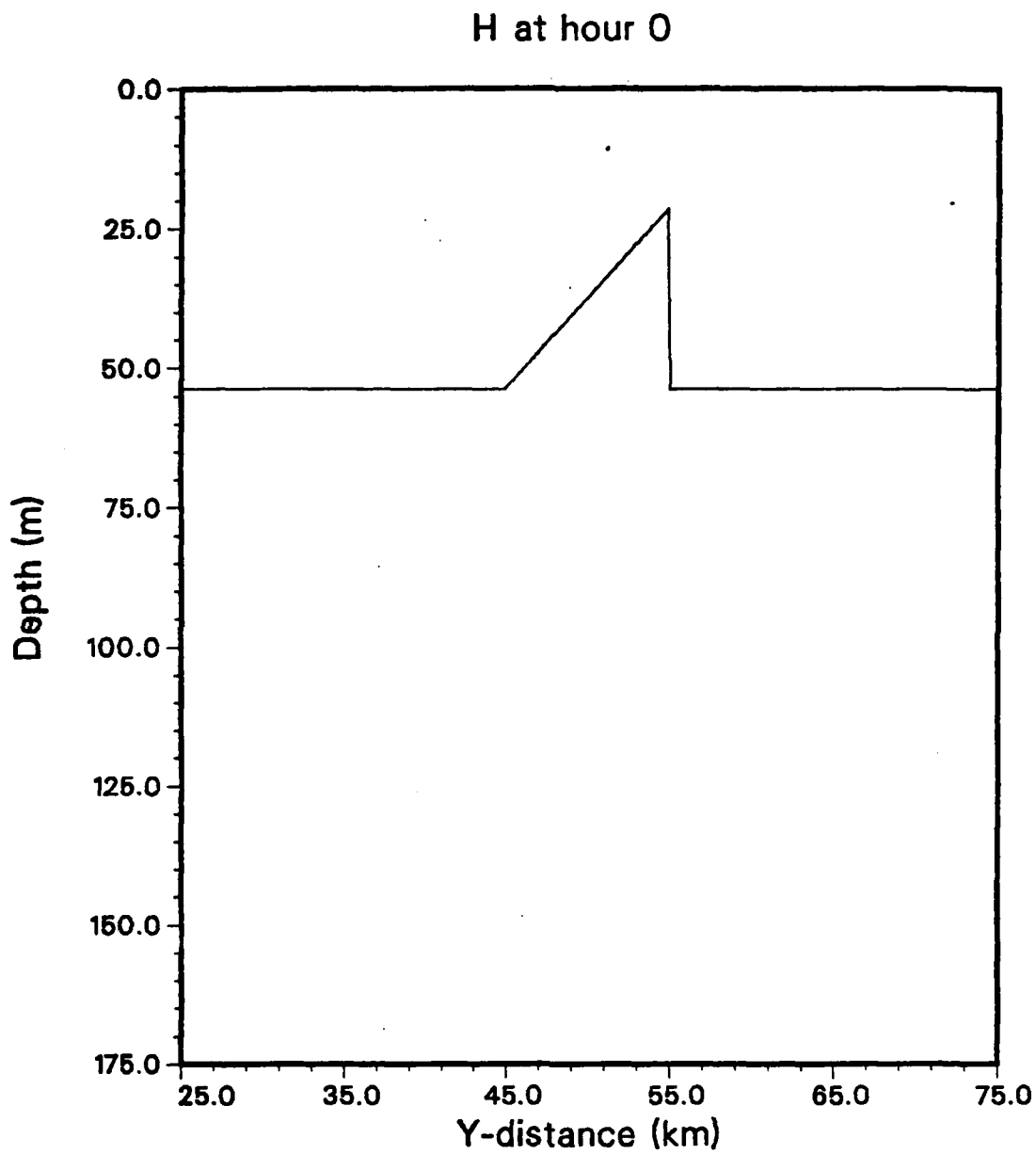
Figure 2. Frcnt 1 Initial Mixed Layer Depth.

23
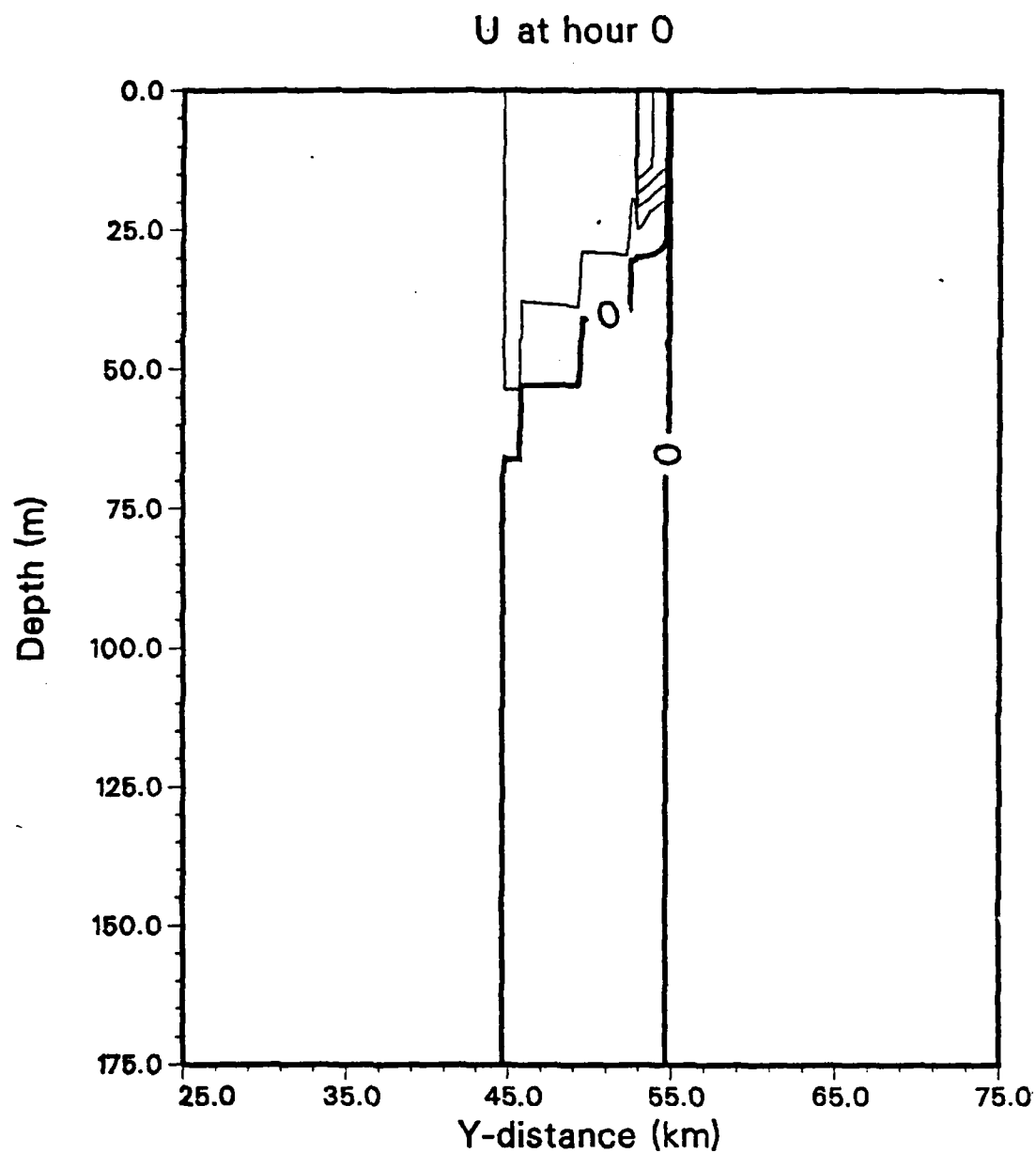
Figure 3. Front 1 Initial U-Geostrophic Velocity. Contour interval is 8 cm/s.

T at hour 0
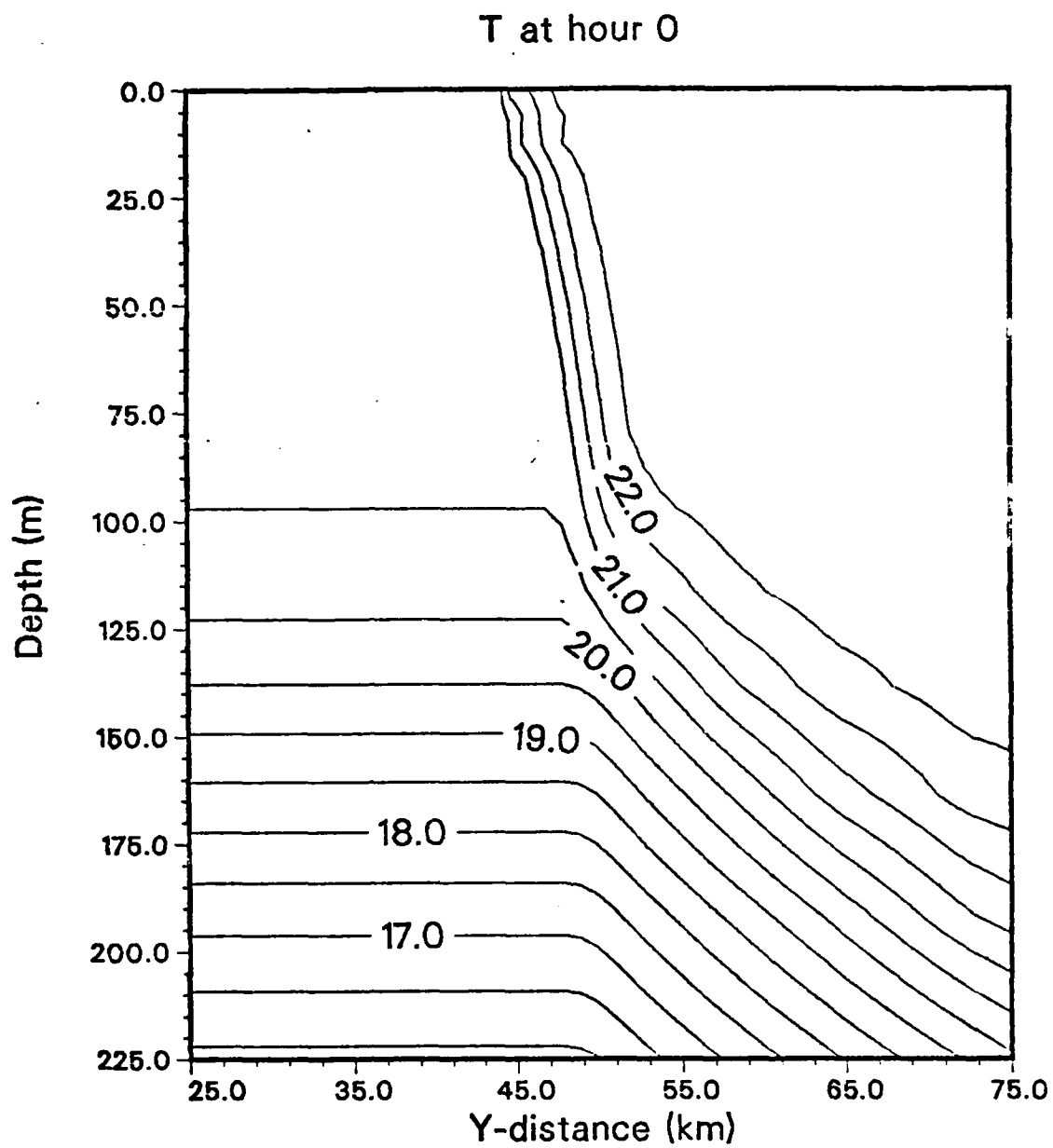
Figure 4. Front 2 Initial Temperature. Only the middle section of the grid and the upper 225 m are shown. Contour interval is 0.5 deg C.
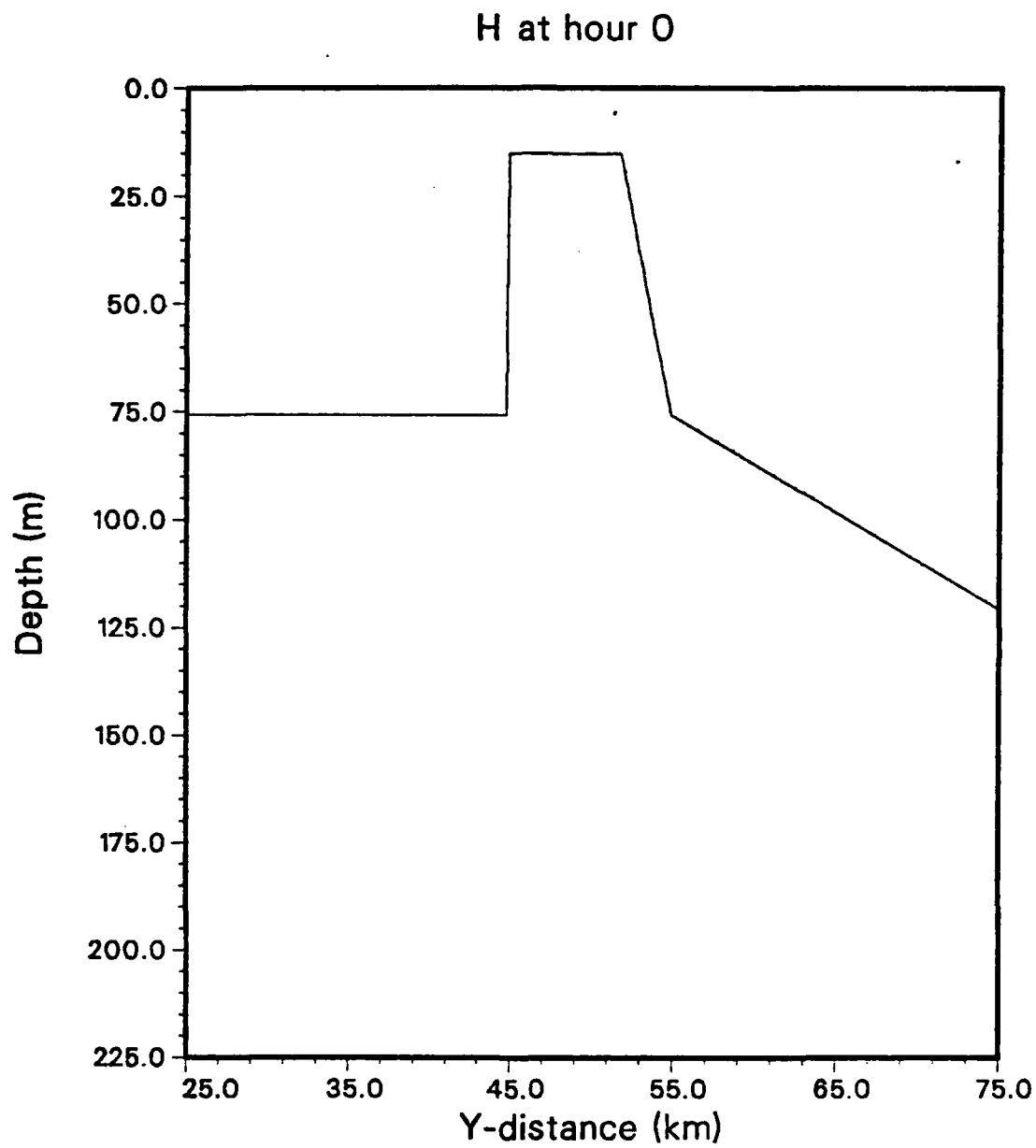
Figure 5.   Front 2 Initial Mixed Layer Depth.

U at hour 0
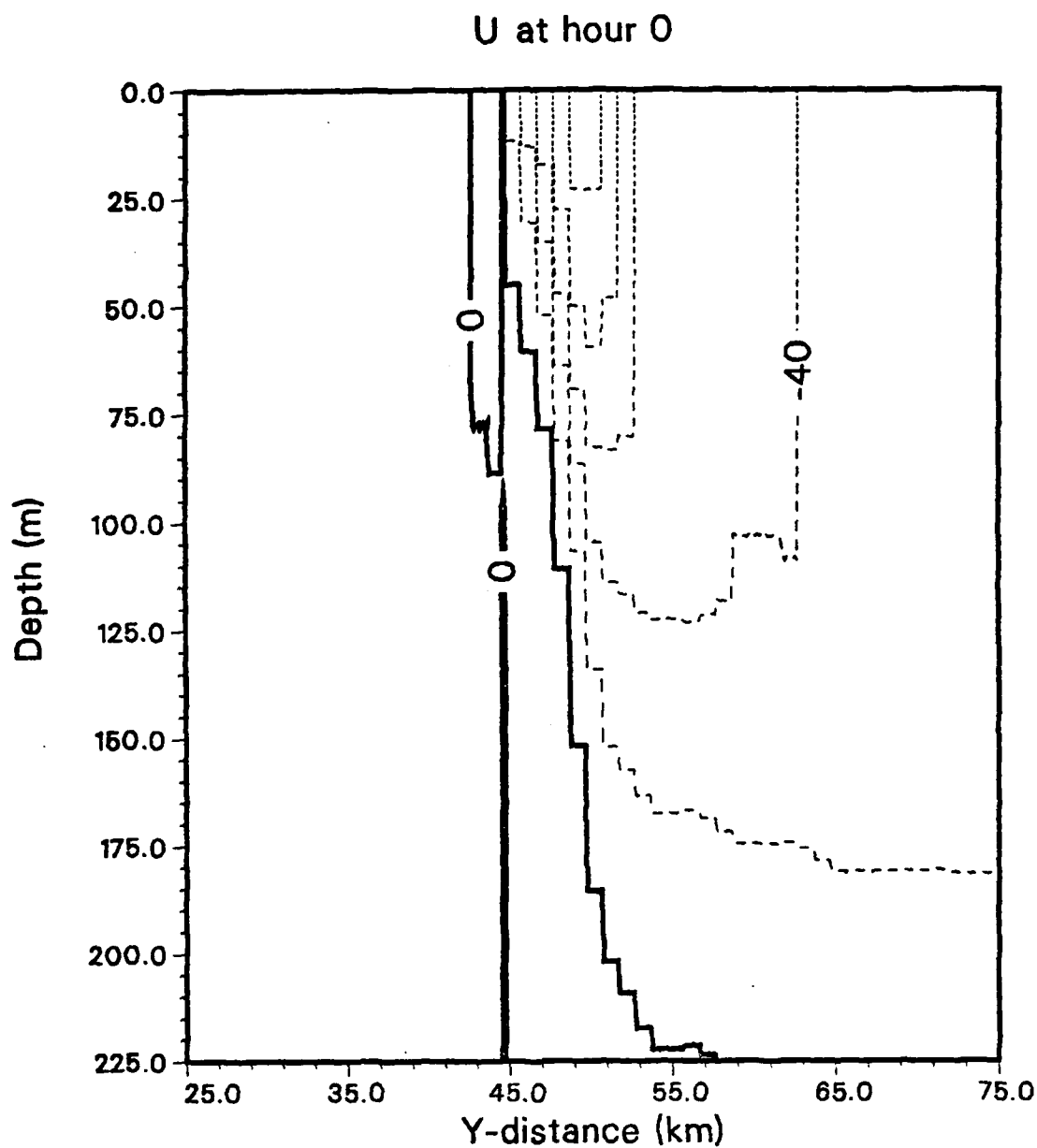
Figure 6. Front 2 Initial U-Geostrophic Velocity. Contour interval is 20 cm/s. Dashed lines indicate negative values.

27

deepened and that the temperature jump also increased
slightly. In a two-dimensional model, De Szoeke (1980)
examined the effects of wind stress only in his version of
the Niiler (1975) model and found that in the case of
constant wind stress, the mixed layer deepened rapidly in
the first half pendulum-day (t=Pi/f), and then slowed. An
additional effect of the wind stress is the possible augmen-
tation of a quasi-geostrophic frontal shear (in the along-
front direction) which could increase vertical mixing as
prescribed by the initial value of the Gradient Richardson
Number:

$$Ri = \frac{-\frac{g}{\rho}\frac{\partial \rho}{\partial z}}{\left|\frac{\partial \vec{V}}{\partial z}\right|^2} < \frac{1}{4}$$

A surface heating-cooling cycle can lead to stratifica-
tion under light to moderate winds which will tend to modu-
late any mixing tendencies brought about by wind-generated
turbulence. Niiler (1975) showed that surface heating halts
the deepening of the mixed layer. We expect the same result
in our model. Mellor and Durbin (1975) investigated a case
of a combined constant wind stress (2 dynes/cm^2) and a

constant heating/cooling value (H = ±.01 cm-K/s). For the heating case they found a shallowing and leveling off of the depth of the mixed layer and an ever-increasing temperature jump value at the base of the mixed layer. The same heating condition with a lower wind stress (1 dyne/cm^2) resulted in a shallower mixed layer depth and the establishment of a double thermocline, a remnant of the initial mixed layer and the formation of a new shallower layer due to the influence of heating.

It is expected that inertial currents across the front may play an important role in the across-frontal transport of heat, mass, and momentum. Phasing of inertial wind-driven currents in conjunction with vertical mixing may result in lateral entrainment or "capture" of buoyant (warm) water by the adjacent cooler water during horizontal oscil-lations across the front plane.

C. METHOD

To test the above hypotheses and to establish the basic dependence of frontal response to local atmospheric forcing, four combinations of surface boundary conditions are inves-tigated. These are listed in Table I.

TABLE I
Atmospheric Forcing used in Model Runs

	τ_x(dynes/cm)	τ_y(dynes/cm)	Q(deg C-cm/s)
Case I	+1.0	0	0
Case II	-1.0	0	0
Case III	+1.0	0	-.004
Case IV	-1.0	0	-.004

In the cases above, τ_x is the along-front (x-direction) component of wind stress, τ_y is the cross-front (y-direction) component of wind stress, and heat flux Q is applied to the ocean uniformly at the surface (heat flux is positive upwards, so the negative value indicates warming of the ocean from the air). All four cases are examined for both Front 1 and Front 2.

Cases I and II examine the effects of wind stress parallel to the front only, which will eventually generate a steady Ekman transport perpendicular to the front. The wind stress of 1 dyne/cm^2 corresponds to a wind speed of 7-8 m/s. In all cases the wind stress is spun-up from 0 at t=0 to its maximum absolute value (1.0 dynes/cm^2) by hour 6. From hour 6 to hour 48 it remains constant. Such a short spin-up time is not unreasonable, as winds can change on a shorter time scale, for example, when an atmospheric cold front passes. Cases III and IV impose a constant surface heating on each

of the two preceding cases.   As indicated by the earlier

one-dimensional mixed layer models, we expect that the heat-

ing value will not be overwhelmed by the wind stress, and

that the effects of both dynamic and thermodynamic forcing

will be evident.

The initial conditions for Front 1 are shown in Figs. 1,

2, and 3. Warmer, less dense water resides on the left, and

cooler, denser water resides on the right. The initial con-

ditions for the velocity are determined by the associated

initial density field,   which is balanced by a geostrophic

along-front current directed out of the figure (u positive)

(see Fig. 3).   The mixed layer depth varies from a uniform

depth in the far field to a shallowing through the front.

The model is run for a 48 hour time period for each of the

specified atmospheric forcings shown in Table I.

In Case I we expect to see water from the cold (right)

side transported to the warm (left) side, upwelling on the

cold side at the front and downwelling due to convective and

turbulent mixing on the warm side.   The mixed layer depth

should deepen, and the front should diffuse.   In Case II we

expect the warm water to be transported on the surface to

the cold side, but convective mixing to be absent due to the

31

stable condition of the less dense water overriding the denser water. Upwelling should occur on the warm side at the front, and only minor downwelling should occur on the cold side due to the effect of wind stirring alone. In both Cases III and IV the heating should have a shallowing influence on the mixed layer depth tending to offset deepening and other effects caused by turbulent mixing.

The initial conditions for Front 2 are shown in Figs. 4, 5, and 6. In this configuration, the warmer, less dense water resides on the right and the cooler, denser water resides on the left. The accompanying along-front geostrophic current is directed into the page (u negative) with its maximum value at the surface. The mixed layer depth follows the contours of the upper thermocline, shallowing across the front. The model is initiated and integrated in time as it was for Front 1.

In Case I (wind stress positive, directed out of the figure), we expect the Ekman transport to be toward the left. The results for this case should be analagous to the expected results for Case II applied to Front 1 as previously noted. Case II should be compared to Case I for Front 1 and Cases III and IV should be compared to Cases IV and III respectively of Front 1.

The inertial period for our model is

$$T_i = \frac{2\pi}{f} \approx 20 \text{ hours}$$

at the latitude of 36 deg N. Considering that in this model wind stress does not attain its steady maximum value until 6 hours have elapsed, we should find a maximum in inertial motion somewhat later than half an inertial period after time zero, at perhaps t=15 hours or so.

D. DESCRIPTION OF THE MODEL

The primary documentation for the model is in Adamec, et al (1981). In that paper, the model is cast in radial coordinates to investigate the oceanic response to a stationary radially-symmetric hurricane. In our case, the model is in right-hand Cartesian coordinates and it is two-dimensional (y and z). It is believed that this model is particularly well-suited to the study of upper ocean fronts because it incorporates the Garwood (1977) bulk mixed layer model into the Haney (1980) primitive equation model. The ocean is assumed hydrostatic and incompressible, where density is a function of temperature alone. The Coriolis parameter is constant and there are no fluxes of mass, momentum or heat

normal to any boundary except at the surface, where atmospheric forcing is applied. The horizontal grid spacing is 125 m and the vertical grid spacing is variable over 20 layers from 6 m at the top layer to 64 m at the bottom layer. The domain size in y and z is 100 km by 500 m, respectively. With the front pre-existing as an initial condition, the initial u-component of velocity is in geostrophic balance, and the initial v-component is initially set to zero.

Drawing upon Adamec, et al (1981), highlights of the model are outlined below. Table II lists the pertinent model variables and constants used in the governing equations.

The governing equations in their two-dimensional form are as follows:

$$\frac{\partial u}{\partial t} = -v\frac{\partial u}{\partial y} -w\frac{\partial u}{\partial z} + fv - \frac{\partial}{\partial z}(\overline{u'w'}) \qquad (1)$$

$$\frac{\partial v}{\partial t} = -v\frac{\partial v}{\partial y} - w\frac{\partial v}{\partial z} - fu - \frac{1}{\rho}\frac{\partial p}{\partial y} + A_{M}\frac{\partial^{2}v}{\partial y^{2}} - \frac{\partial}{\partial z}(\overline{v'w'}) \qquad (2)$$

$$\frac{\partial T}{\partial t} = -v\frac{\partial T}{\partial y} - w\frac{\partial T}{\partial z} + A_{T}\frac{\partial^{2}T}{\partial y^{2}} - \frac{\partial}{\partial z}(\overline{w'T'}) \qquad (3)$$

$$\frac{\partial v}{\partial y} + \frac{\partial w}{\partial z} = 0 \qquad (4)$$

TABLE II

Model Constants and Variables

α	coefficient of thermal expansion	2.0E-5 /degC
A_T	horizontal eddy conductivity coefficient for heat	2.5E+5 cm^2/s
A_M	horizontal eddy diffusion coefficient for momentum	2.5E+5 cm^2/s
K_T	vertical eddy conductivity coefficient for heat	0.5 cm^2/s
K_M	vertical eddy diffusion coefficient for momentum	0.5 cm^2/s
ϕ	latitude	36 N
f	Coriolis parameter	8.55E-5/s
g	gravity	981.0 cm/s^2
ρ_o	reference density of seawater	1.0276 g/cm^3
T_o	reference temperature	5 degC
Δt	model timestep	30 s
J	horizontal grid array size	800
K	vertical grid array size	20
$z=-D$	basin depth	500 m
Y	basin width	100 km
u	x (along-front) component of velocity	
v	y (across-front) component of velocity	
T	temperature	
h, H	mixed layer depth	

$$0 = - \frac{\partial \mathcal{v}}{\partial z} - \rho g \qquad (5)$$

$$\rho = \rho_o (1 - \alpha (T - T_o)) \qquad (6)$$

The boundary conditions are:

$$u = 0 , \quad A_M \frac{\partial v}{\partial y} = A_T \frac{\partial T}{\partial y} = 0 \quad @ \ y = 0 , \ 100 \ km \qquad (7)$$

$$w = 0 \ @ \ z = 0 , \ -D \qquad (8)$$

$$-\overline{w'T'} = \frac{Q}{\rho_0 c} \quad , \quad -\overline{u'w'} = \frac{\tau_x}{\rho_0} \quad ; \quad -\overline{v'w'} = 0 \ @ \ z = 0$$

$$-\overline{w'T'} = -\overline{u'w'} = -\overline{v'w'} = 0 \ @ \ z = -D \qquad (9)$$

An equation for the depth, h, of the well-mixed layer is derived by integrating the continuity equation and applying the rigid lid boundary condition (Eq. 8):

$$\frac{\partial h}{\partial t} + w_{-h} = w_e \qquad (10)$$

The vertical turbulent fluxes are parameterized in two different manners depending upon where in the water column they are located. Below the mixed layer, the vertical fluxes are parameterized by eddy viscosity and conductivity coefficients:

$$\overline{u'w'} = -K_M \frac{\partial u}{\partial z}$$

$$\overline{v'w'} = -K_M \frac{\partial v}{\partial z} \qquad (11)$$

$$\overline{w'T'} = -K_T \frac{\partial T}{\partial z}$$

Above the mixed layer, turbulent mixing makes such a method which assumes K_M and K_T constant unrealistic and inaccurate. Thus the Garwood (1977) turbulence closure model is invoked using bulk turbulent kinetic energy equations.

36

The entrainment buoyancy flux is given by:

$$\alpha g(\overline{w'T'})_{-h} = -\langle \overline{w'w'} \rangle^{\frac{1}{2}} \langle \overline{E} \rangle / h \qquad (12)$$

where $\langle \overline{w'w'} \rangle$ and $\langle \overline{E} \rangle$ are the vertical and total components respectively of the turbulent kinetic energy. The mixed layer total turbulent kinetic energy equation and the vertical component of turbulent kinetic energy equation are:

$$\frac{\partial}{\partial t}\left[\frac{h\langle \overline{E} \rangle}{2}\right] = mu_*^3 - \alpha gh(\overline{w'T'})_{-h}/(2Ri^*) - (\langle \overline{E} \rangle^{\frac{1}{2}} + fh)\langle \overline{E} \rangle \qquad (13)$$

$$\begin{aligned}
\frac{\partial}{\partial t}\left[\frac{h\langle \overline{w'w'} \rangle}{2}\right] = {} & \alpha gh((\overline{w'T'})_{-h} - (\overline{w'T'})_0)/2 \\
& + (\langle \overline{E} \rangle - 3\langle \overline{w'w'} \rangle)\langle \overline{E} \rangle^{\frac{1}{2}} \\
& - (\langle \overline{E} \rangle^{\frac{1}{2}} + fh)\langle \overline{E} \rangle/3 \qquad (14)
\end{aligned}$$

where $u_* = \left(\dfrac{\tau_x}{\rho_a}\right)^{\frac{1}{2}}$ is the friction velocity and

$Ri^* = \dfrac{\alpha gh\Delta T}{\Delta u^2 + \Delta v^2}$ is the bulk Richardson Number.

The downward fluxes of momentum $-(\overline{u'w'})$ and $-(\overline{v'w'})$ are computed as:

$$-(\overline{u'w'})_{-h} = w_e \Delta u = -(\overline{w'T'})_{-h}\left(\frac{\Delta u}{\Delta T}\right)$$

$$-(v'w')_{-h} = w_e \Delta v = -(w'T')_{-h}\left(\frac{\Delta v}{\Delta T}\right) \qquad (15)$$

37

where w_e is the entrainment velocity:

$$w_e = \frac{-(\overline{w'T'})_{-h}}{\Delta T} \qquad (16)$$

The entrainment heat flux $(\overline{w'T'})_{-h}$ is the lower boundary condition for the mixed layer temperature profile, and a new mixed layer depth and new momentum and temperature profiles are calculated. The mixed layer depth is independent of the model level depths. If the mixed layer shallows rather than deepens (as would occur if there were insufficient vertical turbulent energy to transport heat down to the depth of the existing mixed layer), then the depth where $(\overline{w'T'}) \longrightarrow 0$ becomes the new mixed layer depth. During mixed layer shallowing, heat, momentum and potential energy are conserved. To prevent the levels beneath the mixed layer from becoming unstable in the numerical process, a dynamic stability condition is imposed such that the Gradient Richardson Number is always greater than 1/4.

The embedding of the mixed layer model within the general circulation model requires communication between the two. The general circulation model is the dynamic portion which calculates changes of u, v, and T at each depth level

due to advective and diffusive processes. These values are
then acted upon by the mixed layer model, which in turn cal-
culates the changes due to surface fluxes and entrainment
mixing, and calculates the new mixed layer depth. These
values are then used by the general circulation model.

III. MODEL RESULTS FOR FRONT 1 CASE I

A. ANALYSIS AND DISCUSSION

Although the front is initially in geostrophic balance,
the imposition of atmospheric forcing causes the front to
undergo a variety of adjustments.   In Case I, a positive
wind stress of 1 dyne/cm^2 is applied.   The front and the
u-component field undergo diffusion, thereby giving rise to
an ageostrophic u-component, which in turn creates a v-com-
ponent. As diffusion occurs through mixing, and as the sur-
face expression of the front is advected to the left in
response to the wind stress,   the along-front jet decreases
in magnitude as well as in horizontal extent.   A small
countercurrent is present at hour 24 due to a reversal in
the slope of the isotherms in the vicinity of the front.
This effect disappears by hour 36, but then reappears at
hour 48.

The base of the front on the right side deepens (as evi-
dent by the isotherms becoming vertical to greater depths)
from about 30 m initially to about 50 m as a result of the
effect of turbulent mixing and the creation of ageostrophic

velocities while undergoing dynamic adjustment (see Fig. 7).
An ageostrophic u-component is evident in Fig. 8 in the area
of y=53 km to 61 km. The mixed layer depth increases as the
upward sloping thermocline erodes within the front because
water is transported across the front, right to left. The
mixing of the cooler water with the warmer water causes the
mixed layer depth to deepen on the left (warm) side. The
axis of maximum v-values lies just above the bottom of the
mixed layer near y=53 km. If the v-profile is examined
(Fig. 9), it is seen that dv/dy > 0 on the right (cold) side
of the frontal axis, and dv/dy < 0 on the left side. The
gradients of v are much stronger on the left side of the
front than they are on the right. The maximum v-velocity is
-8 to -10 cm/s. From continuity, dw/dz < 0 (downwelling) on
the right side of the axis and dw/dz > 0 (upwelling) in a
thin layer on the left side that closely follows the mixed
layer depth. It is noted also that the mixed layer depth
has deepened at the right side of the front. This phenom-
enon is present throughout the model integration. Though
such a condition was not anticipated prior to the running of
the model (we expected an upwelling in the mixed layer on
the right side as a result of the mass transport over the

front towards the left), this depression in depth is
believed to be physically realistic. It is suspected that
this increase in the mixed layer depth occurs in response to
non-stationary adjustment to the atmospheric forcing, as it
also occurs in Case II where the oppositely-directed wind
stress is applied. Because the mixed layer depth responds
to the vertical integral of transport, the fact that the
mixed layer is shallower within the front than in the far
field blocks the flow from penetrating to depth. As the
water encounters this "obstacle", it "backs up" on the right
side and thus forces a depression in the mixed layer. This
explanation must be tempered by the fact that these figures
are instantaneous snapshots in time, and can be deceiving in
attempting to describe processes that have been evolving
over a length of time. Another possibility is that some
type of internal standing wave has been excited which is
causing fluctuations in the mixed layer depth.

The influence of the ageostrophic u-velocity, the core
of the v-velocity lying along the well-mixed layer a the
depression of the mixed layer on the right side of the front
is felt at depths greater than 100 m. Upwelling and down-
welling are evident at these depths (Fig. 7) beneath the
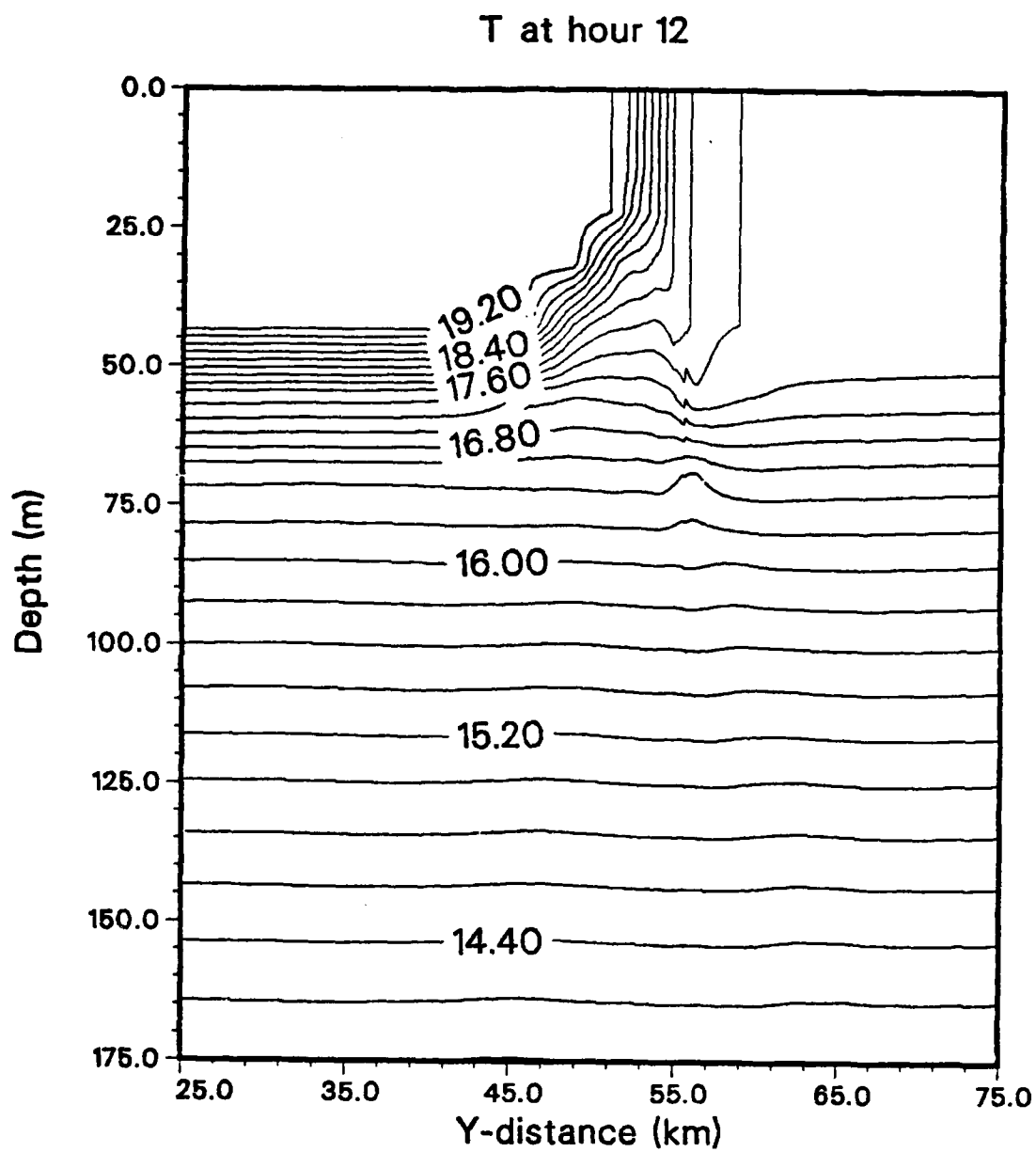right edge of the front.

T at hour 12

Figure 7. Front 1 Case I 12-Hour Temperature. Contour interval is 0.2 deg C.
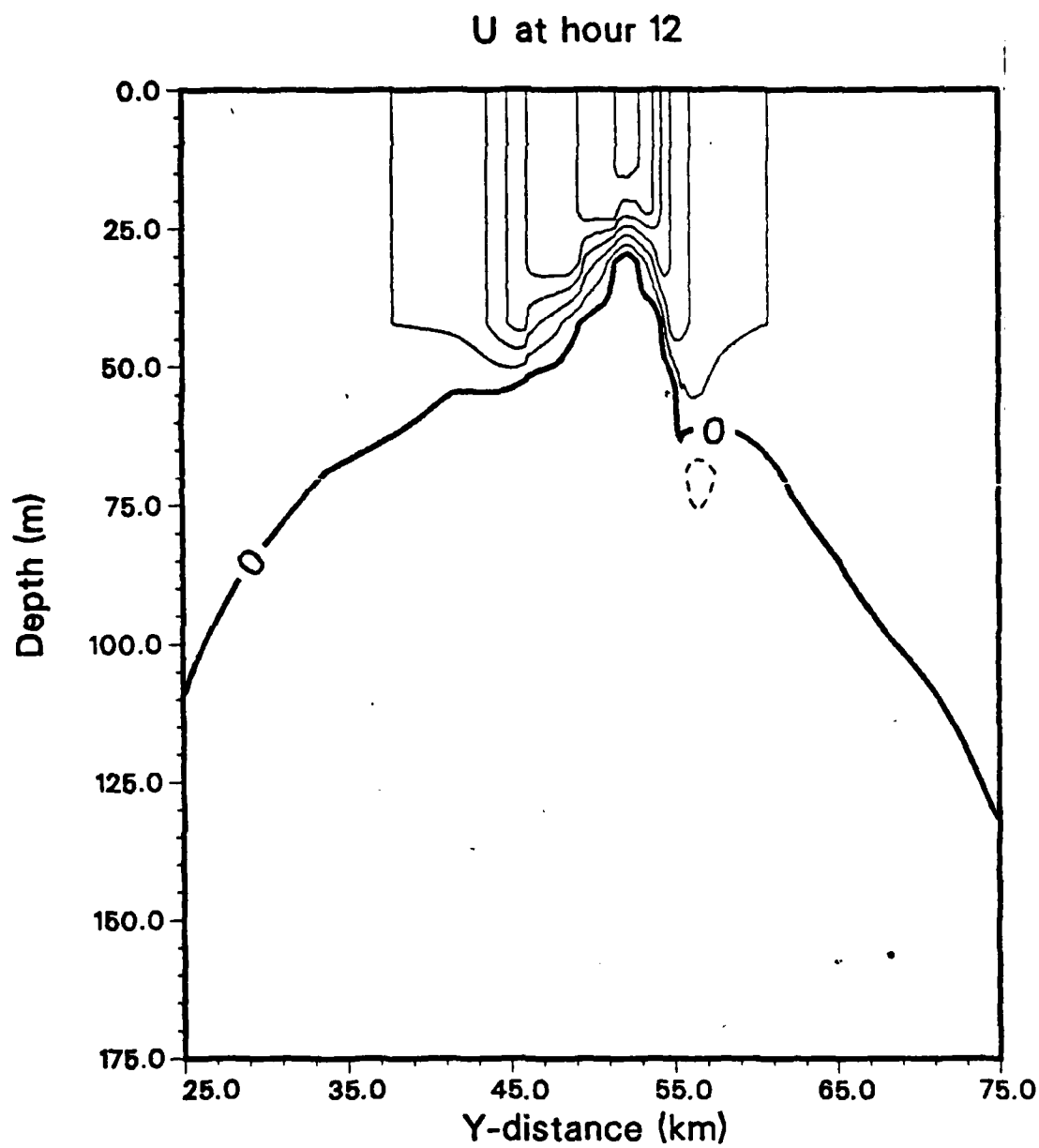
U at hour 12

Figure 8. Front 1 Case I 12-Hour U-Velocity. Contour interval is 8 cm/s.

V at hour 12
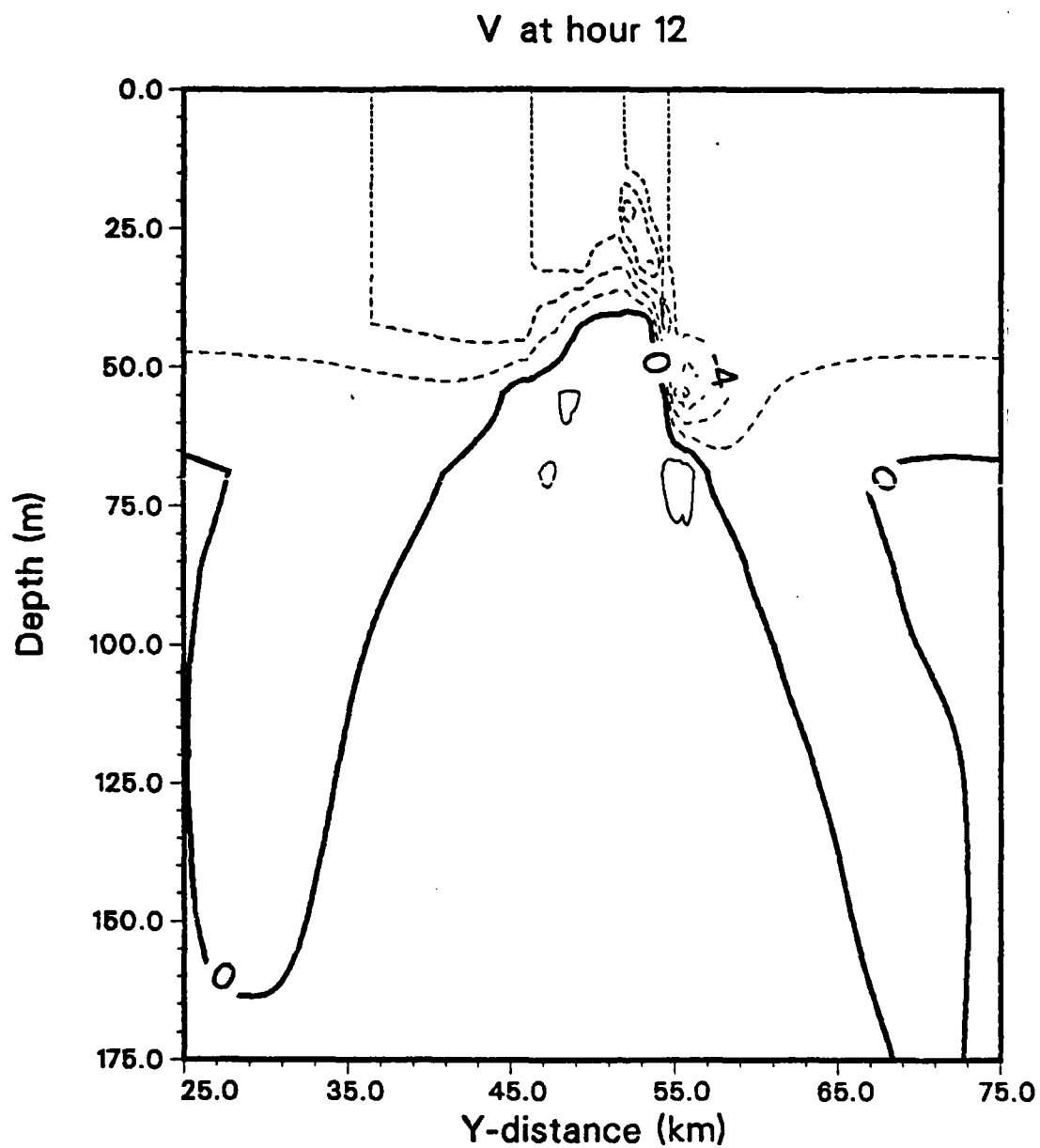
Figure 9.   Front 1 Case I 12-Hour V-Velocity.   Contour
interval is 2 cm/s.   Dashed lines indicate
negative values.

45

Interesting patterns in the v profiles evolve at hours 24 and 48. At 24 hours a small positive v exists. This is contrary to the expected Ekman transport direction in the surface layer, and is probably the result of an oscillation created by the inertial action. Furthermore, at both 24 and 48 hours, two cores of a positive v-component are present symmetrically centered about the base of the mixed layer on either side of the front. These are not present in the front, but form outside the frontal area and extend to the far field where the mixed layer is relatively stable.

The across-front velocity component is in consonance with the direction of the net Ekman transport at all times except hour 24. As noted, this velocity is at a maximum at the base of the mixed layer rather than at the surface. It is non-zero beneath the mixed layer in the middle of the front as well. Thus, it appears that interfacial mixing does occur in this case, and it may be contributing to the vertical mixing of heat in the thermocline at this location.

B. SUMMARY -- CASE I

Under the influence of positive wind stress and no heating, the front has diffused and has been advected in the direction of the surface Ekman transport. Because the front

46

is unsteady under an applied wind stress, ageostrophic velocities are created. Part of the response is frictional due to the turbulent boundary layer or mixed layer processes, and part is inertial due to the applied wind stress boundary condition. A noticeable deepening of the mixed layer occurs at the front on the right (cold) side, and the horizontal variability in mixed layer depth and temperature are reduced significantly under the influence of both vertical and cross-frontal mixing.

IV. MODEL RESULTS FOR FRONT 1 CASE II

A. ANALYSIS AND DISCUSSION

In this case, a negative wind stress (directed into the page) is applied. Wind stirring must overcome static stability as the warmer water will override the cooler water. It will be seen that the wind stress of 1 dyne/cm^2 is sufficient to mix the warmer water which is transported toward the cooler water. There is no evidence of stratification of shallow waters. Recall from Case I that, as the denser water from the right side was being transported to the left, it had to overcome static stability in order to upwell and override the front, and that the mixed layer depth profile posed a vertical barrier to the transport. In this case, the base of the mixed layer is at an incline in the direction of transport and static stability need not be overcome in the transport process. This leads to the expectation that cross-frontal mixing may be minimal in this case.

Diffusion in the temperature field again is evident over the 48 hours, but this time it occurs primarily at the edges of the front. A strong horizontal temperature gradient of

0.6 deg C/1.2 km in the middle of the front is maintained up through 48 hours (see Fig. 10 as representative of this) which was not present in Case I. This lends credence to the hypothesis that cross-frontal mixing is minimal.

Noticeable mixing occurs on the cold side of the front. The isotherms are vertical to greater depths than they were in Case I (see Fig. 10). The turbulent mixing alone not only overcomes static stability but is also able to mix to a relatively greater depth on the right side of the front. The water that is being transported across the front is apparently immediately mixed by wind stirring as no plume of the warm, less dense water is present on the right side.

The along-front current again forms an ageostrophic component as it undergoes adjustment, and is especially evident on the right side of the front around y=55 km (Fig. 11) where it exists to a greater extent both horizontally and vertically than was seen in Case I. The core of the along-front jet does decrease in speed and diffuse in time. By hour 36 the maximum value of u has been reduced to slightly more than 8 cm/s. The creation of this ageostrophic velocity accompanied by a v-component leads to strong downwelling around y=55 km underneath the front (Fig. 10) and remains
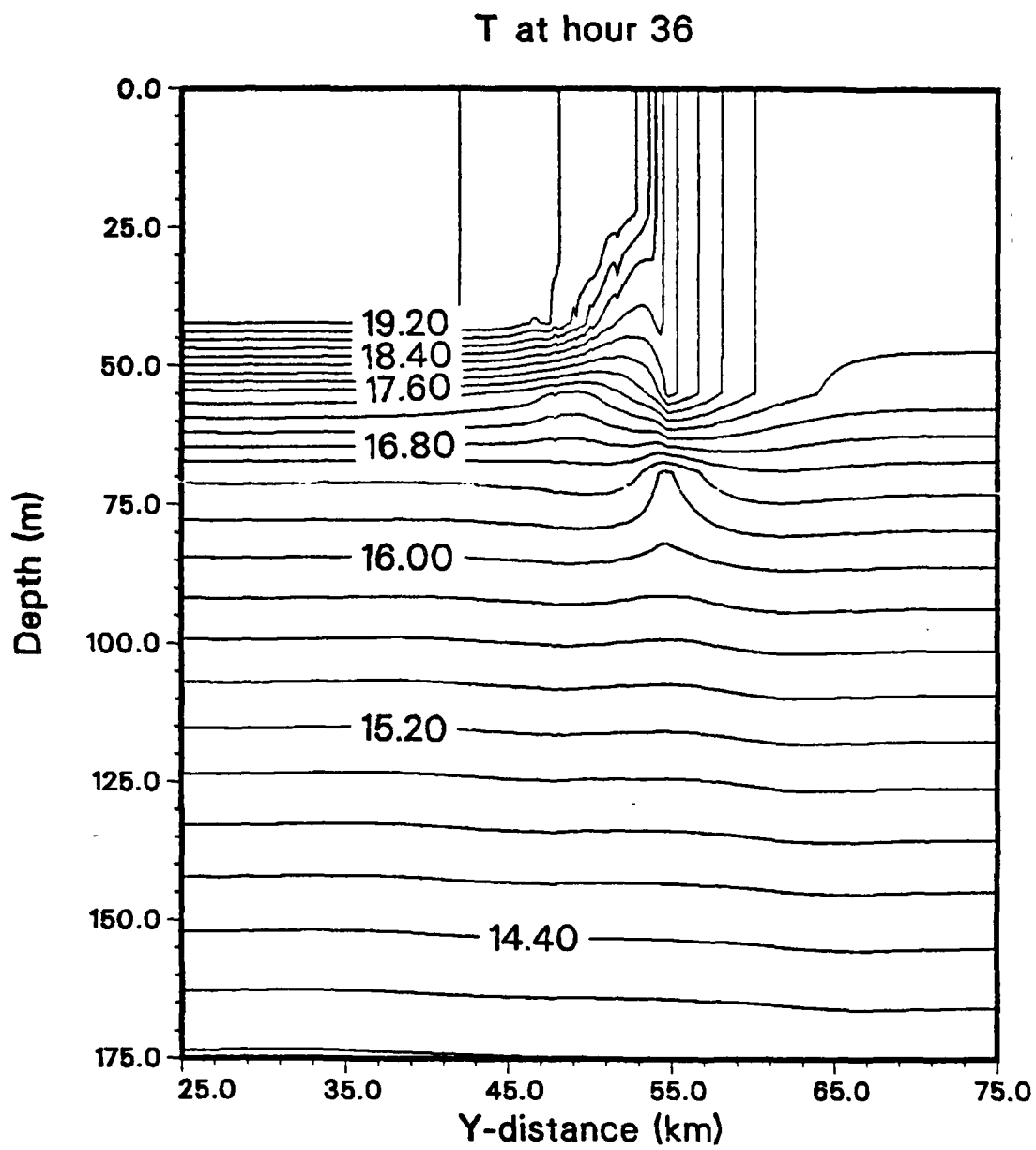
T at hour 36

Figure 10. Front 1 Case II 36-Hour Temperature. Contour interval is 0.2 deg C.

over the 48 hour integration. A strong core of negative across-front velocity of over -6 cm/s is created in this area (Fig. 12), and there is an attendant sharp upwelling in the isotherms at 75 m and wave-like fluctuations present to depths beyond 175 m. In the areas where dv/dy > 0 (dw/dz < 0), downwelling is seen in the front, and where dv/dy < 0 (dw/dz > 0), upwelling is seen. In the surface layer, the v-component is positive and in the direction of Ekman transport. It is concentrated in a jet in the area of the tightest horizontal temperature gradient over the shallow peak in the mixed layer depth. All of these tendencies and trends persist over the 48 hour integration.

A deepening in the mixed layer occurs to the right of the front near y=55 km and progresses outward in time. The shallow peak in the mixed layer depth within the front is mostly preserved, though some erosion and mixing obviously has occurred (compare Figs. 13 and 14). This further supports the hypothesis that minimal cross-frontal mixing occurs. Examination of the corresponding v-fields also show little cross-frontal mixing.

B. SUMMARY -- CASE II

In this case of a forcing of a negative wind stress and no heating, the temperature structure of the front retains a strong horizontal gradient over the 48-hour integration. Diffusion of the front occurs, but it is concentrated at the boundaries of the front. Wind stirring overcomes the static stability of transported water once it crosses the front. The creation under adjustment of a large ageostrophic u-velocity and an accompanying v-velocity give rise to strong upwelling and downwelling features within the front. The shallow peak of the mixed layer depth within the front is preserved over time. The fact that this peak is maintained, the horizontal temperature gradient retains a tight structure, and the v-field is mainly constrained to the ageostrophic areas and surface layer, suggests that interfacial or cross-frontal mixing is minimal.
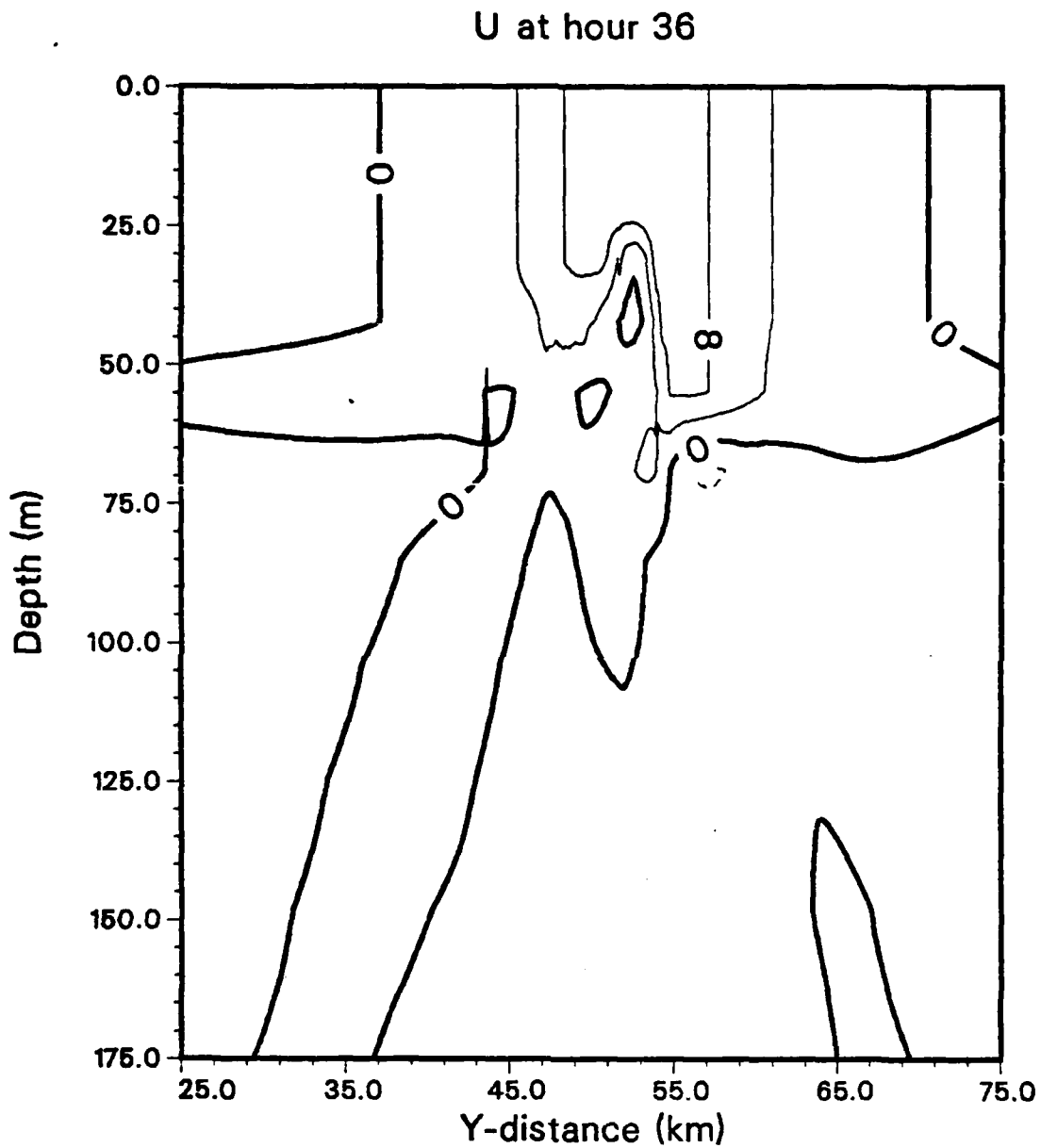
Figure 11.   Front 1 Case II 36-Hour U-Velocity.   Contour
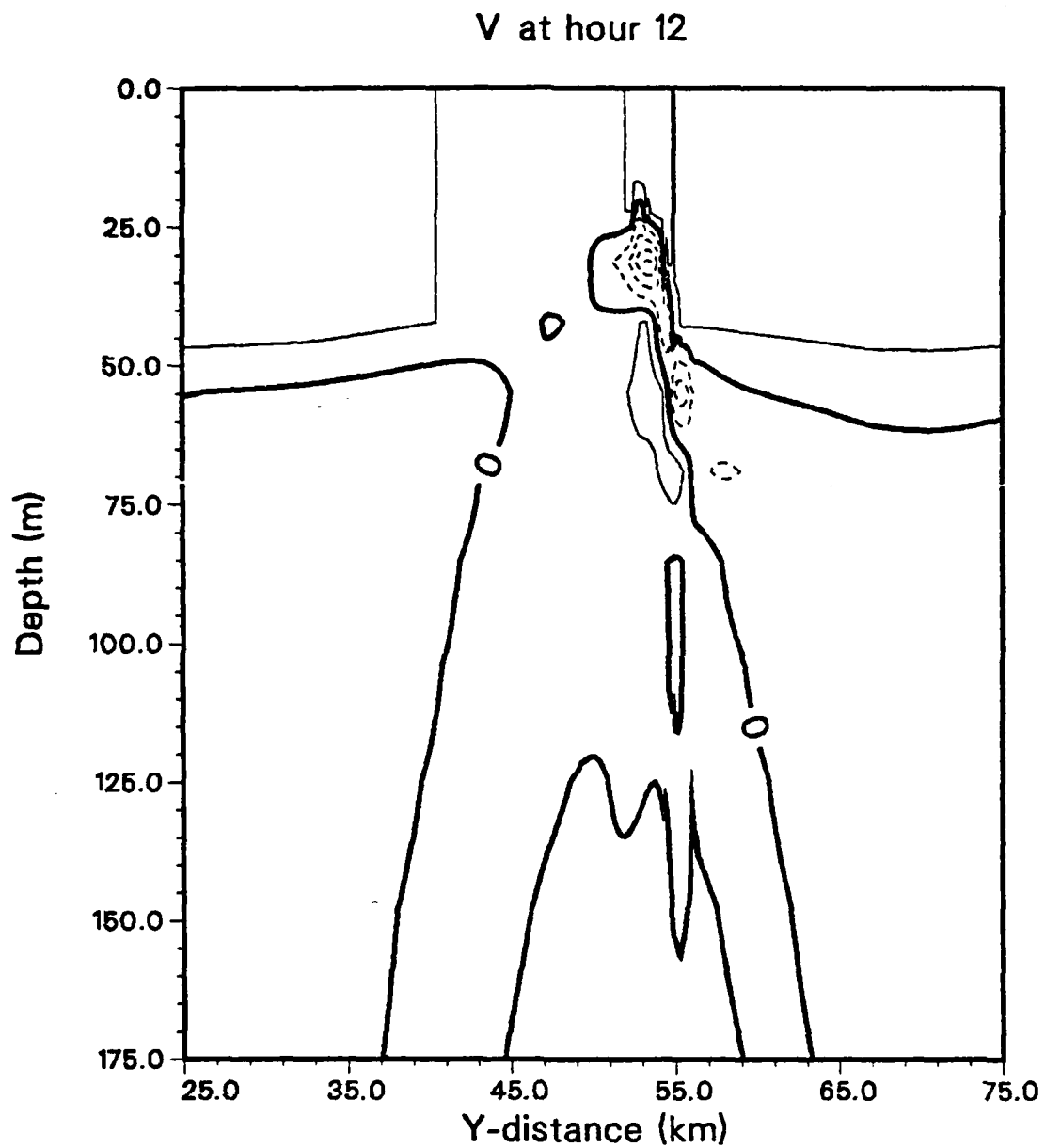   interval is 4 cm/s.

Figure 12.   Front 1 Case II 12-Hour V-Velocity.   Contour
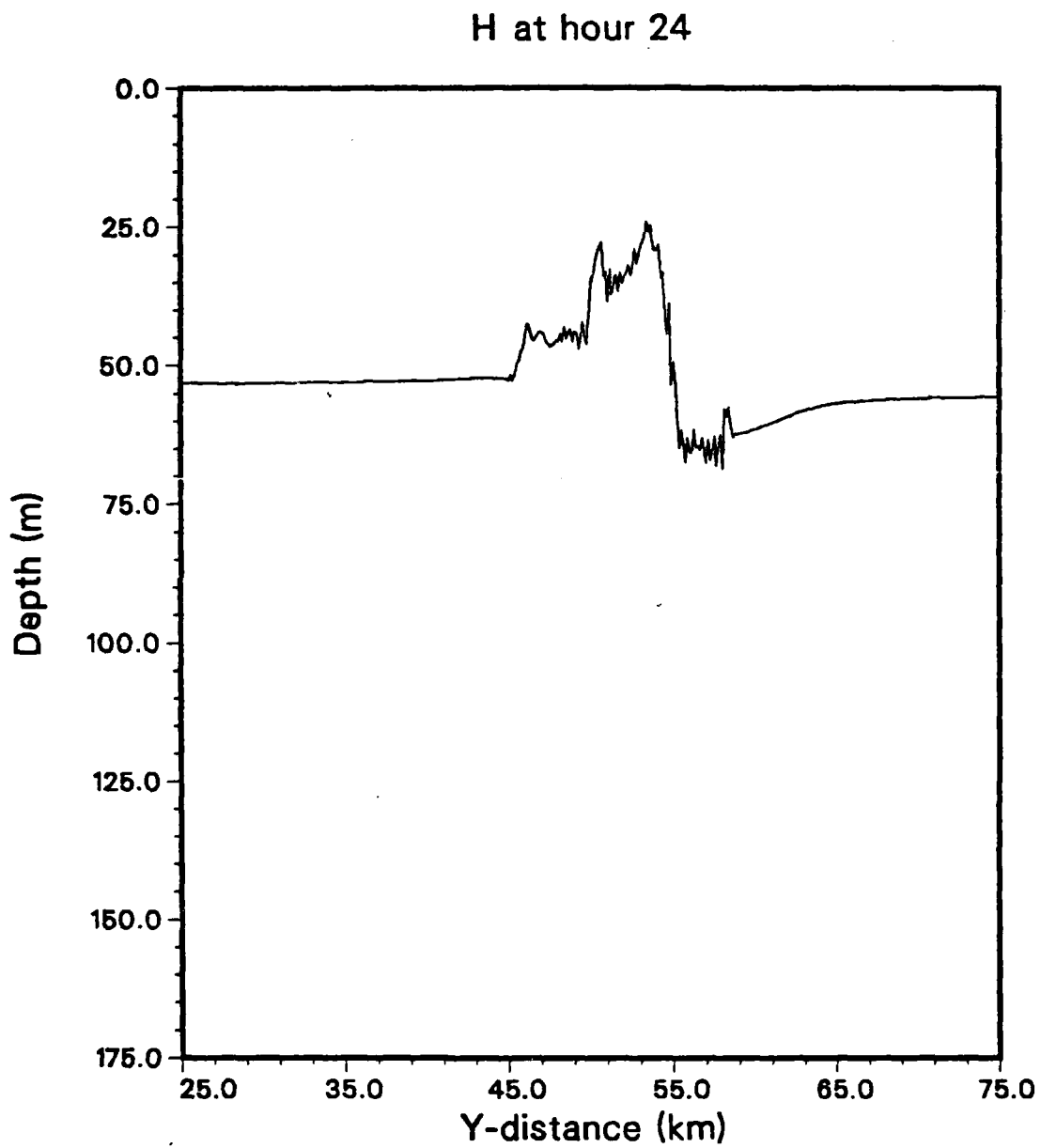   interval 2 cm/s.

H at hour 24

Figure 13. Front 1 Case II 24-Hour Mixed Layer Depth.
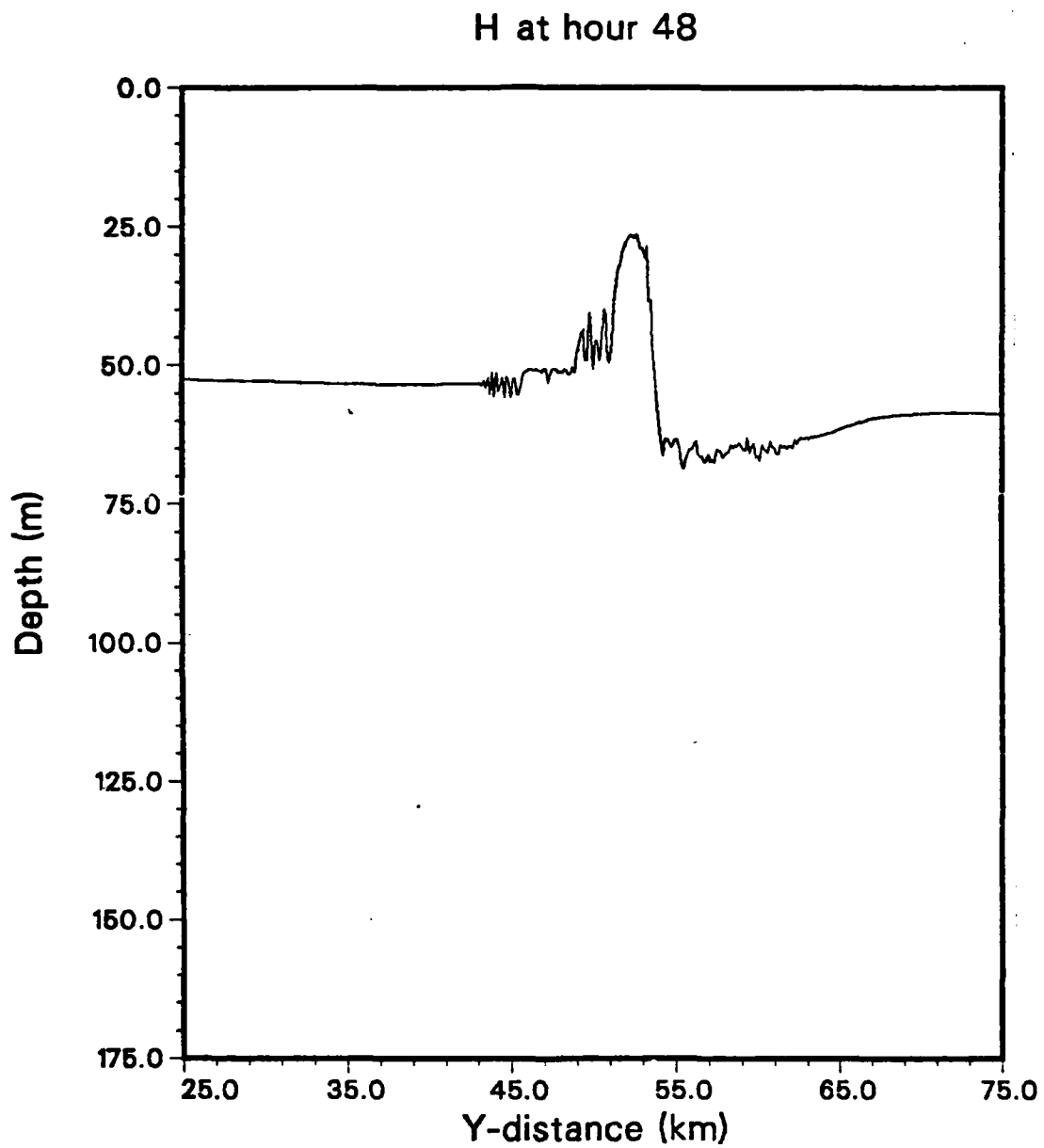
Figure 14. Front 1 Case II 48-Hour Mixed Layer Depth.

V. MODEL RESULTS FOR FRONT 1 CASE III

A. ANALYSIS AND DISCUSSION

A uniform surface heating is applied with the identical
wind stress of Case I. The magnitude of each forcing is
such that influences from both are expected to be mani-
fested. In examining Figs. 15 and 16, the obvious effect of
heating is the adjustment of the temperature structure on
either side of the front. At first examination, it appears
that the heating is having the opposite effect of what is
expected - that is, it appears to cool the mixed layer
rather than warm it. In reality, the heat is carried down
to depths of 50 m and warms the water there. Cooling occurs
between 32 and 50 m depth, which is readily seen in Fig. 17.
Mixing may create a dynamic instability in the thermocline,
and vertical diffusion of heat by $K_T * d^2 T / dy^2$ may cause the
intermediate water to be cooled and the deep mixed layer to
be warmed. This basic structure remains over the 48-hour
integration. The front undergoes diffusion and is advected
to the left, as occurred in Case I. The front is manifested
to a lesser depth in accordance with the heating process -
downwelling and mixing have been moderated by the heating.
Though some wave-like action is seen in the temperature

field beneath the mixed layer, the magnitude is not as great as in the case of wind stress alone. The mixed layer depth has shallowed to about 43 m under heating alone in the areas outside the front (see Fig. 16). This shallowing occurs because the atmospheric forcing (heating and wind) is input as a body force over the entire mixed layer. The heating has the effect of making the mixed layer depth more uniform. The marked deepening in the mixed layer depth that occurred in Cases I and II at the right (cold) side of the front is not present in this case. The deepening of the mixed layer affects the u-field. The ageostrophic u-component does not develop to as great an extent as it did in Case I. The general along-front current appears much as it did in Case I, except that its vertical extent is also constrained by the shallower mixed layer depth. In both cases, maximum speeds agree over the 48-hour integration, and they are advected with the front as it responds to the mass transport.

The v-field follows the same trends as it did under wind stress alone. At 12 hours, v is directed to the left as expected following the transport, and at 24 hours the v-velocity reverses and establishes the layers of concentrated positive v-values centered symmetrically about the mixed

T at hour 12

Figure 15. Front 1 Case III 12-Hour Temperature. Contour
interval is 0.2 deg C.

H at hour 12

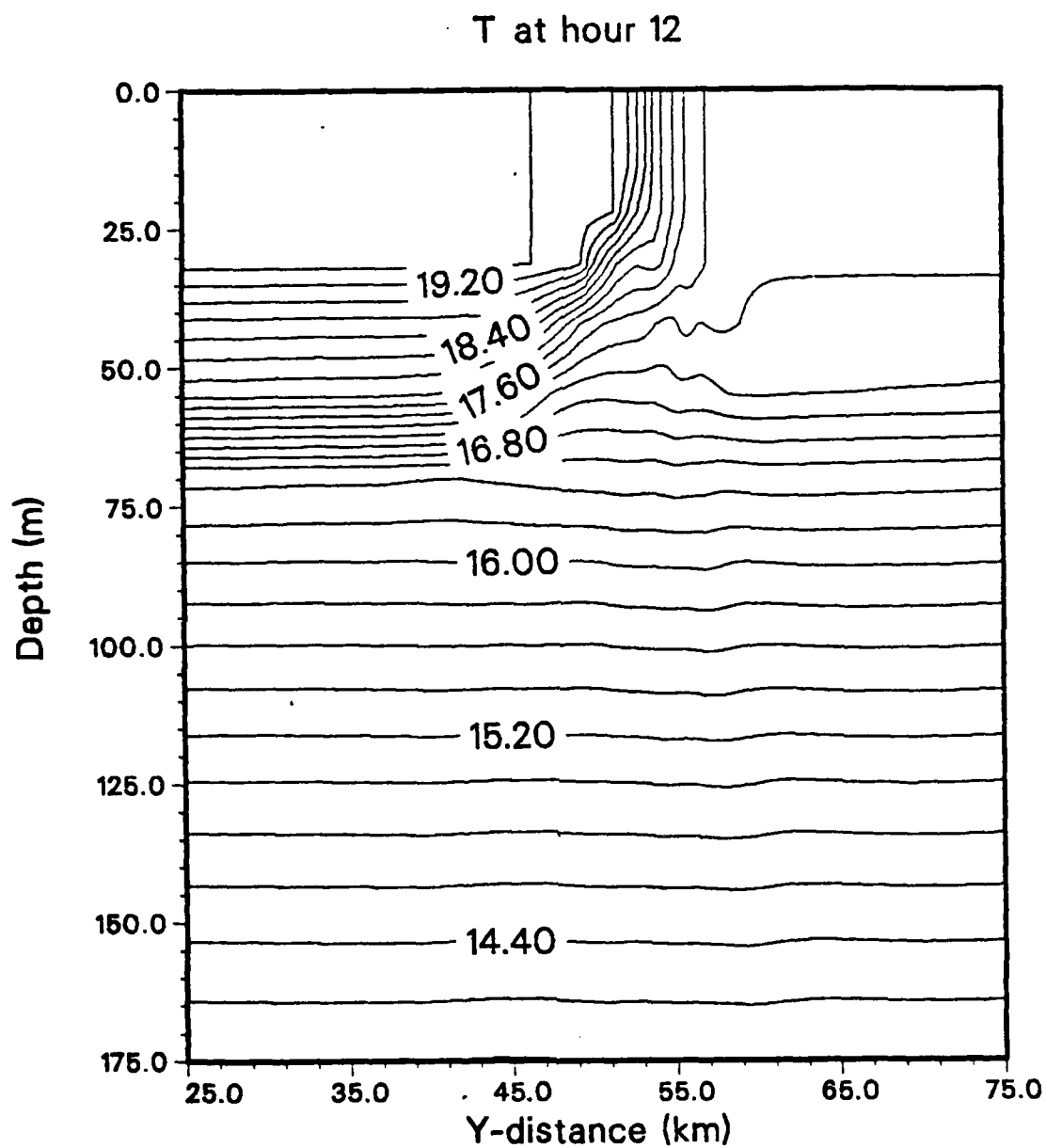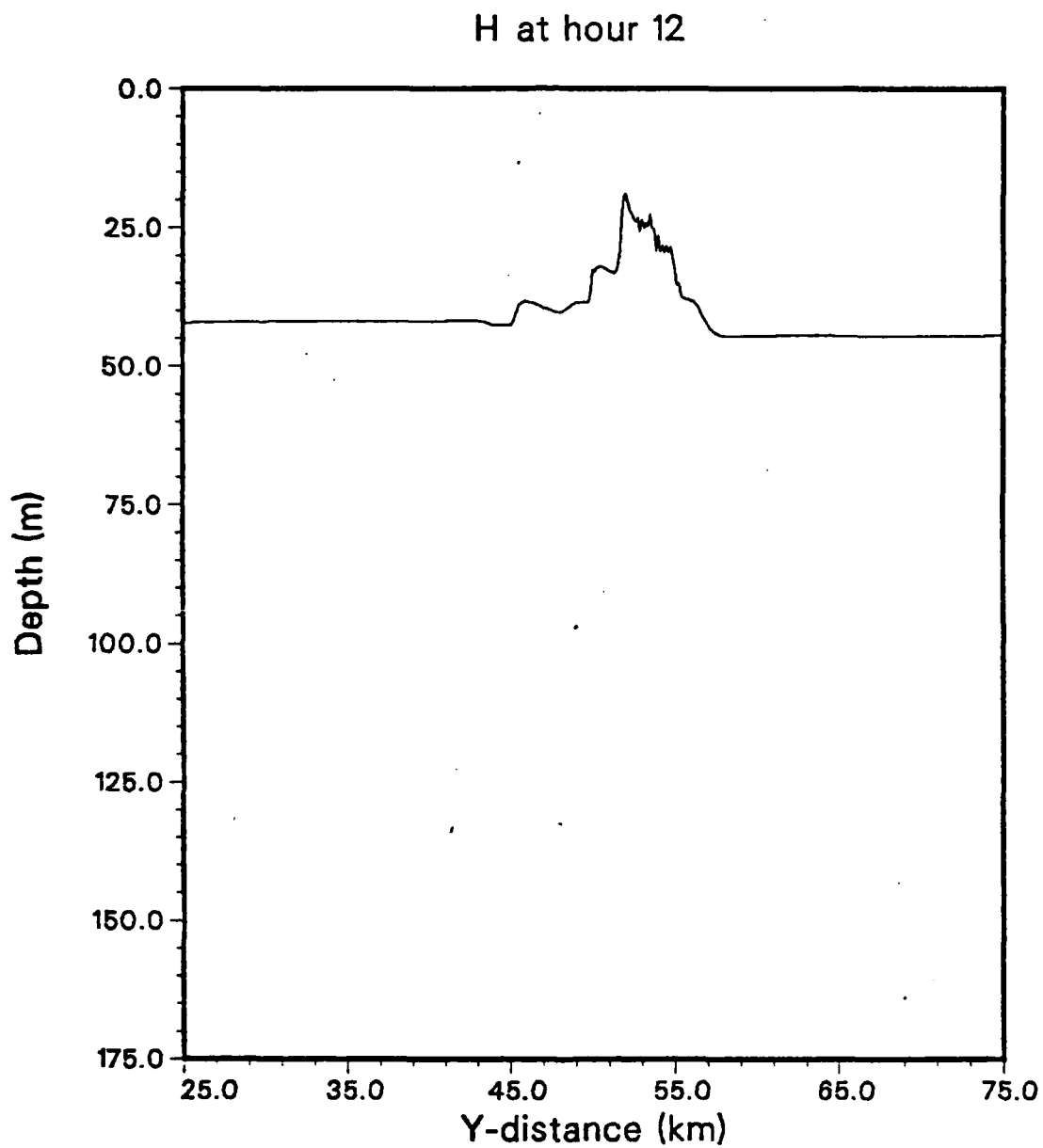Figure 16. Front 1 Case III 12-Hour Mixed Layer Depth.
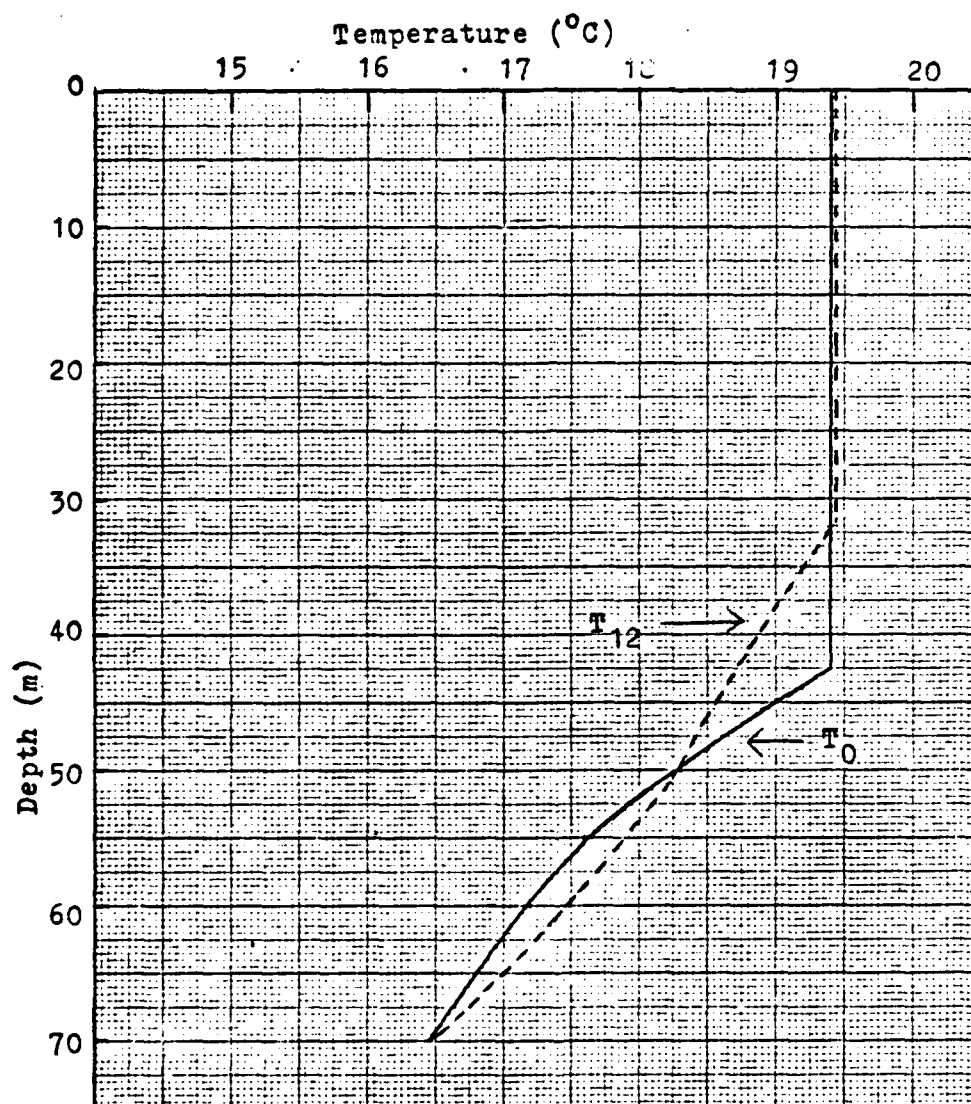
Figure 17. Front 1 Case III - T vs z Profile. Profile taken at y=35 km for t=0 and t=12 hours.

61

layer depth. At 36 hours, v returns to a negative value and at 48 hours, though still negative, v is much decreased in magnitude. Again, cells of positive v-velocities are present at about the mixed layer depth. The across-front velocity does penetrate the front and the shallow peak of the mixed layer (see Fig. 18) which is indicative of cross-frontal mixing. The shallow section of mixed layer itself is eroded and smoothes cut over the 48-hour integration as it did in Case I (Fig. 19).

B. SUMMARY -- CASE III

The effects of both wind stress and heating are clear in this case. The wind stress induces a mass transport to the right, moving cooler, denser water into warmer, less dense water. This water not only upwells and moves over the front, but also moves across the frontal interface. At 24 and 48 hours, the v-field appears to be influenced by inertial oscillations with a reversal in direction occurring in the surface layer at 24 hours and a near-reversal at 48 hours. Cores of positive velocities are established centered about the mixed layer depth outside of the front. The front both diffuses and moves to the left in time.
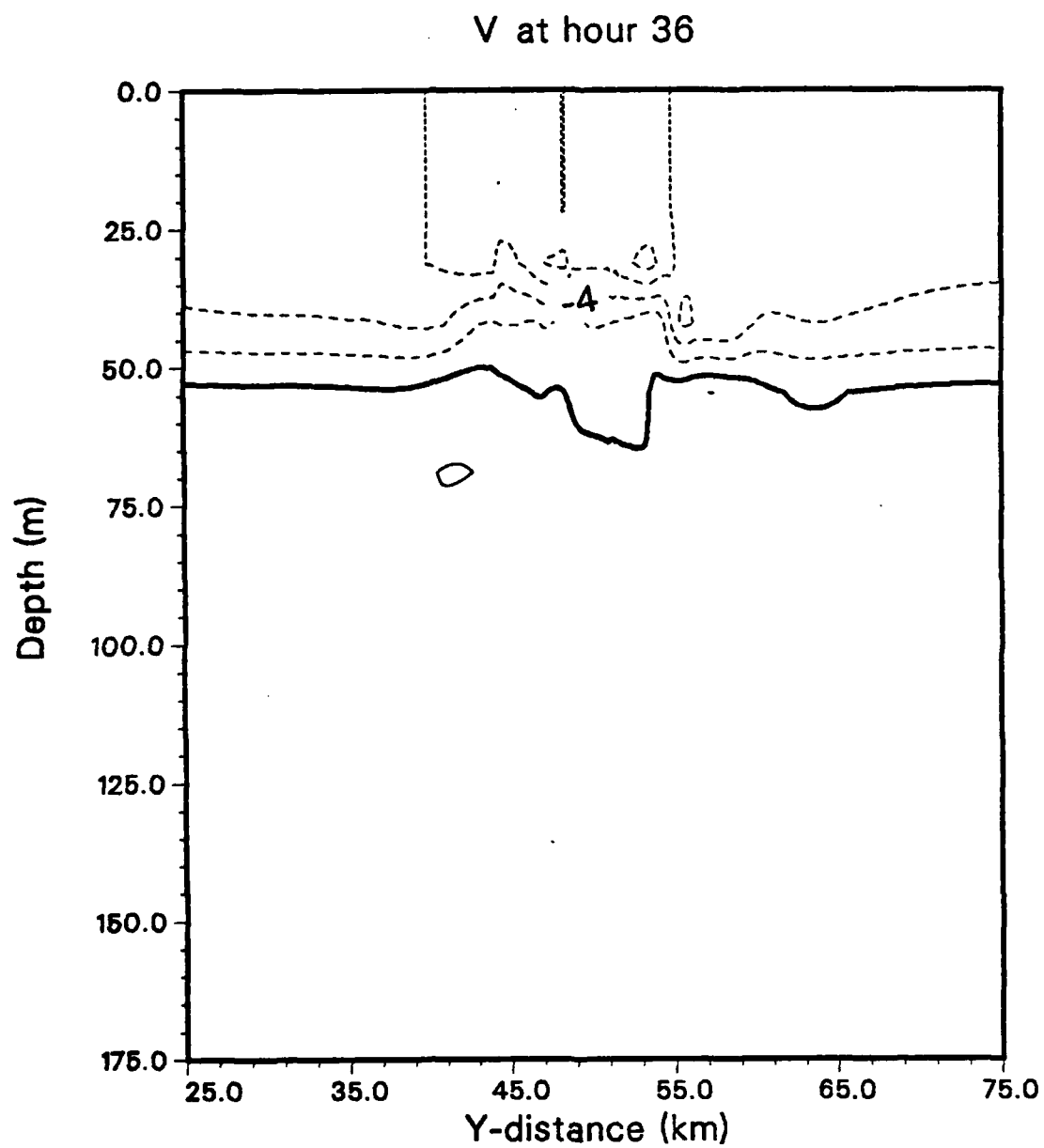
Figure 18. Frcnt 1 Case III 36-Hour V-Velocity. Contour
interval is 2 cm/s.

H at hour 48

Depth (m) vs Y-distance (km)
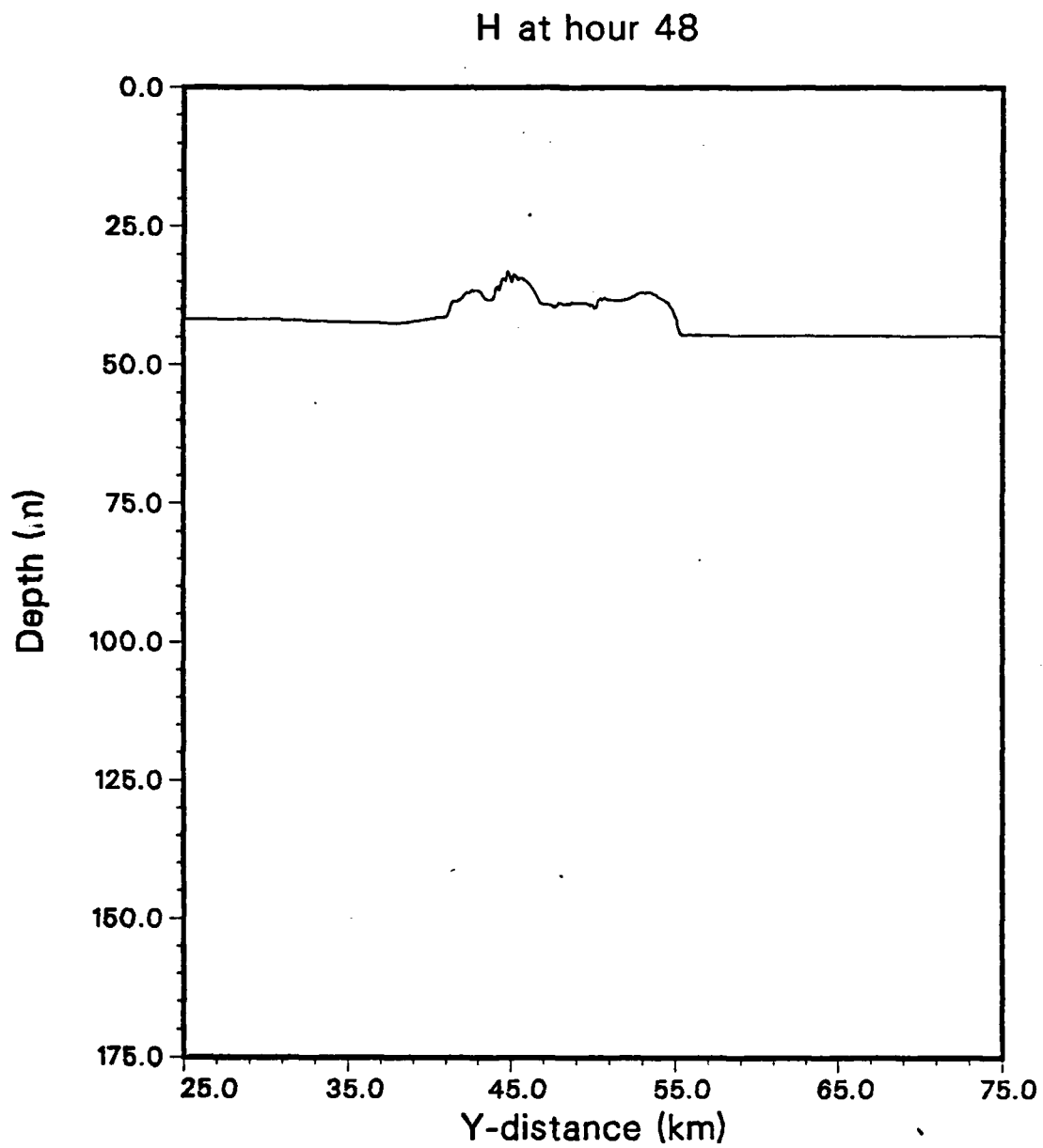
Figure 19.   Front 1 Case III 48-Hour Mixed Layer Depth.

Heating shallows the mixed layer depth as expected, and thereby restricts the vertical extent of the velocity fields. Heating also prevents the immediate deepening of the mixed layer on the right side of the front, which was also seen in both Cases I and II. The heat manifests itself at the initial mixed layer depth where the isotherms become more stratified.

VI. MODEL RESULTS FOR FRONT 1 CASE IV

A. ANALYSIS AND DISCUSSION

Case IV combines a negative wind stress and a uniform
surface heating. The mixed layer shallows noticeably and
heat is carried to the bottom of the mixed layer at depths
of 55 to 70 m as in Case III (see Figs. 20 and 21). The
heating does have an interesting effect when compared with
the wind-stress-only forcing of Case II. The sharp dip in
the isotherms in the middle of the front is not evident here
as it was in Case II. Horizontal diffusion of the tempera-
ture structure occurs more rapidly and attains a gradient of
1.6 deg C/5.6 km by hour 12 (see Fig. 20). The along-front
velocity is limited in its vertical development on the right
side of the front near y=57 km (Fig. 22) and follows both
the horizontal and vertical diffusion tendencies of the den-
sity front. The across-front velocity has a narrow, verti-
cally-oriented core of negative values with a maximum of -6
cm/s on the right side of the front between 25 and 50 m
depth as in Case II. Since this maximum of v-velocity
exists in an area where there is little u-velocity, its

existence cannot be attributed to a response to the ageostrophic u-component. The position of this v-velocity correlates well with the upwelling/downwelling pattern evident in the isotherms in Fig. 20, and also with wave patterns in the isotherms over the entire depth extent in the right half of Fig. 23. We suspect that such a large area of v-component created below the mixed layer is a response to the warming of the water at the initial mixed layer depth which has shoaled, re-oriented the isotherms and created vertical velocity. Furthermore, wind-generated mixing forces vertical motions in the water mass to a great depth, inducing a v-component there.

In this case, the front diffuses horizontally more rapidly than under wind stress forcing alone. The front spreads like a warm, less-dense plume overriding the cool, denser water (compare Fig. 24 to Fig. 20). The along-front current shifts with the front. The mixed layer loses its shallow section within the front and smoothes out, which did not happen in Case II. The peak in the mixed layer was maintained much longer. With heating, there is less of a temperature difference and less of a shallowing from the far-field mixed layers to the shallow mid-frontal mixed

67

T at hour 12
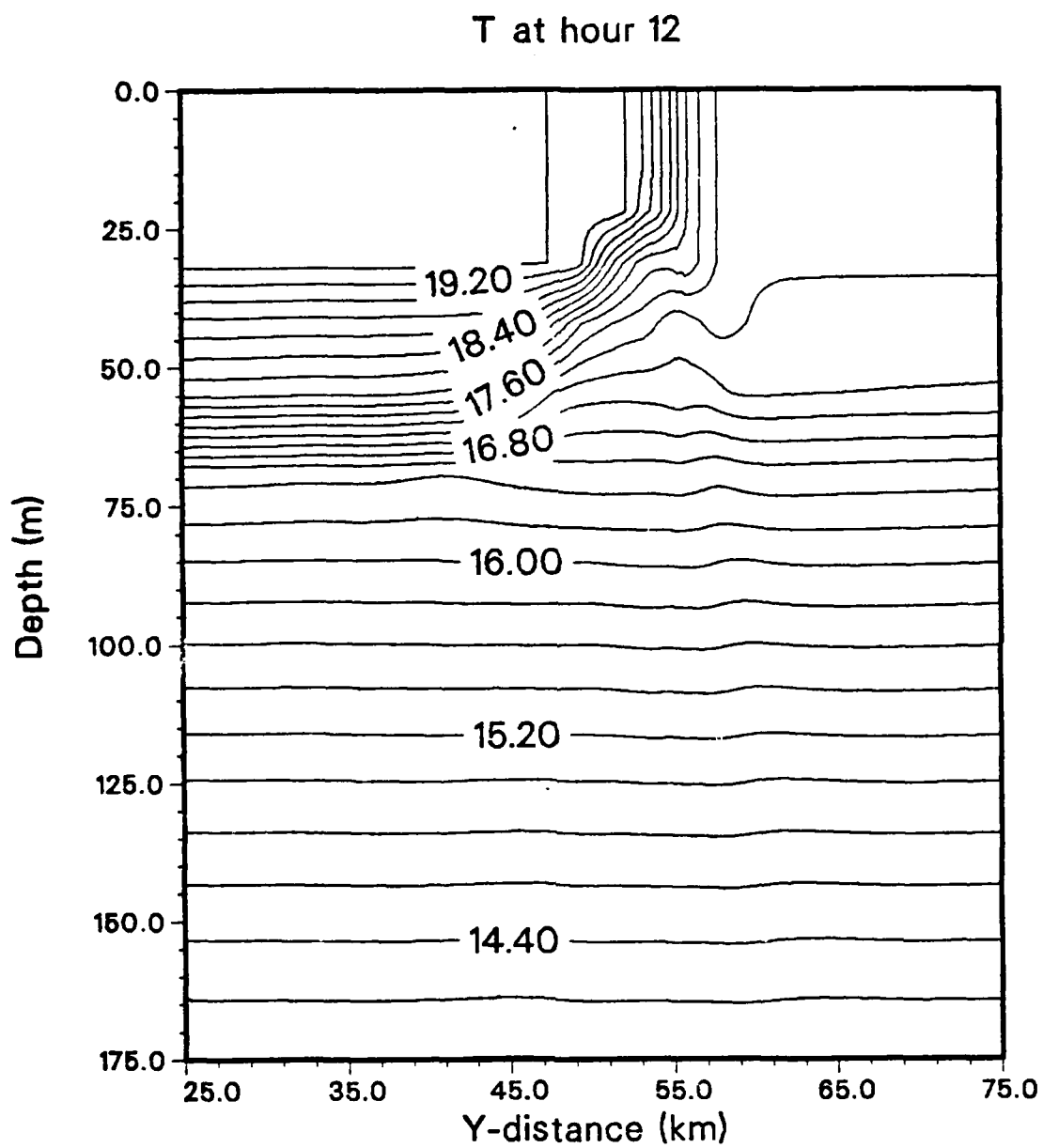
Figure 20.   Front 1 Case IV 12-Hour Temperature.   Contour
interval is 0.2 deg C.

H at hour 12
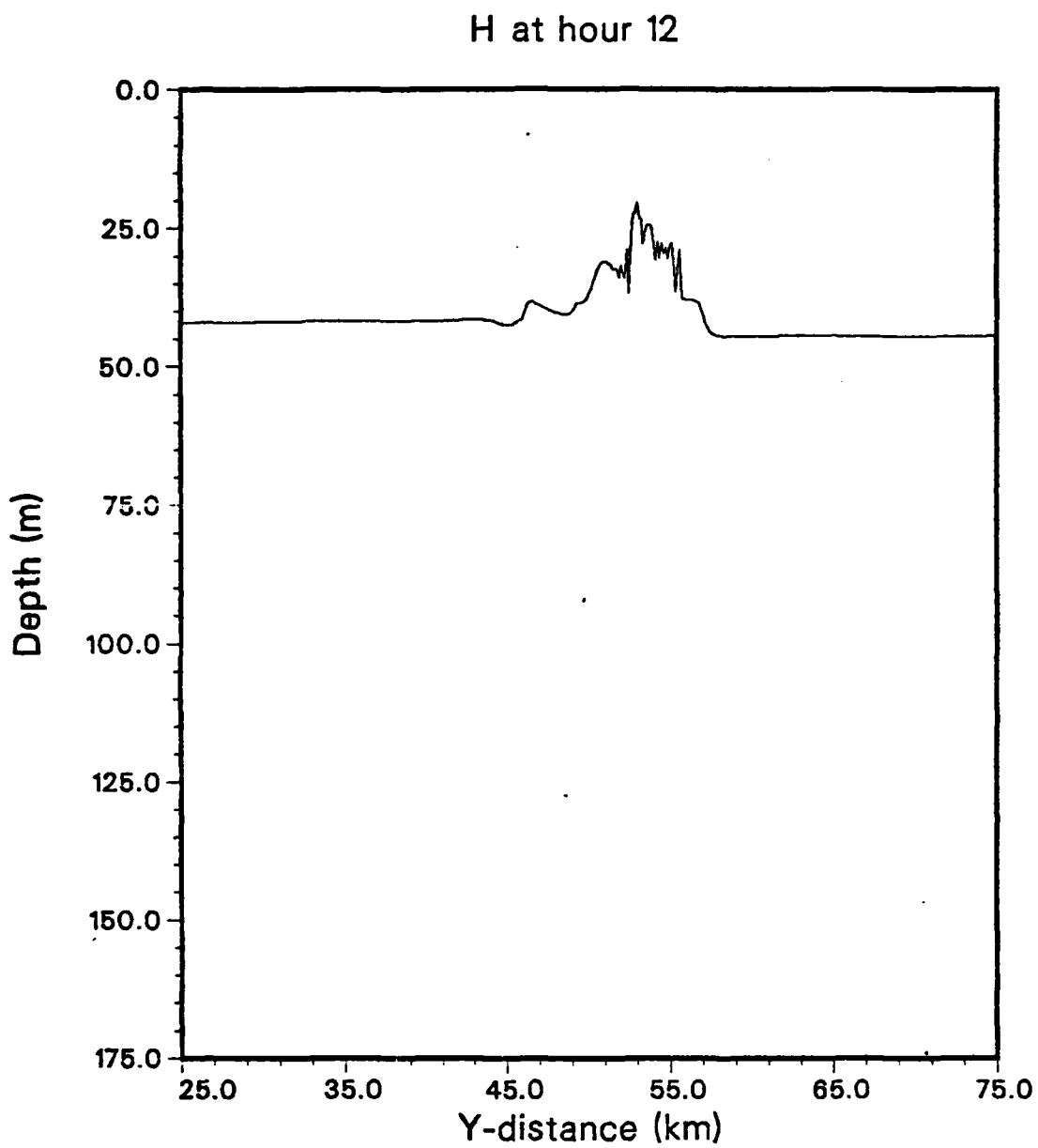
Figure 21. Front 1 Case IV 12-Hour Mixed Layer Depth.

U at hour 12
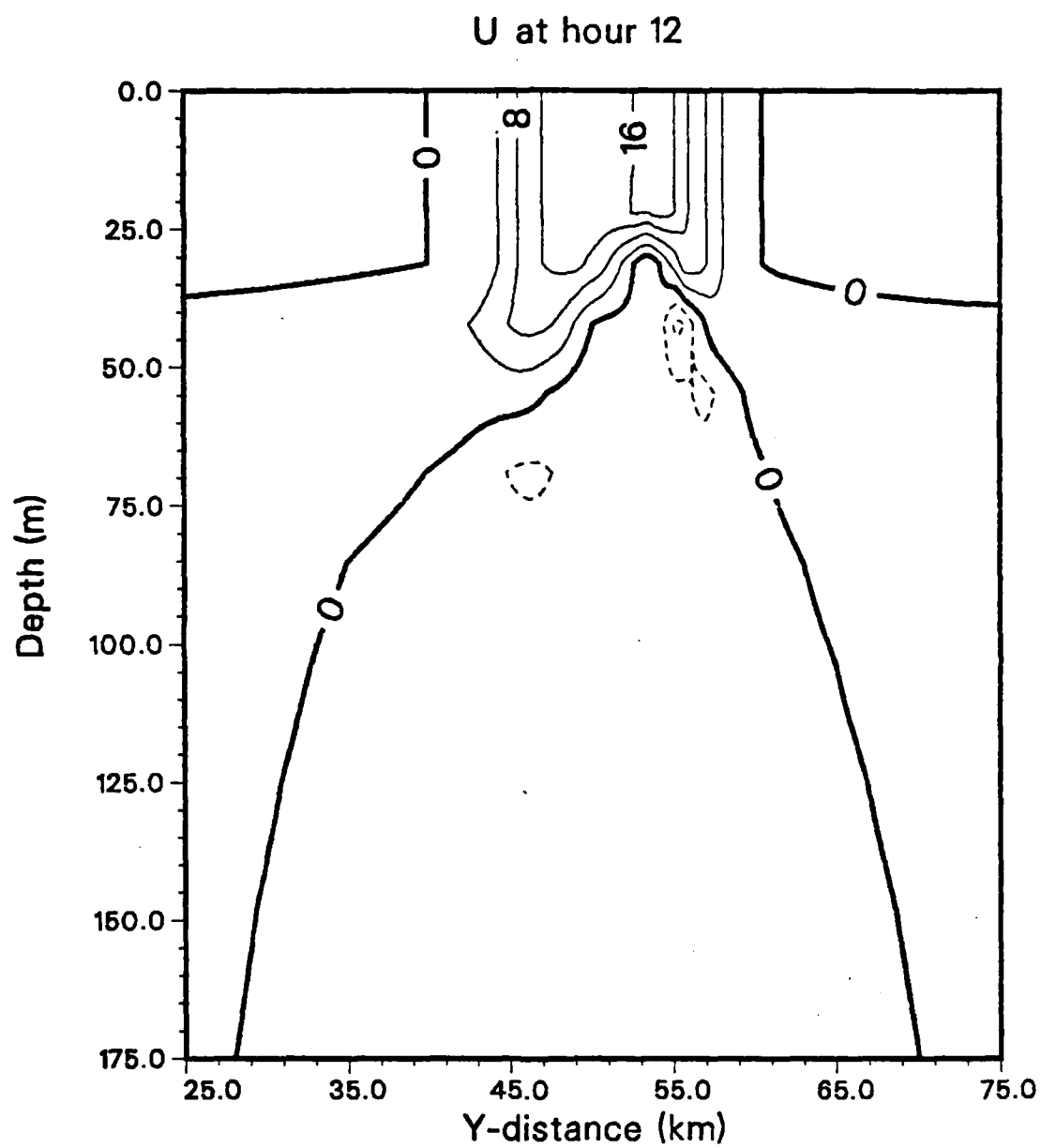
Figure 22.   Front 1 Case IV 12-Hour U-Velocity.   Contour
interval is 4 cm/s.

V at hour 12
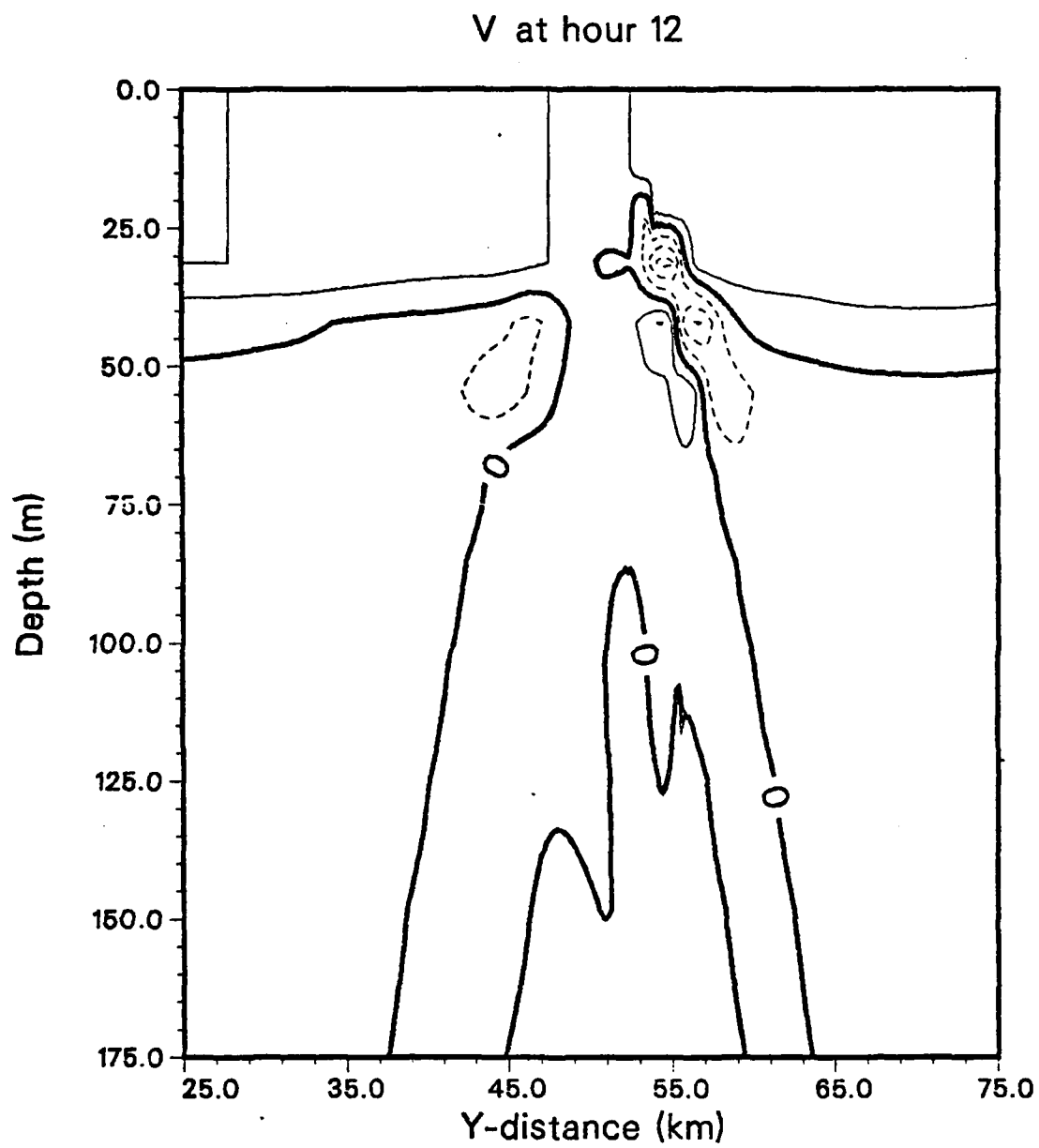
Figure 23. Front 1 Case IV 12-Hour V-Velocity. Contour interval is 2 cm/s.

layer, which probably accounts for the quicker breakdown of the shallow section of the mixed layer.

The v-field in the surface layer is advected to the right, with a maximum value located at the surface within the front. By hour 24, strong horizontal cells of a v-component have formed about the mixed layer depth. In this case, the values are negative, whereas in Cases I and III they were positive. (Case II never formed them.). These cells disappear at hour 36 and reappear at hour 48, as they did in Cases I and III. The mechanism that explains the appearance of negative v values is unclear.

The trends to 48 hours show further diffusion and advection of the warm frontal plume to the right. There is smoothing of the horizontal distribution of mixed layer depth. The surface front patterns of u- and v-velocity are all advected to the right.

T at hour 36
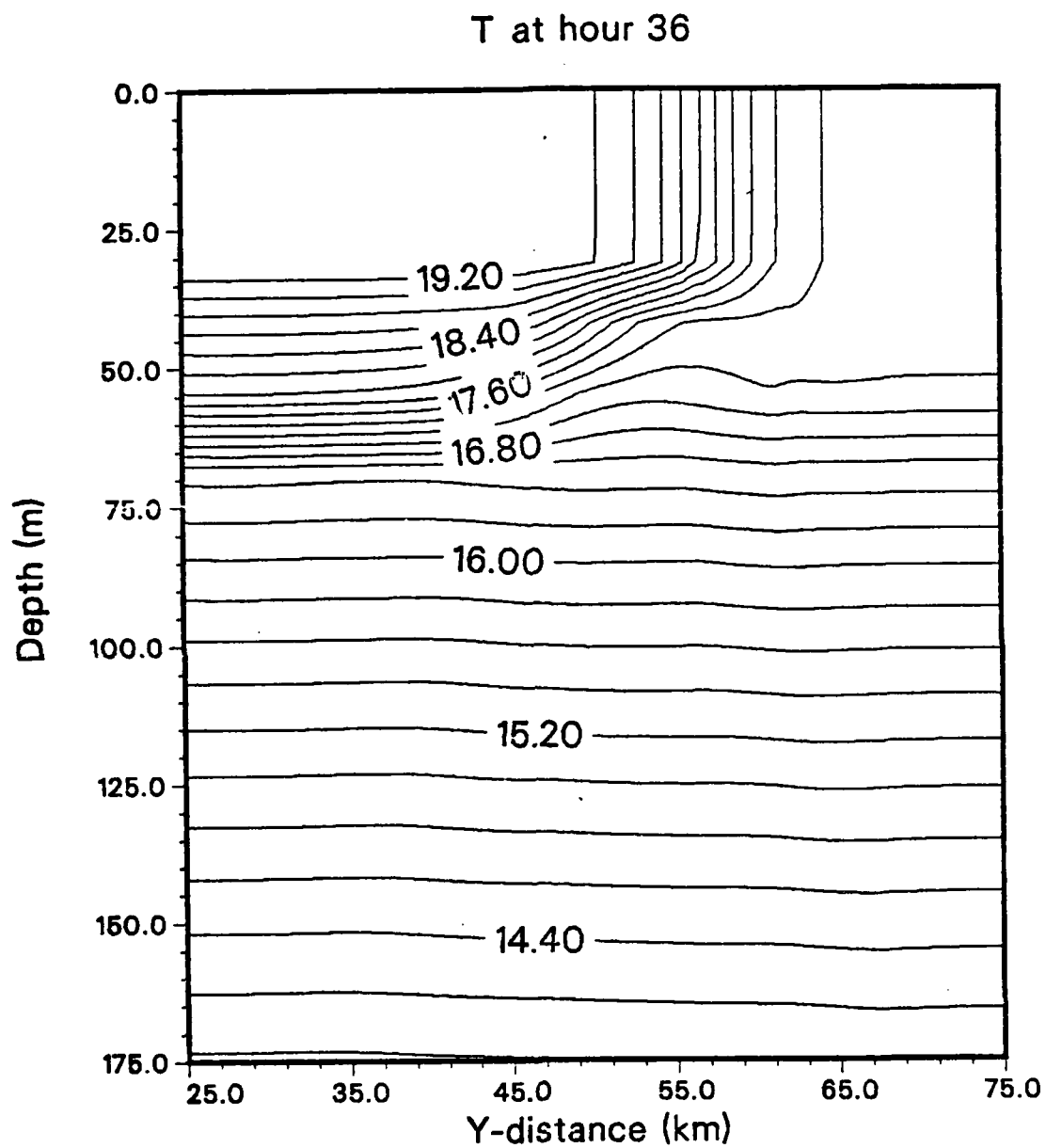
Figure 24. Front 1 Case IV 36-Hour Temperature. Contour interval is 0.2 deg C.

B. SUMMARY -- CASE IV

Application of a negative wind stress and surface heat-
ing results in the front moving as a warm overriding plume
to the right. The mixed layer initially shallows due to the
heating, and over the 48 hour integration breaks down and
smoothes out in the horizontal. The along-front velocity is
advected and diffused in the mixed layer.   The pattern of
across-front velocity shifts to the right in the surface
layer, with its maximum value centered over the shallowest
portion of the mixed layer. A v-component develops to quite
a great depth on the right side of front due to motion gen-
erated by heating and turbulent mixing.   Cells of negative
v-component are formed at hours 24 and 48 which are centered
about the mixed layer depth.

VII. MODEL RESULTS FOR FRONT 2 CASE I

A. ANALYSIS AND DISCUSSION

The initial conditions for Front 2 are shown in Figs. 4, 5, and 6. The front extends throughout the depth of the basin and is oriented such that warmer, less dense water is on the right and cooler, denser water is on the left. Many of the dynamical features of Front 1 are expected to be repeated for Front 2. In comparing Front 2 to Front 1, the horizontal axes are oppositely-directed to the frontal orientation. The thermocline slopes upward in the positive y-direction for Front 1, but downward for Front 2.

The wind stress of Case I applied to Front 2 creates a transport directed to the left. Warmer, less dense water moves towards the cooler, denser water. In this case, diffusion in the temperature field is present for the duration of the integration. The horizontal temperature gradient remains large (1.0 deg C/1.2 km) in the middle of the front with the majority of the diffusion occurring at the right boundary. Mixing on the cool (left) side of the front extends from the surface to 135 m which is below the initial

depth of the mixed layer.   Results of downwelling are seen

at the left frontal boundary, near y=42 km.   Apparently,

there is no chance for a stable, overriding warm plume to

develop before it is mixed into the ambient cool water pool.

These phercmena in the temperature field were also seen in

Case II for Front 1.   Much more dramatic oscillations occur

in the isctherms, primarily on the right side between 53 km

and 70 km,   where the entire field is inclined.   They are

also visible cn the left side superimposed upon an inclina-

ticn of the entire field sloping downward to the right (Fig.

25).   The isctherms show a definite trend towards becoming

more unifcrmly inclined beneath the mixed layer across the

entire horizcntal expanse, with the steeply-inclined field

on the right beccming more horizontal.   Downwelling causes

the left side to slope dcwnward to the right and upwelling

lifts the isotherms on the right side.

The mixed layer depth undergces major changes over the

entire domain.   On the left side,   it deepens to where the

depth in the far field is approximately 125 m (Fig.   26).

Since this deepening occurs by 3 hours of integration, such

a drastic deepening probably resulted from the initial mixed

layer depth being inserted at too shallow a depth in this

T at hour 36
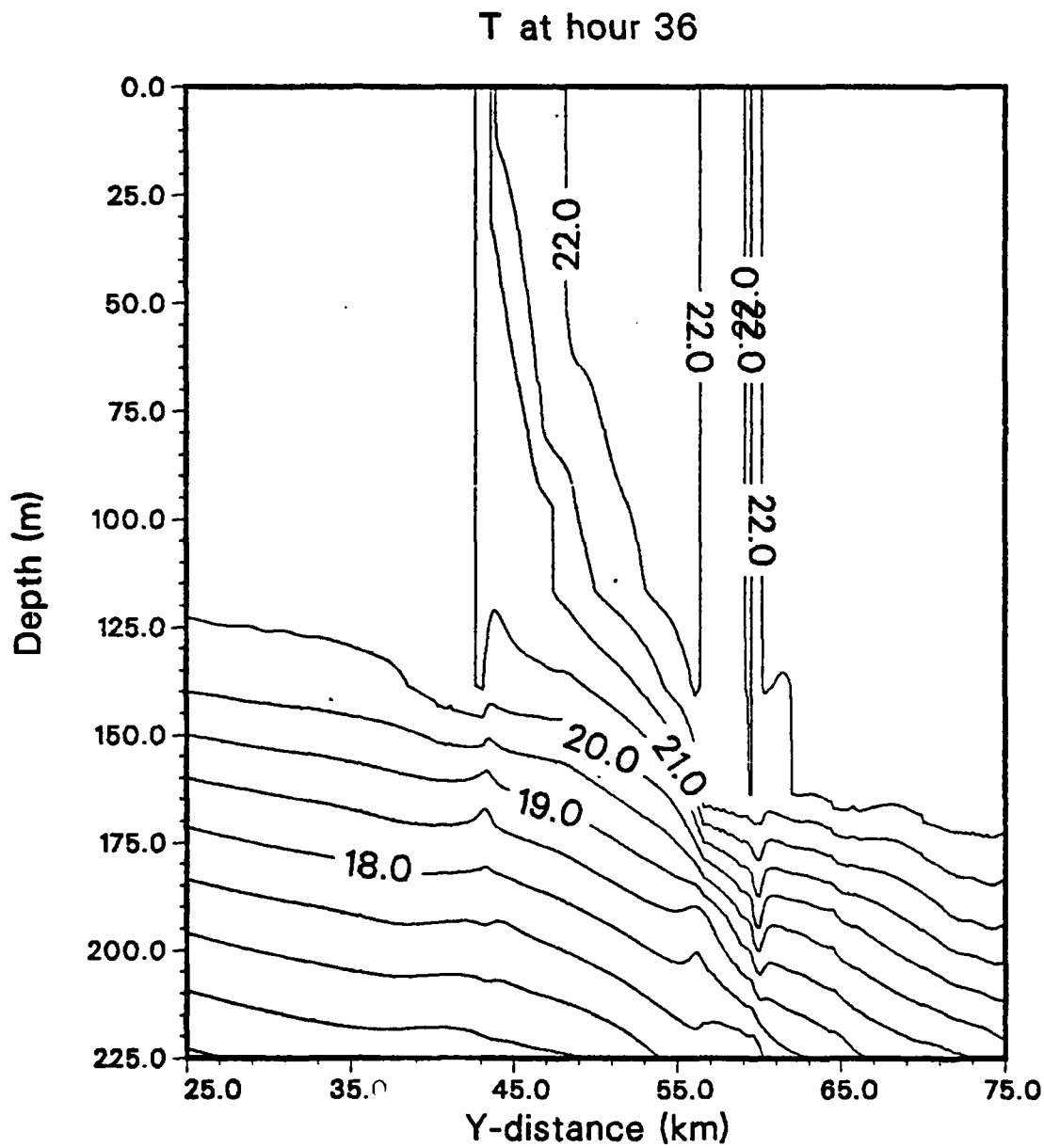
Figure 25.   Frcnt 2 Case I 36-Hour Temperature.   Contour
interval is 0.5 deg C.

area. As in Front 1 Case II, a downward bulge in the mixed layer extending to 155 m occurs at the left frontal boundary at y=43 km (Fig. 26). In this case, the downward bulge does not correspond to the side on which the waters would tend to "back up" prior to crossing over the front as in Front 1 Case I. As strong mixing is implied by the vertical orientation of the isotherms at that location, the bulge is believed to be associated with a cooling of the waters in that area as a result of enhanced vertical mixing caused by the ageostrophic along-front velocity shear (Fig. 27). Within the front, a shallow peak in the mixed layer depth is maintained at the left boundary, though over time it does deepen slightly and erode through mixing. There is much variability in the mixed layer depths on the right side of the front, but it appears that the general trend is for deepening to occur in the far field beyond y=55 km (Fig. 26).

Along with the isotherms, the along-front u-velocity diffuses and decreases its maximum speed over time. As already seen, an ageostrophic component forms on the left frontal boundary and stimulates mixing there. The remnants of a tight horizontal velocity gradient are seen after 48

H at hour 36
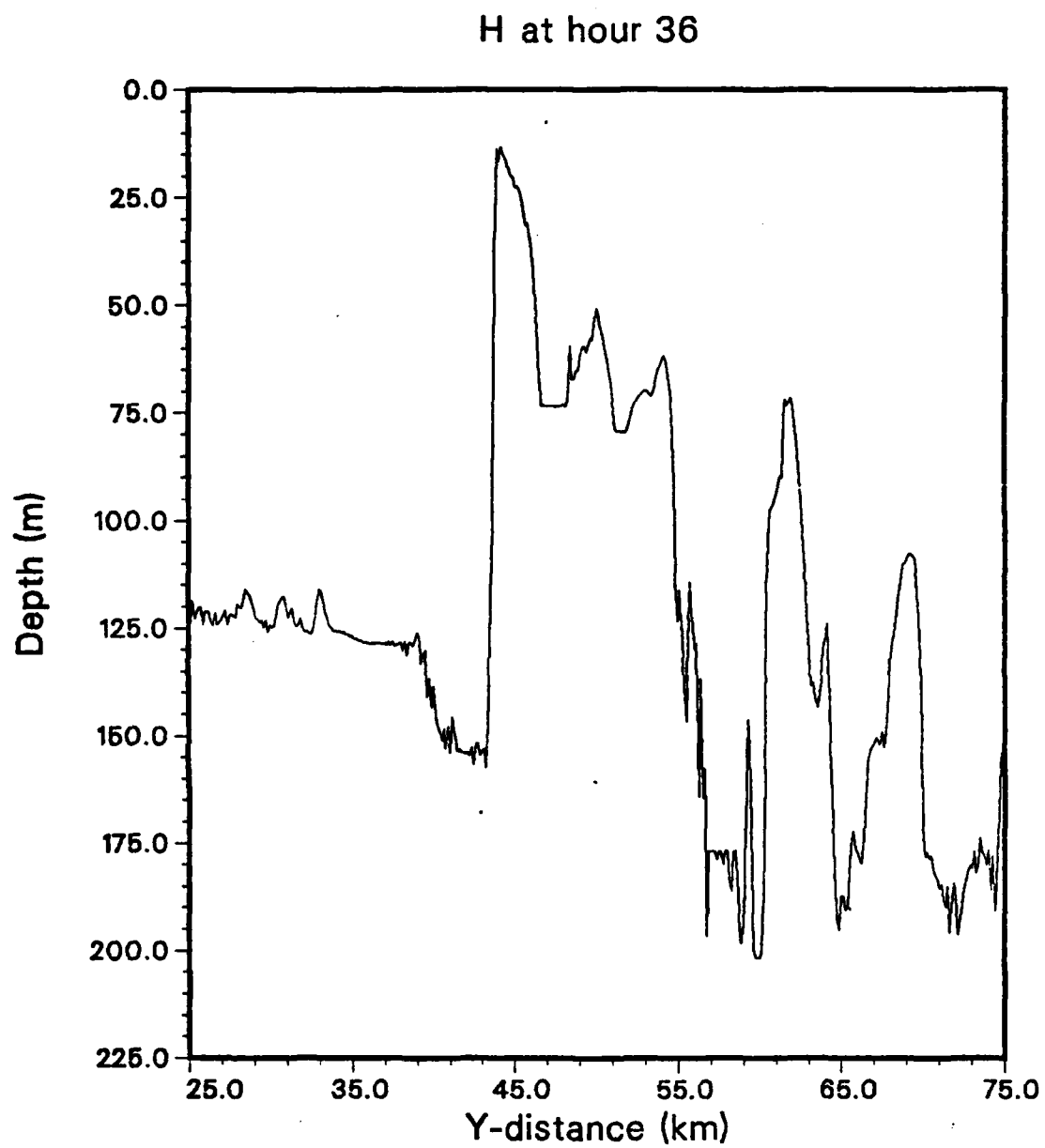
Figure 26. Front 2 Case I 36-Hour Mixed Layer Depth.

U at hour 12
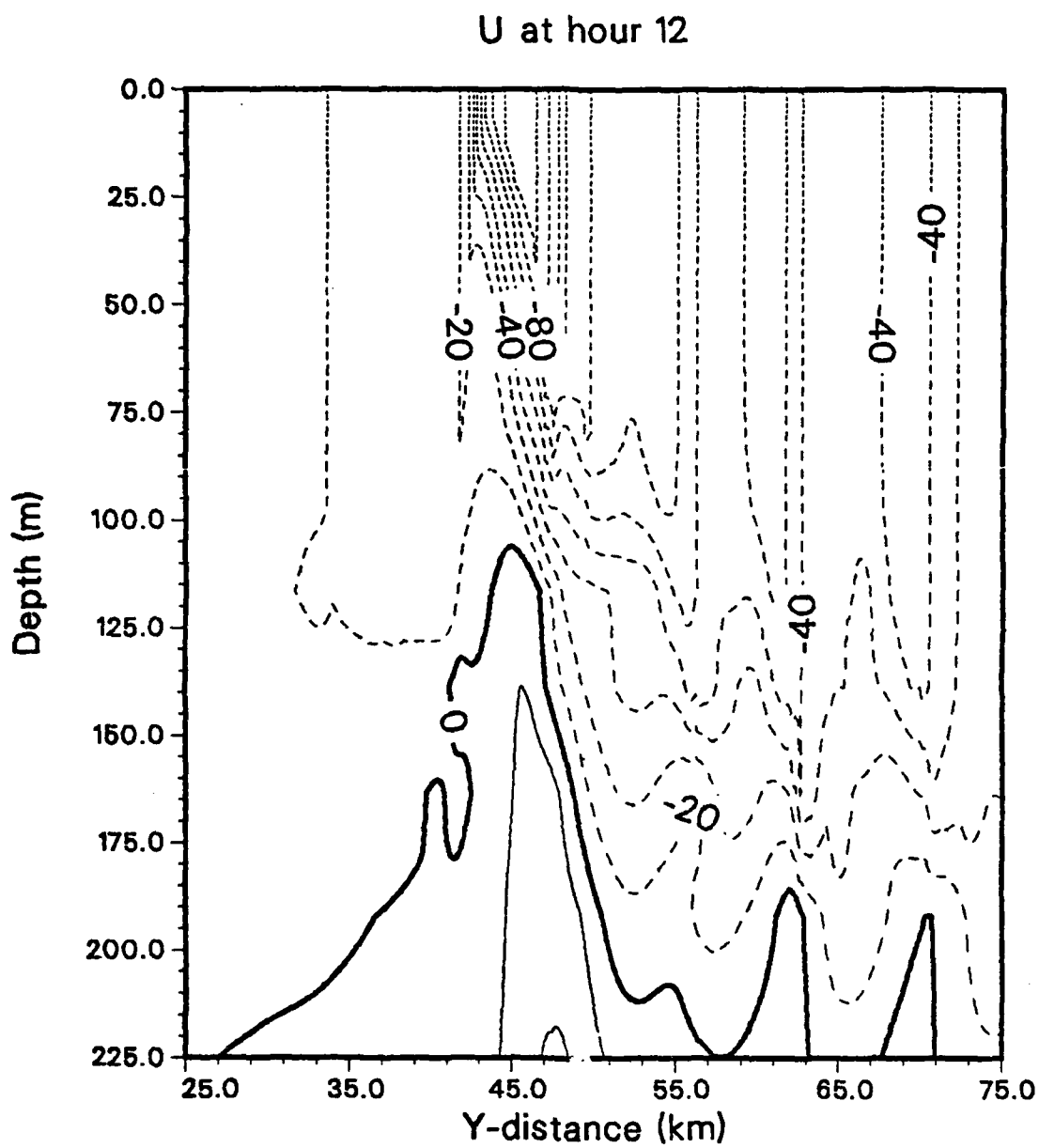
Figure 27. Front 2 Case I 12-Hour U-Velocity. Contour interval is 10 cm/s.

hours, though little or no advection of the along-front cur-
rent occurs in response to the wind-generated transport.
Wave-like oscillations appear to propagate along the deeper
extremities of the u-field, but no phase relation between
isotachs or with other fields is readily apparent.

The across-front v-velocity does correlate with the
direction of transport up through hour 9. An oscillatory
pattern exists in the v field over the 48-hour integration.
At hour 12, the entire v-field is positive, but this may be
a response to the ageostrophic u-velocity, and it is strong
enough to overcome the across-front transport velocity. At
24 hours, v is in the direction of transport and a maximum
of -20 cm/s appears at the surface within the front over the
shallowest section of mixed layer depths at y=43 km (Fig.
28), and remains through hour 36. This is reassuring as it
was expected that the inherent static stability of the water
masses would minimize deep cross-frontal mixing, similar to
what was seen in Front 1 Case II. The isotachs very defi-
nitely terminate at the left boundary of the front, but they
also exist beneath the mixed layer and do cross the front
beneath the mixed layer. At hour 48, v is positive again,
perhaps due to inertial actions. It is proposed (though it

is certainly not as clear as it was for Front 1) that
cross-frontal mixing, though inhibited, occurs here to a
greater extent than it did for Front 1. The majority of the
mass transport appears to exist in the mixed layer and
passes over, rather than through, the shallow mid-frontal
depth of the mixed layer. The reasons for the variations
between the fronts may be due to the greater u-component
(both in speed and in areal coverage) present with Front 2.

B. SUMMARY -- CASE I

Several complexities have been incorporated into the
modeling of Front 2. First, the isotherms slope downward to
the right over the entire right half of the basin. Hence,
the front not only exists at the surface but is "connected"
through the depth of the basin. This establishes an initial
u-velocity which exists over the same area. Adjustment to
the wind stress may not be confined solely to the upper few
meters, as dynamic responses may be transmitted to depths
beyond those directly affected in the surface layer. Also,
the mixed layer depth is artificially inserted as an initial
condition, and may not be the most perfect fit to the temp-
erature field. Though this mixed layer configuration may
exaggerate or suppress actual features, it is nevertheless
felt to be a reasonable approximation of an actual front.

82

V at hour 24
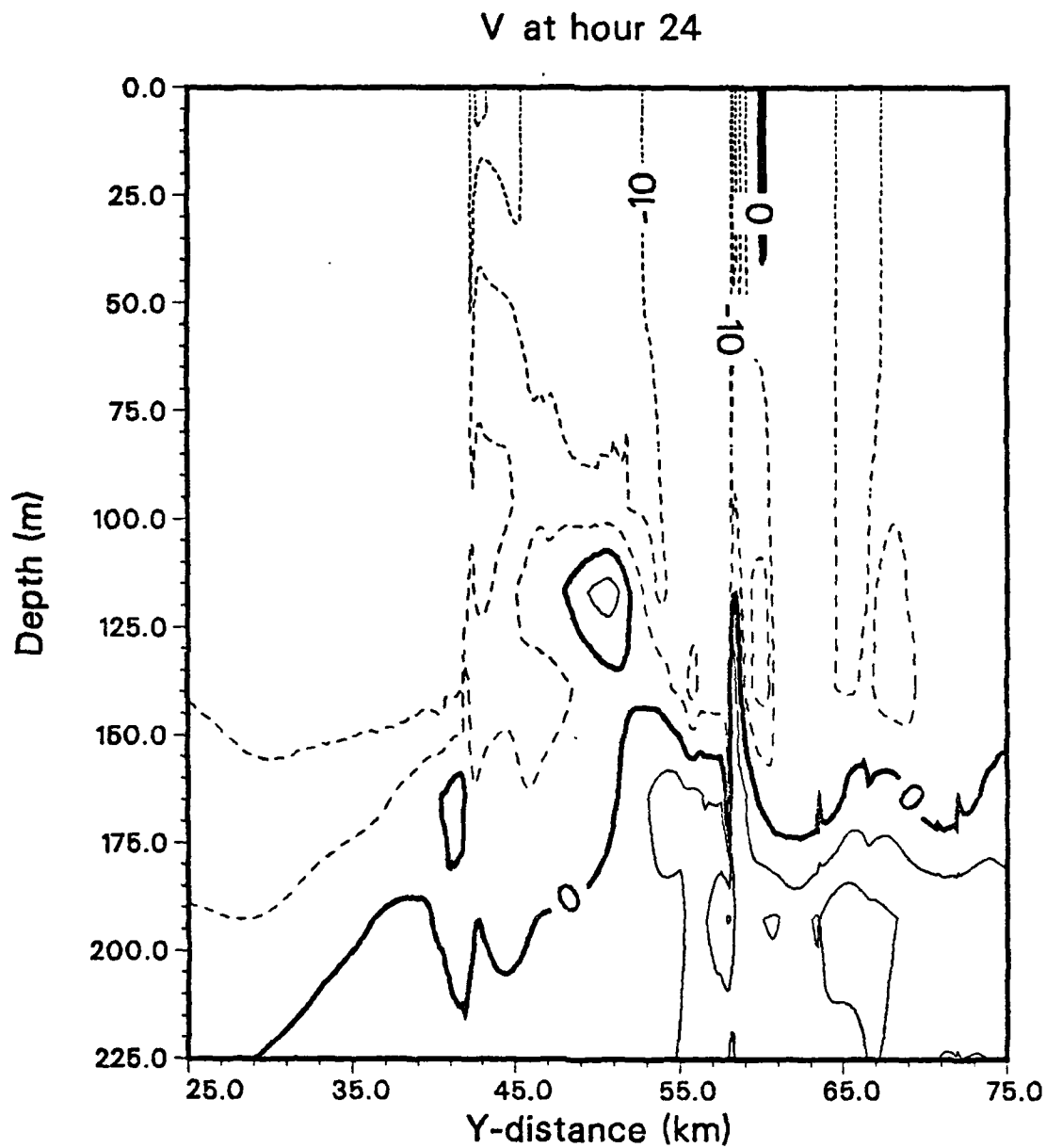
Figure 28.   Front 2 Case I 24-Hour V-Velocity.   Contour
interval is 5 cm/s.

The responses are much more complicated in structure in Front 2 than they were in Front 1. Beyond 12 hours, the front shows little advective response to the mass transport. One reason this occurs is because the front exists over such a great depth. The original thermal structure and temperature gradient are maintained in the middle of the front, with horizontal diffusion occurring primarily at the right boundary. Mixing in the surface layer occurs as the isotherms become vertical to greater depths over time. At the left boundary of the front, downwelling is quite evident and the waters mix easily due to the creation of an ageostrophic u-component which enhances the wind stirring. Wave-like oscillations are evident in the temperature field beneath the mixed layer, and the entire deep temperature field becomes more uniform in slope over the 48-hour integration.

The mixed layer depth must be considered in three separate regimes - left side, frontal, and right side. On the left, the mixed layer depth increases by almost 50 m at the frontal boundary, where mixing is enhanced due to the influence of the ageostrophic current. The mixed layer bulges downward, then rises sharply to its shallow peak at the front. This shallow section remains throughout the 48 hour

integration though it does deepen slightly due to mixing. On the right side, the mixed layer deepens and becomes more horizontal though there are strong fluctuations over intervals of 4 km and less.

Two primary trends are observed in the along-front u-velocity: 1) the u-component diffuses in time, still retaining its basic shape but decreasing in speed and horizontal gradient; 2) an ageostrophic component is evident, primarily extending outwards from the left boundary of the front and which is believed to "drive" the downward bulge in the mixed layer there.

The across-front velocity component is concentrated at the surface in the direction of transport between 0 and 9 hours and at 24 and 36 hours. The front poses no barrier to the v-velocity at 12, 24, or 48 hours. The 36-hour fields are the only ones which have essentially no cross-front velocity component other than in the surface layer. Because the initial horizontal temperature gradient is preserved in the middle of the front, and because the shallow portion of the mixed layer depth is still evident after 48 hours, suggest that little cross-frontal mixing occurs.

VIII. MODEL RESULTS FOR FRONT 2 CASE II

A. ANALYSIS AND DISCUSSION

With the wind stress opposite from that of Case I, the
net Ekman transport is left to right, and cooler, denser
water will be transported toward warmer, less dense water.
There are similarities here to the results of Front 1 Case
I. The front becomes much more diffuse at the surface and
the horizontal temperature gradient is not preserved as it
was in the preceding case (see Fig. 29). It has decreased
to 1.5 deg C/6.4 km. The horizontal field on the left side
reorients by inclining down to the right, and the inclined
field on the right becomes more horizontal. The total
effect is to make the temperature field more level beneath
the mixed layer. Wave-like fluctuations are also seen in
the isotherms (Fig. 29). Vertical mixing can be readily
seen to have occurred within the front by the steep slope of
the isotherms.

The mixed layer depth immediately adjusts in the left
far field to around 125 m as it did in Case I, but a much
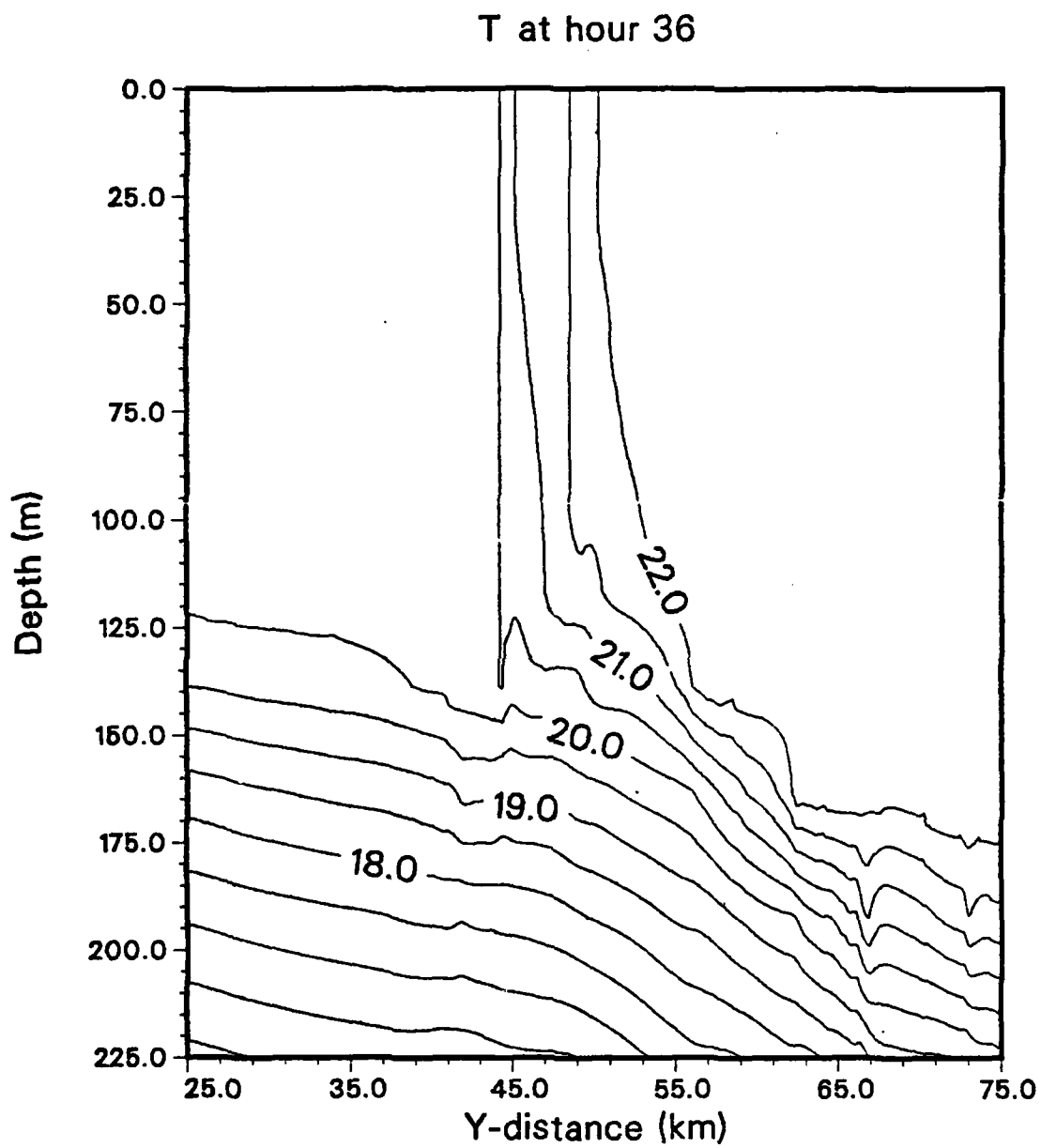greater downward bulge in the mixed layer forms at the left

T at hour 36

Figure 29. Front 2 Case II 36-Hour Temperature. Contour
interval is 0.5 deg C.

boundary of the front around y=42 km and remains over the 48 hour integration (Fig. 30). This result is consistent with the interpretation proposed for Front 1 Case I, where the shallower mixed layer within the front acted as a barrier to mass transport, causing the transported water to "back up". The mixed layer peak within the front deepens and erodes. The right side far field is again variable but shows the same tendencies to deepen.

The ageostrophic u-velocity (not shown) is very similar to the isotach pattern which evolved for Case I. A core of maximum velocity is advected to the right which correlates with the advection of the front. The biggest difference is that the isotachs appear at a greater depth just inside the left frontal boundary.

The expected direction of the across-front velocity is left to right, the direction of the net Ekman transport. As in Case I, a wave oscillation is evident. At 12 and 48 hours this is clearly so, with the velocity field existent along the entire section of the front from the base of the front at around 150 m up to the surface (Fig. 31). The maximum velocity occurs at a depth beneath the shallow mid-frontal section of the mixed layer, which seems to
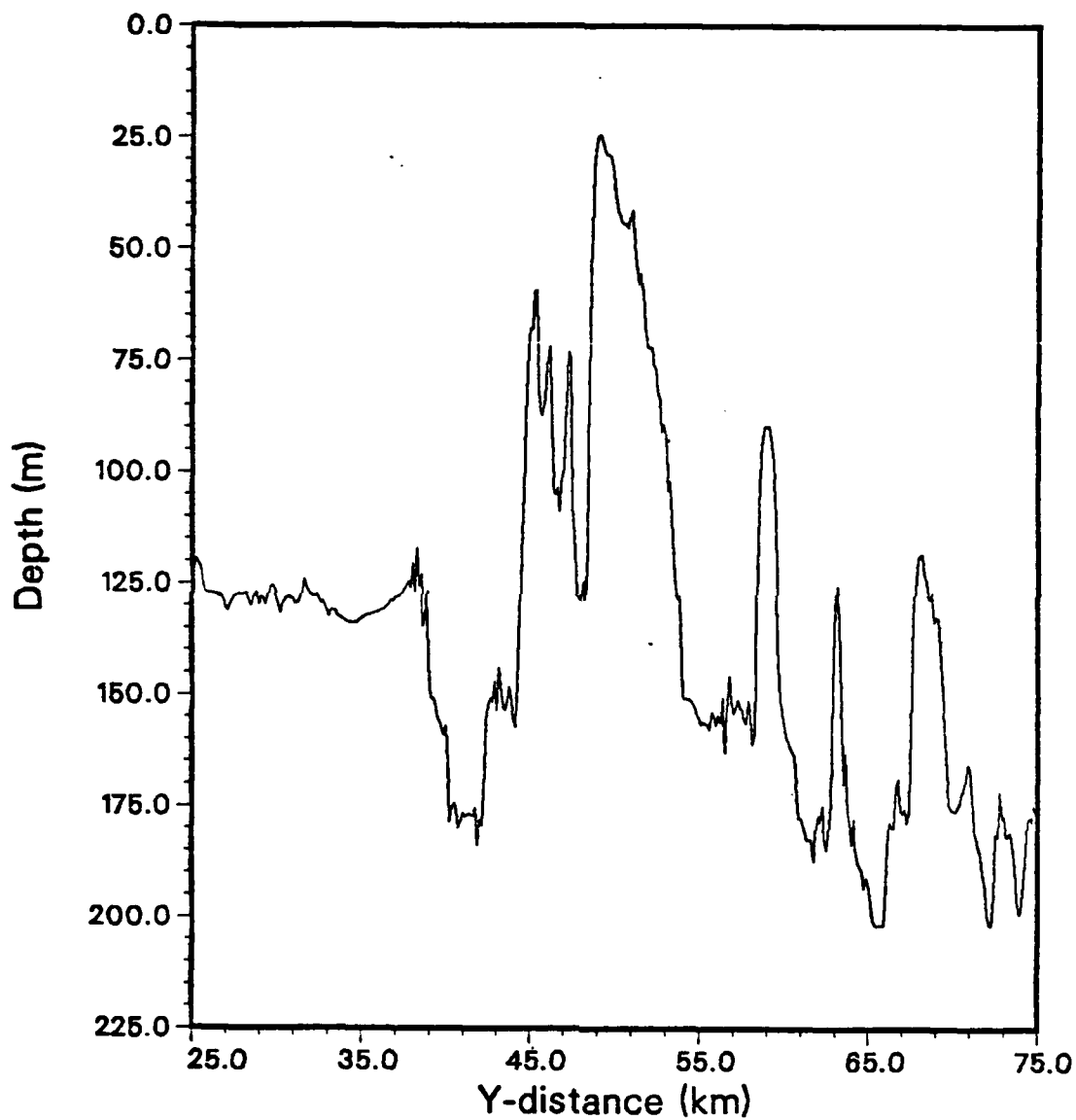
H at hour 48

Figure 30. Frent 2 Case II 48-Hour Mixed Layer Depth.

contribute to cross-frontal mixing, erosion of the mixed layer depth within the front, and weakening of the frontal horizontal temperature gradient. At 24 hours, the v-velocity field is reversed, and negative velocities predominate in the front and beneath the mixed layer. Inertial motions probably account for this reversal.

B. SUMMARY -- CASE II

The temperature structure of the front shows vertical mixing and horizontal diffusion occurring over the 48-hour integration. The horizontal temperature gradient is decreased due to the effect of convective mixing of the cooler water which is transported to the warmer water by wind stirring. The across-front velocity patterns penetrate the mixed layer within the front and establish cross-frontal mixing. The entire temperature field in the vicinity of the front undergoes an adjustment which inclines all the isotherms downward to the right in a rather uniform pattern.

The mixed layer undergoes major adjustment over the 48-hour integration, but the primary trends are a deepening on both sides of the front, a leveling off on the right side and a breakdown of the shallow section within the front due to mixing and diffusion. By extrapolating the processes
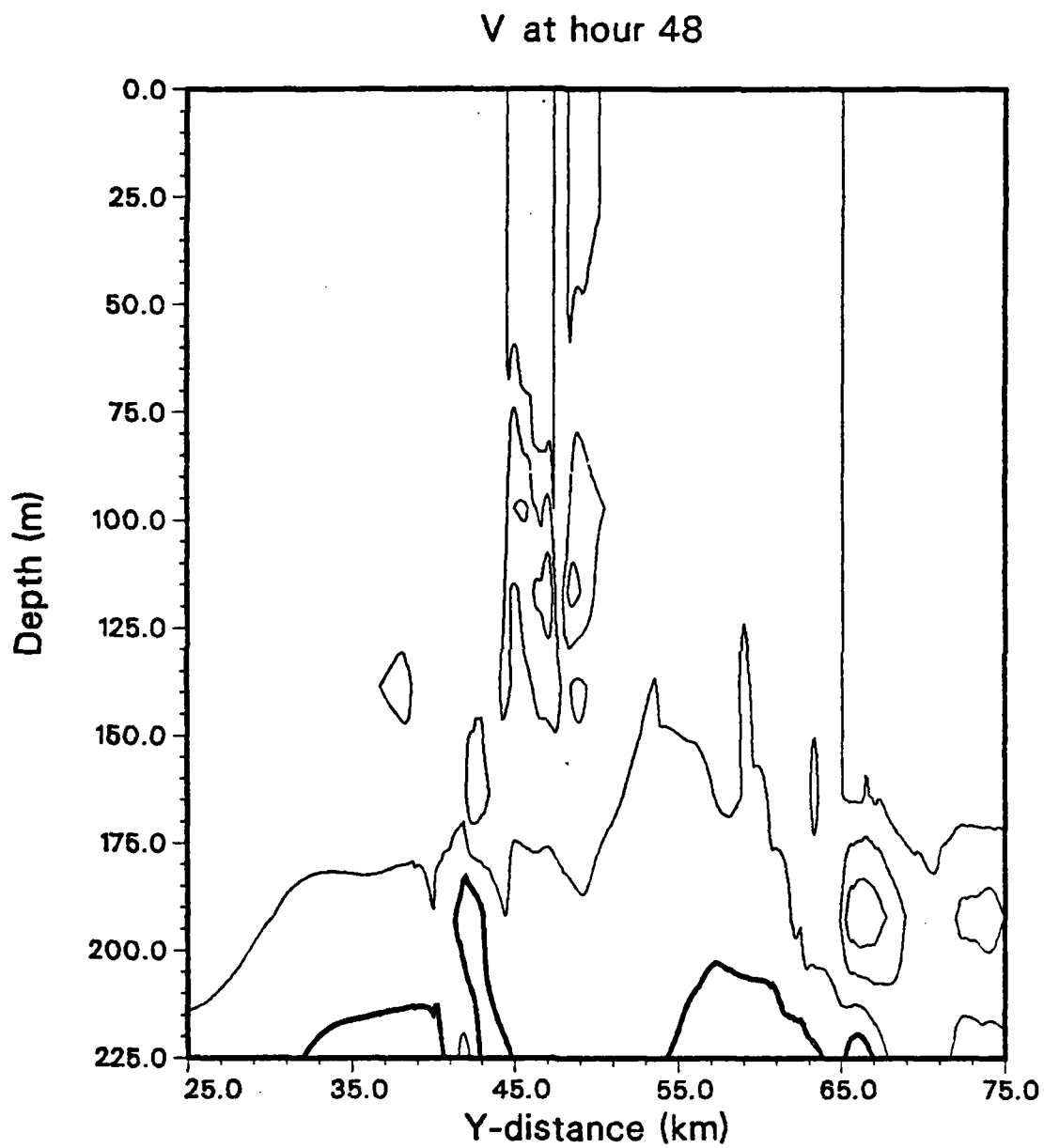
V at hour 48

Figure 31. Front 2 Case II 48-Hour V-Velocity. Contour interval is 5 cm/s.

91

occurring at 48 hours, it is presumed that the mixed layer depth would eventually even out with little or no remains of a frontal peak. As in other cases, a marked deepening in the mixed layer occurs at the left boundary of the front.

IX. MODEL RESULTS FOR FRONT 2 CASE III

A. ANALYSIS AND DISCUSSION

Constant surface heating is combined with a positive wind stress. As the net Ekman transport will be from right to left, and with heating, we expect to see the formation of a warm plume of water on the surface in the cool (left) ambient pool. The surface heating should enhance the inherent static stability and prevent the wind from completely mixing the transported warm waters. This effect does happen prior to the 12 hour point and becomes more pronounced over the entire integration (see Fig. 32). Downwelling and mixing of the warmed surface waters with the cooler underlying waters are observed at the leading edge of the progressing front. Upwelling on the right side of the cooler water which replaces water lost due to transport is clearly seen by comparing successive temperature fields. The front shows a tendency to almost split at 30 m depth into a shallow surface front and a deeper front. Perhaps a different combination of forcing would make this happen.
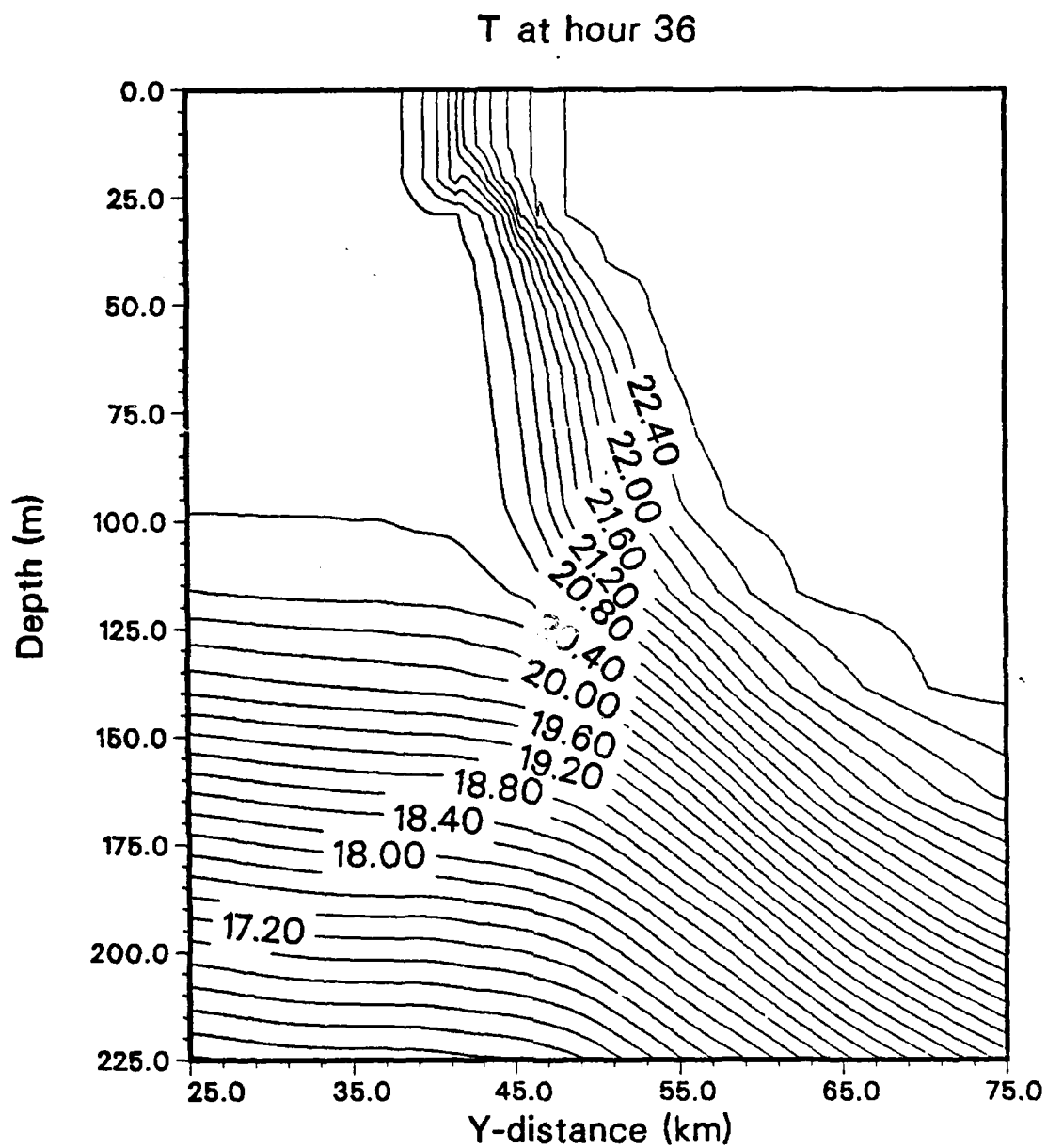
T at hour 36

Figure 32.   Front 2 Case III 36-Hour Temperature.   Contour
interval is 0.2 deg C.

The isotherms are much smoother than for the cases of wind stress alone. As in Case I, the originally-horizontal field on the left side becomes inclined, and the originally-inclined field on the right side becomes level. The effect is not as dramatic as before.

The mixed layer quickly responds to the applied heating. By 12 hours the mixed layer has re-formed in the far field at 40 m. The shallow section within the front is advected with the plume of the front and moves into the cooler (left) side. The original shallow section of the mixed layer depth at the right boundary of the front has deepened to the mean far-field value prior to hour 12, "filling in" at the rear as the shallow frontal peak is advected. This shallow "bubble" progresses to the left with the front causing shallowing in advance of the front and deepening behind. The mixed layer responds with changes of up to 10 to 15 m on a time scale of something less than 12 hours (compare Fig. 33 to Fig. 5).

The along-front velocity maintains a constant shape and configuration over the 48-hour integration. The maximum speed decreases slowly over time from 100 cm/s at the start to 60 cm/s by hour 36. The horizontal gradient on the right

MICROCOPY RESOLUTION TEST CHART

NATIONAL BUREAU OF STANDARDS-1963-A

H at hour 36
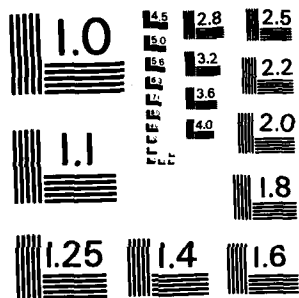
Figure 33. Front 2 Case III 36-Hour Mixed Layer Depth.

side decreases rapidly but on the left side is preserved
(Fig. 34) This is due to the advance of the plume and the
resistance to mixing that the heating has established.

At 24 and 36 hours, the across-front velocity is neg-
ative, with the maximum of -10 cm/s occurring within the
moving plume of overriding warm water (Fig. 35). A wave
oscillation in the v field is evident, and has the same
direction and time scale as those of Cases I and II. At 12
hours, v is positive, which is probably a response to the
ageostrophic u-component created as the front undergoes
adjustment. At 48 hours the v-field has a small positive
and may be inertial motion.

B. SUMMARY -- CASE III

The application of heating is able to generate and pre-
serve a warm plume which overrides the cooler water in
response to net Ekman transport. Some downwelling is
implied at the leading edge of the front. The isotherms
show a "kirk" and an ageostrophic u-velocity is there. Some
of the surface-warmed water is mixed into the ambient pool.
On the right "upstream" side, upwelling occurs as cooler
water is brought up to replace that lost by transport.

U at hour 36
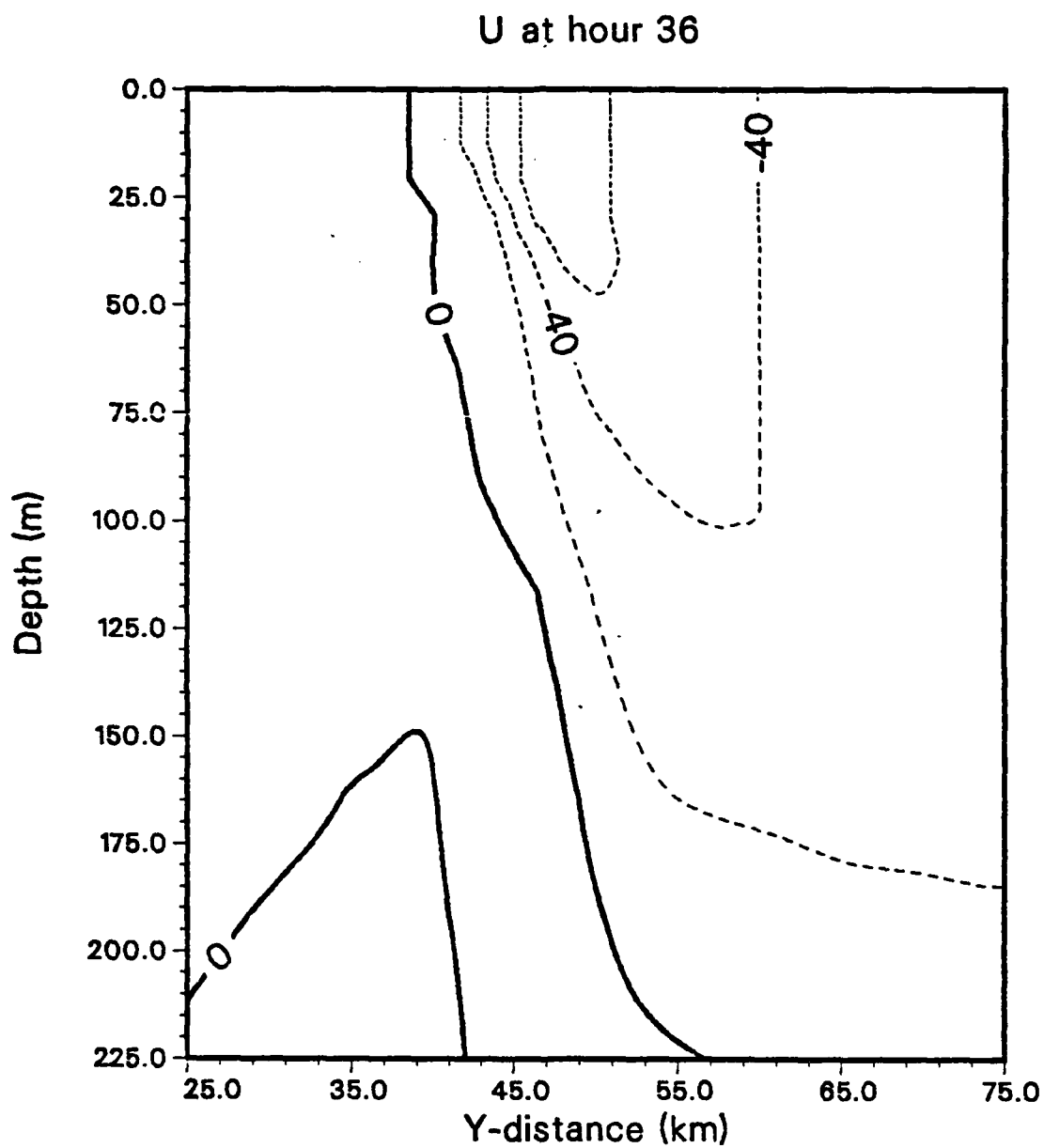
Figure 34.   Front 2 Case III 36-Hour U-Velocity.   Contour increment is 20 cm/s.

98

V at hour 24
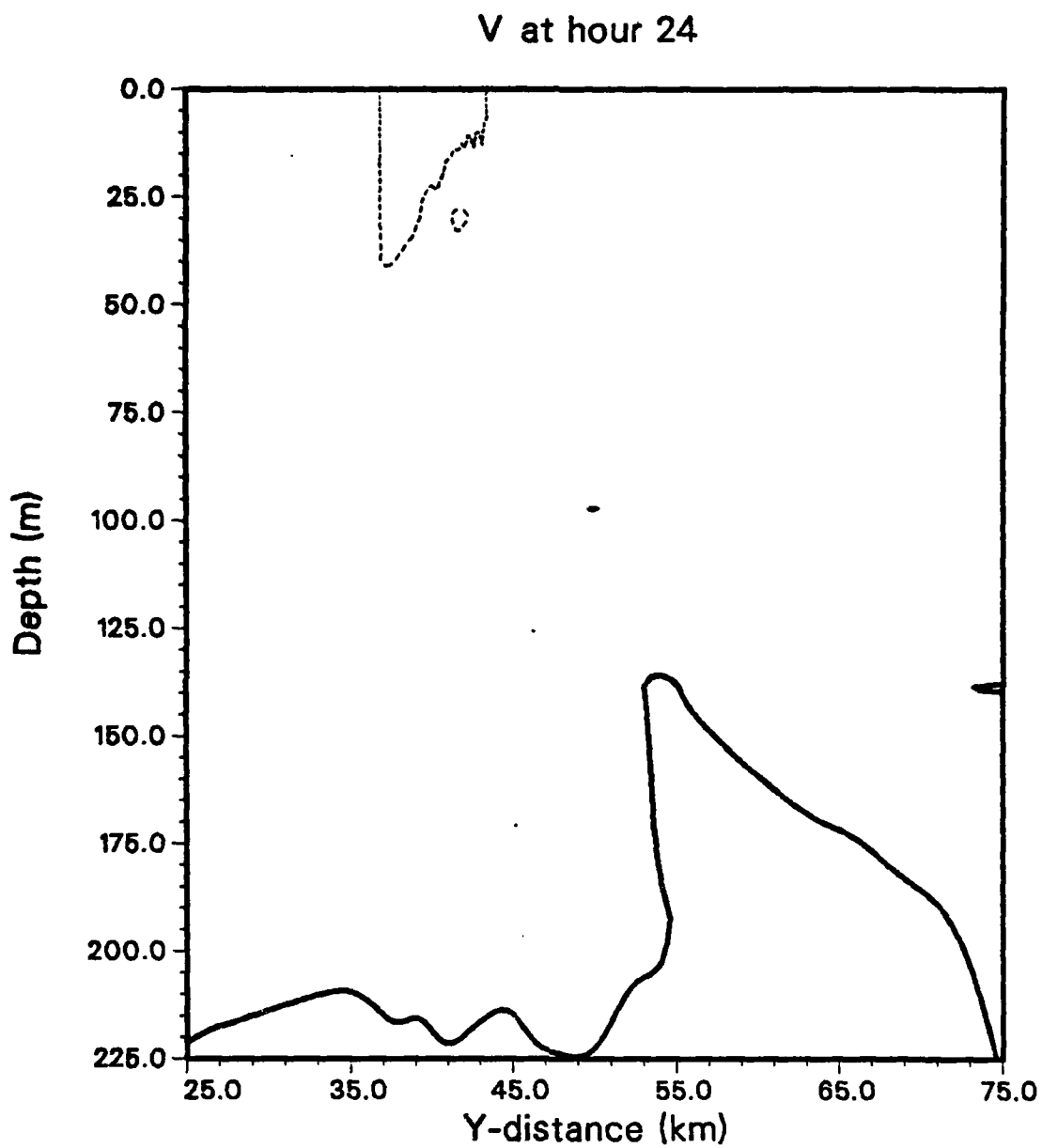
Figure 35. Frcnt 2 Case III 24-Hour V-Velocity. Contour
interval is 10 cm/s.

99

The mixed layer depth shallows to a constant depth outside
of the frontal area under the uniform heating, and the shal-
lower peak existent within the front is advected with the
front in a response to the mass transport. The across-front
velocity generally shows a maximum at the surface within the
front the direction of net Ekman transport, though reversals
in direction occur with time as a result of ageostrophic
responses.

X. MODEL RESULTS FOR FRONT 2 CASE IV

A. ANALYSIS AND DISCUSSION

The combined effects of surface heating and a negative wind stress act to push the upper 150 m of the front into the warmer water on the right side. Vertical mixing is pronounced as seen by the vertical orientation of the surfaced isotherms (Fig. 36). This result is expected as convective mixing is coupled with wind stirring. Diffusion and horizontal mixing cause the frontal horizontal temperature gradient to decrease continually over the 48-hour integration. Here too, the entire field develops a downslope to the right as in the preceding three cases.

The mixed layer is initially shallowed to around 40 m by the applied heating, and the shallow section located within the front breaks down and approaches the level of the overall mixed layer (Fig. 37). This result is expected based on previous cases which combined the action of convective mixing and wind stirring.

The u-velocity field has an ageostrophic component at the left boundary as a response to the adjustment.
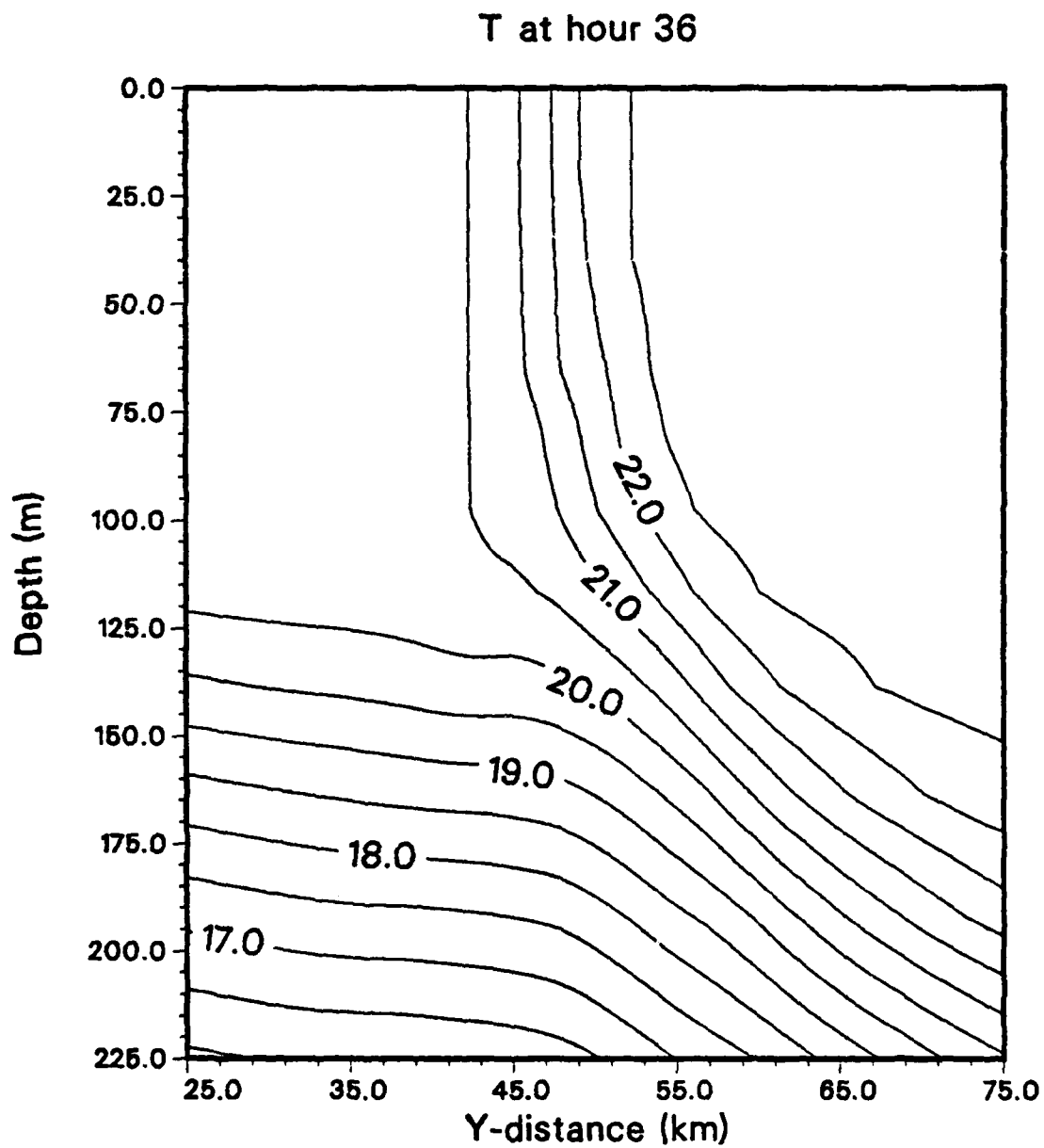
Figure 36. Front 2 Case IV 36-Hour Temperature. Contour interval is 0.5 deg C.

H at hour 36
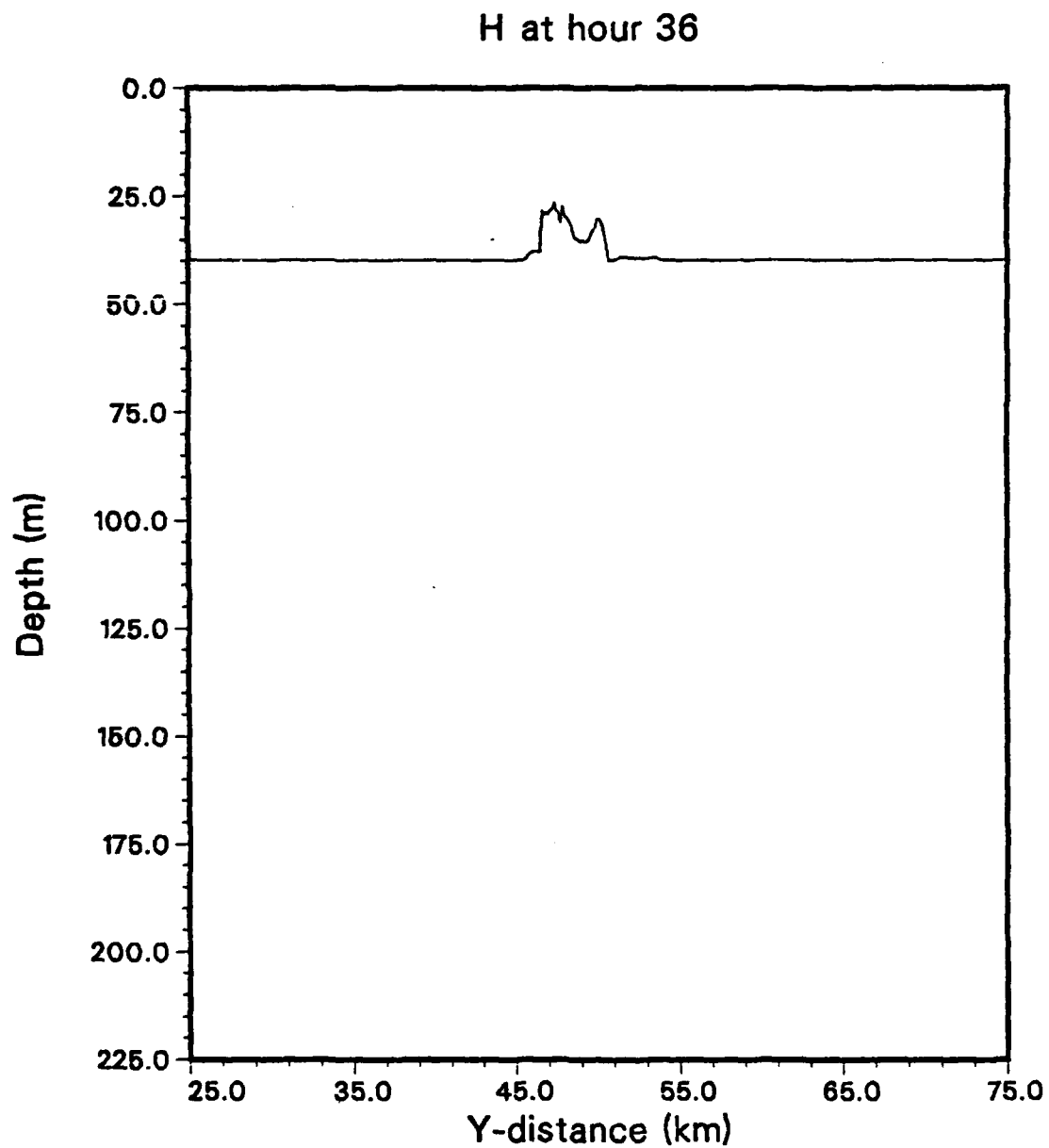
Figure 37. Front 2 Case IV 36-Hour Mixed Layer Depth.

Basically the u-velocity decreases its maximum speed and weakens its horizontal gradient over the 48-hour integration. The across-front v-velocity is in the direction of transport at 12 and 48 hours and extends from the surface, through the mixed layer depth, and down to a depth below 100 m. Once again, cross-frontal mixing occurs. At 24 hours, the v-field is reversed over the entire upper 200 m. At 36 hours, the v-field exists only in the shallow surface layer, and, by 48 hours, the field returns to the positive direction. Some type of oscillation is evident in the v field (refer to Figs. 38, 39, 40, and 41). At hour 12, the field is positive everywhere. At hour 24, it is negative everywhere. At hour 36, it is negative in the shallow depths only. At 48 hours, it is again positive everywhere. This pattern occurred in the previous three cases, and it is strongly suggestive of some type of oscillation in the v-component both in direction and in depth-extent.

B. SUMMARY -- CASE IV

The adjustment of the front under a negative wind stress and surface heating is affected by both convective mixing and wind-stirring in the vertical. Cross-frontal mixing is evident in the horizontal. The front is "pushed back" into

the warmer water on the right by the transport of cooler water. The front diffuses over time.

The mixed layer depth shallows outside of the front due to the surface heating, and the shallow portion within the front is eroded through mixing and approaches the depth of the far field. The u-velocity follows an uneventful pattern of diffusion and a decrease in maximum speed as the front adjusts. The direction of the v-velocity correlates to the direction of net Ekman transport only at 12 and 48 hours. Between those times, an oscillatory pattern in direction and depth is observed. This is the same pattern which was observed in the v-fields of Cases I, II, and III. The v-field indicates cross-frontal mixing as it extends over a great depth. It is independent of the mixed layer depth.

V at hour 12
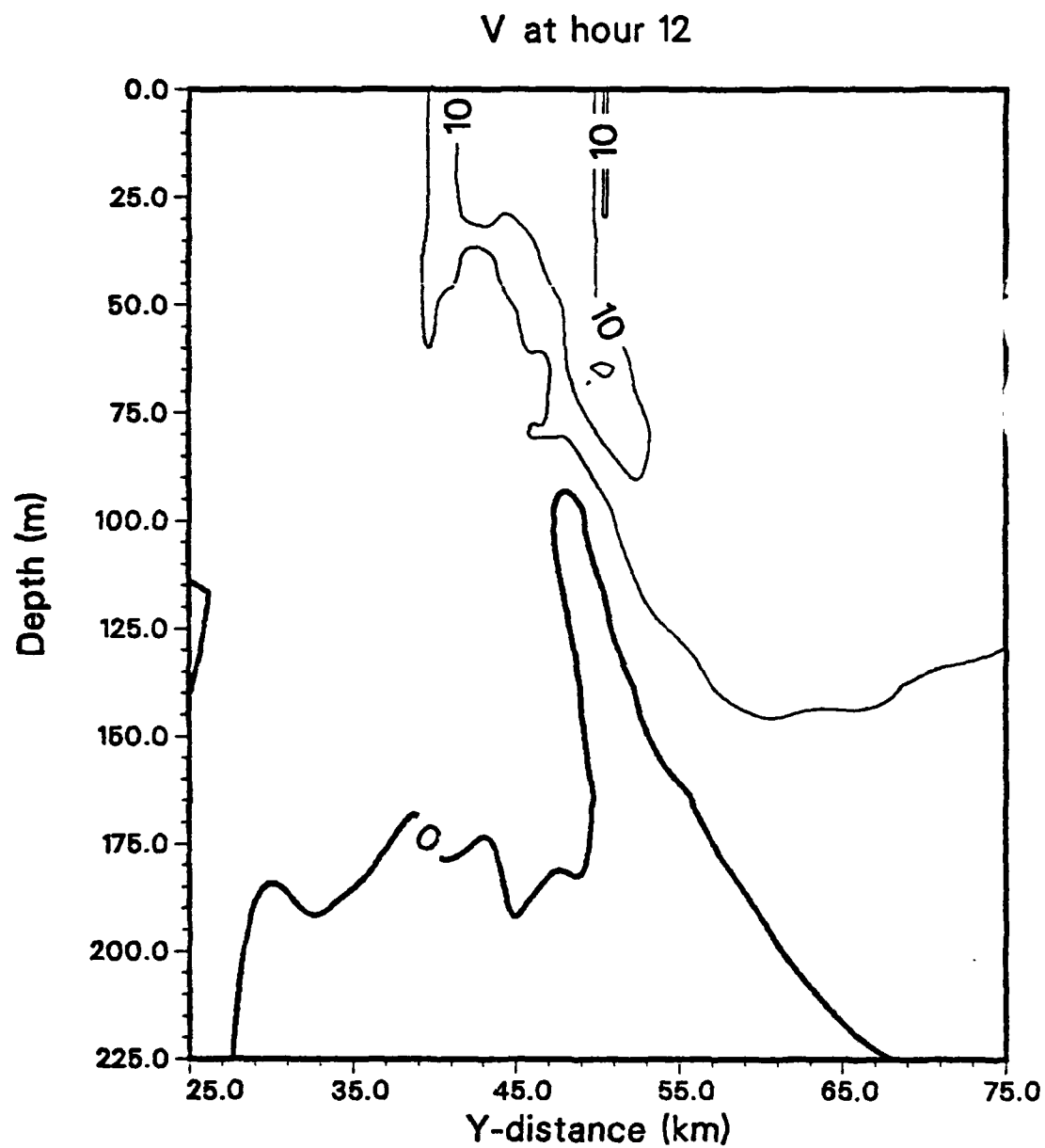
Figure 38.   Front 2 Case IV 12-Hour V-Velocity.   Contour
interval is 5 cm/s.

V at hour 24
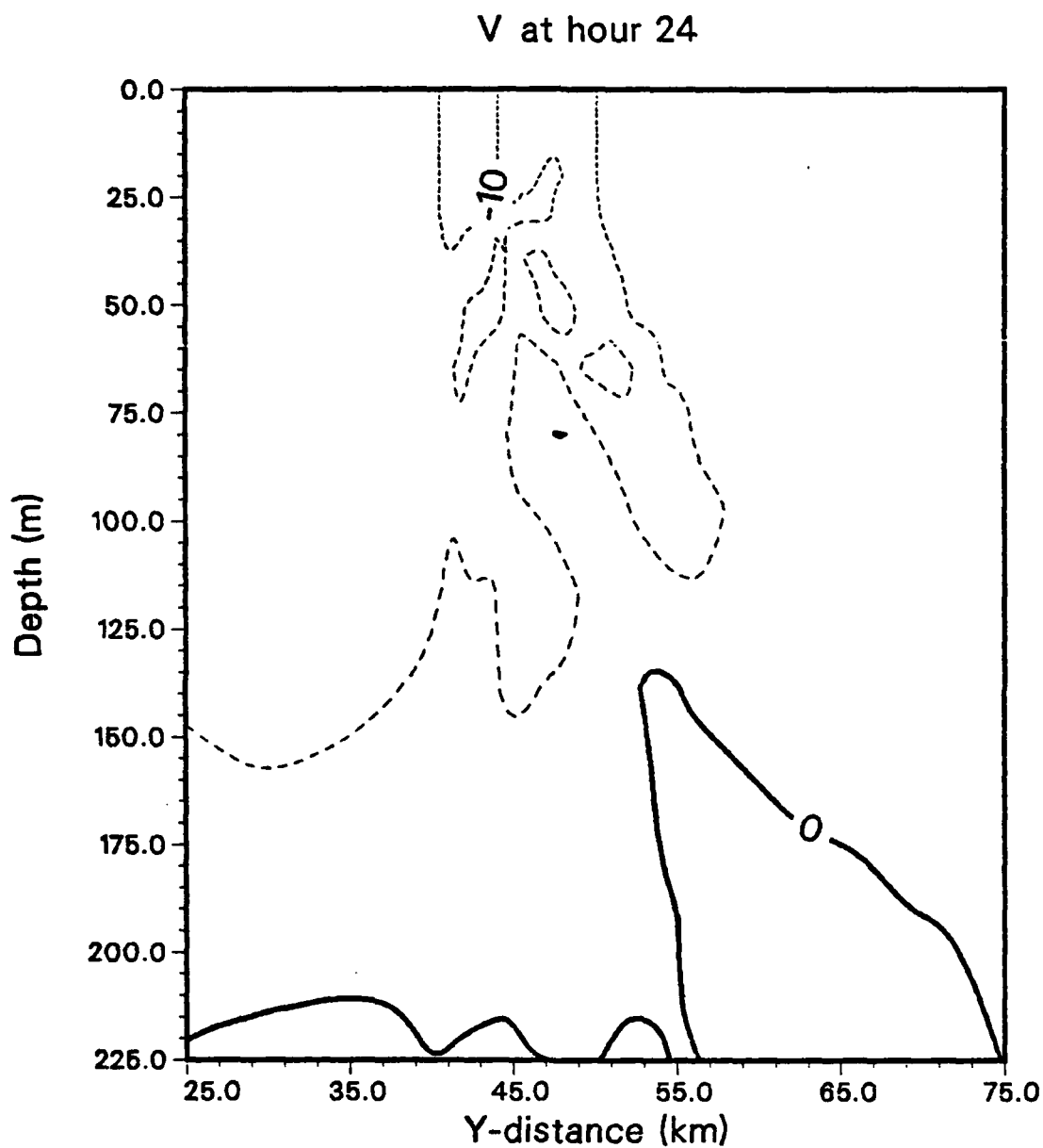
Figure 39. Front 2 Case IV 24-Hour V-Velocity. Contour interval is 5 cm/s.

V at hour 36
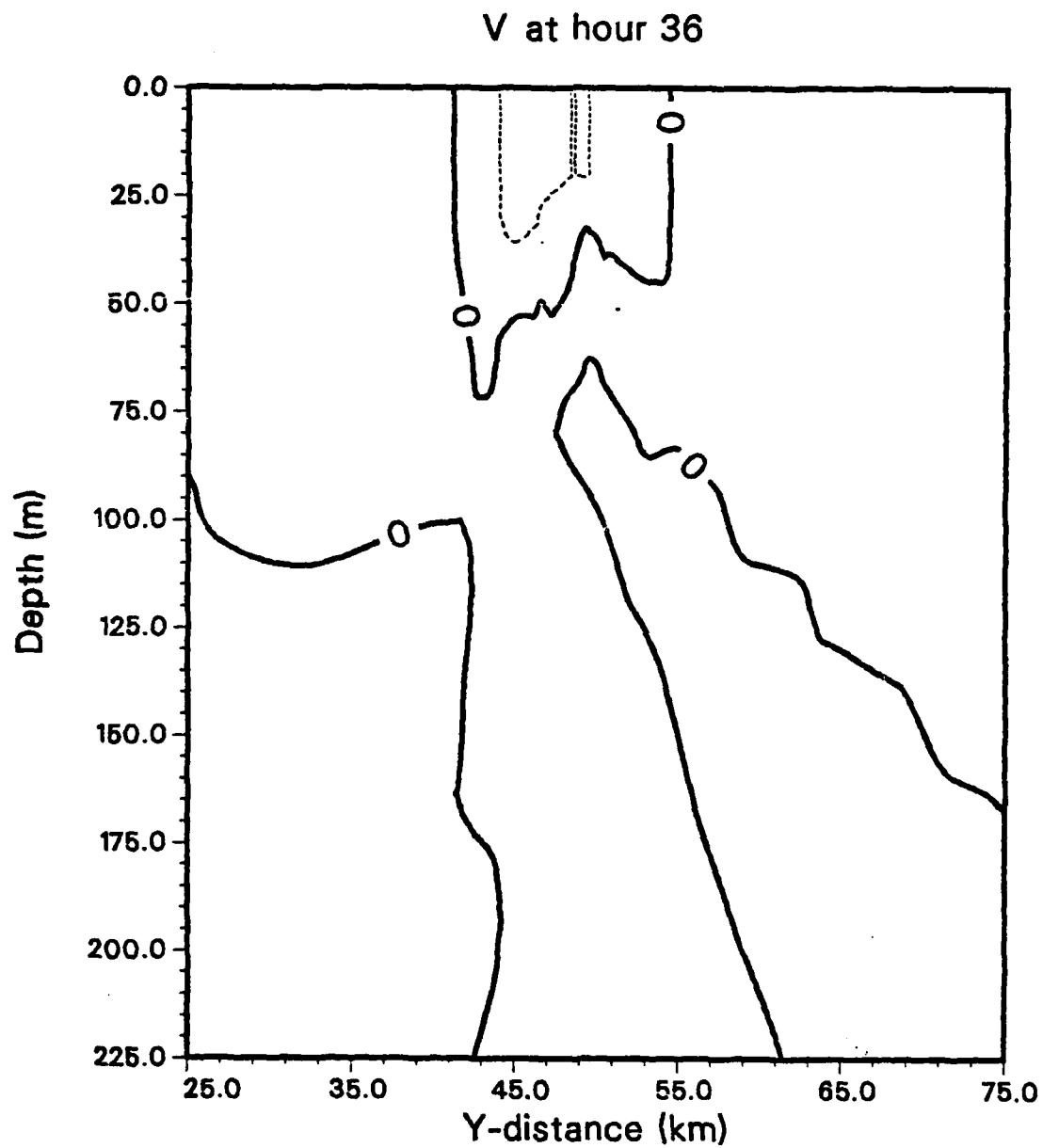
Figure 40. Front 2 Case IV 36-Hour V-Velocity. Contour interval is 5 cm/s.
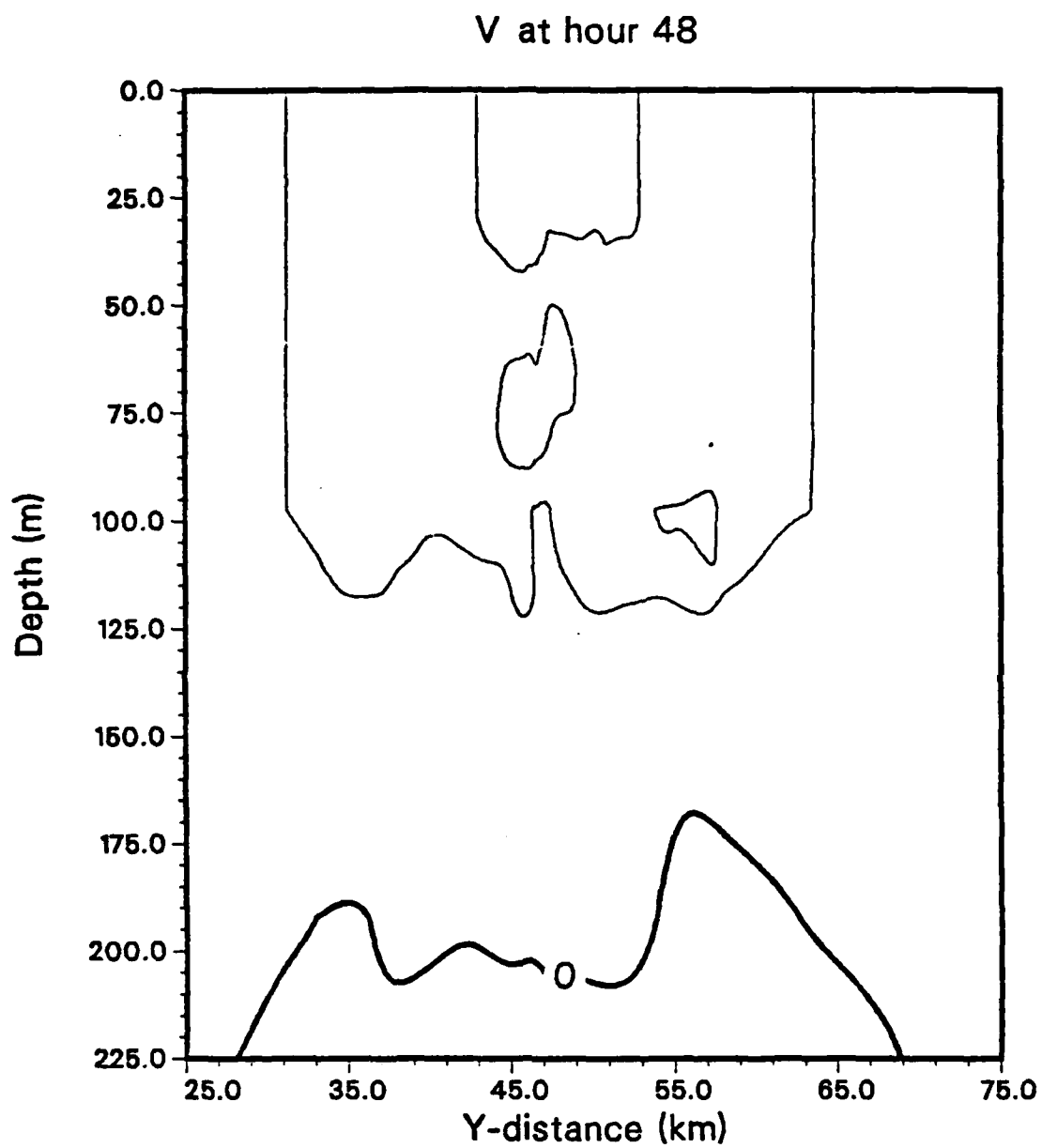
Figure 41. Front 2 Case IV 48-Hour V-Velocity. Contour interval is 5 cm/s.

XI. CONCLUSIONS AND RECOMMENDATIONS

A. GENERAL

This thesis has examined the unsteady response of two oceanic fronts to the local atmospheric forcings of wind stress and surface heat flux. The simplicity of Front 1 enabled identification of basic processes stimulated by the forcings, processes which were not so clearly seen in Front 2. Front 2 was a more realistic simulation of an oceanic front, and, hopefully, it will serve as a stepping stone for further investigations into fronts and testing of this frontal model.

There are a few very general properties that exist for both Fronts 1 and 2, and which bear out our hypotheses stated in Chapter 2.B.:

1) Wind direction plays a primary role in frontal adjustment. In the cases where warmer, less dense water is transported to cooler, denser water, the structure of the front is preserved. The mixed layer depth is also preserved, and little cross-frontal mixing occurs.

2) In the cases where cooler, denser water is transported to warmer, less dense water, the horizontal temperature gradient is diffused, the mixed layer depth within the

front breaks down and deepens, and much cross-frontal mixing occurs. Convective mixing occurs along with wind stirring.

3)   A uniform constant surface heat flux shallows the mixed layer outside of the frontal zone to a depth which is proportional to the amount of heat flux. The combination of a +1 dyne/cm^2 wind stress and a surface heat flux of -0.004 deg-cm/s mixes heat down to a depth of the initial mixed layer and leads to stratification there. Stratification of the isotherms at the surface did not occur. For the cases in which the heat flux is applied, turbulent mixing is restrained in the vertical, which agrees with the results of Niiler (1975) and Mellor and Durbin (1975).

4)   In areas of the frontal zone where ageostrophic velocities are created, vertical mixing is increased.

5)   Mixed layers deepen rapidly within the first 12 hours under wind stress alone as the fronts undergo initial adjustment. Beyond 12 hours, adjustments are confined to an area around the the basic depth attained during the initial adjustment period.   Niiler (1975), Mellor and Durbin (1975) and De Szceke (1980) all reported this phenomenon.

6)   A time-dependent pattern in the direction and depth-influence of the across-front velocity exists.   It is

probably due to inertial oscillations created by the atmos-
pheric forcing.

It was surprising to see the downward bulge in the mixed
layer at the cold-side boundary of both fronts in the wind
stress only cases. It is unclear as to why this happens,
though some speculative reasons were provided.

In Front 1, the formation of cores of positive v-veloc-
ity which are symmetric about the mixed layer depth are
intriguing. Inertial oscillations may provide an
explanation.

The tilting down to the right of the entire temperature
field in Front 2 in all four cases is a major adjustment,
and one which is independent of wind stress direction and
heating. It would appear that this tilt is a response to
the re-orientation of the oceanic current fields.

B. RECOMMENDATIONS

There is both further investigation that can be done
with the results of this thesis, as well as new work which
is suggested by these results. The results of these eight
model runs could be further quantified by using a finer con-
tour interval for the fields, and by producing fields for
gradients, ageostrophic velocities, and the like. The

inertial actions could be investigated to encompass magnitudes, directions, depths and areas affected. It would be instructive to examine (y,z) streamfunctions. The model could be tested by conducting parametric sensitivity studies of the constants used in the governing equations and mixed layer equations.

New work might include using different combinations of these atmospheric forcings both in magnitude and direction. Inclusion of a wind stress in the y-direction would certainly prove to be of interest, as would a diurnal heating/cooling cycle. Other atmospheric forcings could be applied. Evaporation and precipitation might be incorporated. The equation of state could be expanded to include salinity, and an initial salinity field could be inserted and monitored over time. Cf course, a three-dimensional version of this model would be valuable. More simulations of observed fronts using data acquired in the field would provide further insight into the applicability of the model. Data acquired by Johannessen, et al (1977) of the Maltese front would be a recommended starting point.

Computer central processor unit (CPU) time was extensive for each of these model runs. They each averaged over four

hours of CPU time to run, providing no stopping and restart-
ing were required. Such a model is far from being useful
operationally for real-time assessment of ocean structure to
provide, for example, input for acoustic forecasting models.
However, for basic research, this model appears to be a pow-
erful tool for deciphering the complexities of ocean frontal
dynamics and thermodynamics.

LIST OF REFERENCES

Adamec, D., R.L. Elsberry, R.W. Garwood, Jr., and R.L. Haney, 1981: An embedded mixed layer-ocean circulation model. Dyn. of Atmos. and Oceans, 6, 69-96.

Bang, N.D., 1973: Characteristics of an intense ocean frontal system in the upwell regime west of Cape Town. Tellus, 25, 256-265.

Briscce, M.G., C.M. Johannessen, and S. Vincenzi, 1974: The Maltese oceanic front: a surface description by ship and aircraft. Deep Sea Res., 21, 247-262.

Camerlengo, A., 1982: Large-scale response of the Pacific Ocean subarctic front to momentum transfer: a numerical study. J. Phys. Oceanogr., 12, 1106-1121.

Cromwell, T., and J.L. Reid, Jr., 1956: A study of oceanic fronts. Tellus, 8, 94-101.

Cushman-Roisin, B., 1981: Effects of horizontal advection on upper ocean mixing: a case of frontogenesis. J. Phys. Oceanogr., 11, 1345-1356.

De Szceke, R.A., 1980: On the effects of horizontal variability of wind stress on the dynamics of the ocean mixed layer. J. Phys. Oceanogr., 10, 1439-1454.

Elsberry, R.L., and R.W. Garwood, Jr., 1979: First-generation numerical ocean prediction models - goal for the 1980's. Naval Postgraduate School Report 63-79-007, 41 pp.

Endoh, M., C. N. K. Mooers, and W. R. Johnson, 1981: A coastal upwelling circulation model with eddy viscosity depending on Richardson Number. Coastal Upwelling, F. A. Richards, Ed. Am. Geophys. U., 529 pp.

Garvine, R.W., 1974: Dynamics of small-scale oceanic fronts. J. Phys. Oceanogr., 4, 557-569.

Garvine, R.W., 1979a: An integral hydrodynamic model of upper ocean frontal dynamics: Part I. Development and analysis. J. Phys. Oceanogr., 9, 1-18.

Garvine, R.W., 1979b: An integral hydrodynamic model of upper ocean frontal dynamics: Part II. Physical characteristics and comparison with observations. J. Phys. Oceanogr., 9, 19-36.

Garvine, R.W., 1980: The circulation dynamics and
thermodynamics of upper ocean density fronts. J. Phys.
Oceanogr., 10, 2058-2081.

Garwood, R.W., Jr., 1977: An oceanic mixed layer model
capable of simulating cyclic states. J. Phys. Ocean-
ogr., 7, 455-468.

Haney, R.I., 1980: A numerical case study of the
development of large-scale thermal anomolies in the cen-
tral north Pacific Ocean. J. Phys. Oceanogr., 10,
541-556.

Johannessen, C.M., D. Good, and C. Smallenburger, 1977:
Observation of an oceanic front in the Ionian Sea during
early winter 1970. J. Geophys. Res., 82, 1381-1391.

Johnson, D. R. and C. N. K. Mooers, 1981: Internal
cross-shelf flow reversals during coastal upwelling.
Coastal Upwelling, F. A. Richards, Ed. Am. Geophys. U.,
529 pp.

Kao, T.W., 1980: The dynamics of oceanic fronts. Part I:
The Gulf Stream. J. Phys. Oceanogr., 10, 483-492.

Katz, E.J., 1969: Further study of a front in the Sargasso
Sea. Tellus, 21, 259-269.

Mellor, G.L., and P.A. Durbin, 1975: The structure and
dynamics of the ocean surface mixed layer. J. Phys.
Oceanogr., 5, 718-728.

Mooers, C. N. K., 1978: Oceanic fronts: A summary
of a Chapman Conference. EOS, 59, No. 5, 484-491.

Niiler, P.P., 1975: Deepening of the wind-mixed layer.
J. Mar. Res., 33, 405-422.

Niiler, P.P., 1982: 'Fronts-80' - a study of the North
Pacific subtropical front. Nav. Res. Rev., 34, No. 3,
41-50.

Roden, G.I., 1971: Aspects of the transition zone in the
northeastern Pacific. J. Geophys. Res., 76, 3462-3475.

Roden, G.I., 1972: Temperature and salinity fronts at the
boundaries of the subarctic-subtropical transition zone
in the western Pacific. J. Geophys. Res., 77,
7175-7187.

Roden, G.I., 1974: Thermohaline structure, fronts, and
sea-air energy exchange of the trade wind region east of
Hawaii. J. Phys. Oceanogr., 4, 168-182.

Roden, G.I., 1975: On North Pacific temperature, salinity, sound velocity, and density fronts and their relation to the wind and energy flux fields. J. Phys. Oceanogr., 5, 557-571.

Roden, G.I., 1976: On the structure and prediction of oceanic fronts. Nav Res. Reviews, 29, No. 1, 18-35.

Roden, G.I., 1977: Oceanic subarctic fronts of the central Pacific: structure of and response to atmospheric forcing. J. Phys. Oceanogr., 7, 761-778.

Roden, G.I., 1980: On the subtropical frontal zone north of Hawaii during winter. J. Phys. Oceanogr., 10, 342-362.

Suginohara, N., 1977: Upwelling front and two-celled circulation. J. Oceanogr. Soc. Japan, 33, 115-130.

Voorhis, A.D., and J.B. Hersey, 1964: Oceanic thermal fronts in the Sargasso Sea. J. Geophys. Res., 69, 3809-3814.

INITIAL DISTRIBUTION LIST

		No. Copies
1.	Defense Technical Information Center Cameron Station Alexandria, VA 22314	2
2.	Library, Code 0142 Naval Postgraduate School Monterey, CA 93940	2
3.	Chairman, Code 68Mr Department of Oceanography Naval Postgraduate School Monterey, CA 93940	1
4.	Chairman, Code 63Rd Department of Meteorology Naval Postgraduate School Monterey, CA 93940	1
5.	Professor R. W. Garwood, Code 68Gd Department of Oceanography Naval Postgraduate School Monterey, CA 93940	2
6.	Mr. D. A. Adamec, Code 63Ac Department of Meteorology Naval Postgraduate School Monterey, CA 93940	1
7.	Professor R. L. Elsberry, Code 63Es Department of Meteorology Naval Postgraduate School Monterey, CA 93940	1
8.	Professor R. L. Haney, Code 63Hy Department of Meteorology Naval Postgraduate School Monterey, CA 93940	1
9.	LT Christopher J. Hall, USN Naval Oceanography Command Center Box 31 Rota, SP FPO New York 09540	2
10.	LTJG D. C. Durban, USN Naval Postgraduate School SMC Box 2645 Monterey, CA 93940	1

11. Director   1
    Naval Oceanography Command
    Naval Observatory
    34th and Massachusetts Avenue NW
    Washington, D.C. 20390

12. Commander   1
    Naval Oceanography Command
    NSTL Station
    Bay St. Louis, MS 39522

13. Commanding Officer   1
    Naval Oceanographic Office
    NSTL Station
    Bay St. Louis, MS 39522

14. Commanding Officer   1
    Fleet Numerical Oceanography Center
    Monterey, CA 93940

15. Commanding Officer   1
    Naval Ocean Research and Development Activity
    NSTL Station
    Bay St. Louis, MS 39522

16. Commanding Officer   1
    Naval Environmental Prediction Research Facility
    Monterey, CA 93940

17. Chairman, Oceanography Department   1
    U.S. Naval Academy
    Annapolis, MD 21402

18. Chief of Naval Research   1
    800 N. Quincy Street
    Arlington, VA 22217

19. Office of Naval Research (Code 420)   1
    Naval Ocean Research and Development Activity
    NSTL Station
    Bay St. Louis, MS 39522

20. Scientific Liaison Office   1
    Office of Naval Research
    Scripps Institution of Oceanography
    La Jolla, CA 92037

21. Library   1
    Department of Oceanography
    University of Washington
    Seattle, WA 98105

22. Library   1
    CICESE
    P.O. Box 4803
    San Ysidro, CA 92073

23. Library   1
    School of Oceanography
    Oregon State University
    Corvallis, OR 97331

24. Commander   1
    Oceanography Systems Pacific
    Box 1390
    Pearl Harbor, HI 96860

END

DATE
FILMED

9-83

DT